University of Nevada, Reno

Improving Potable Reuse Water Quality by Understanding *N*-nitrosodimethylamine Precursors and Bulk Organic Matter Present during Advanced Oxidation Processes

A dissertation submitted in partial fulfillment of the requirements for the degree of Doctor of Philosophy in Civil and Environmental Engineering

by

Mingrui Song

Dr. David Hanigan/Dissertation Advisor

December 2022

THE GRADUATE SCHOOL

We recommend that the dissertation
prepared under our supervision by

Mingrui Song

entitled

Improving Potable Reuse Water Quality by Understanding N-nitrosodimethylamine Precursors and Bulk Organic Matter Present during Advanced Oxidation Processes

be accepted in partial fulfillment of the
requirements for the degree of

Doctor of Philosophy

David Hanigan, Ph.D.
Advisor

Yu Yang, Ph.D.
Committee Member

Eric A. Marchand, Ph.D.
Committee Member

Sage Hiibel, Ph.D.
Committee Member

Kerri Jean Ormerod, Ph.D.
Graduate School Representative

Markus Kemmelmeier, Ph.D., Dean
Graduate School

December, 2022

ABSTRACT

Planned potable reuse is becoming a common strategy to relieve water scarcity throughout the world. Full-advanced treatment (FAT) systems consist of ultrafiltration/microfiltration, reverse osmosis (RO), and ultraviolet/advanced oxidation processes (UV-AOP) and are utilized at potable reuse facilities to degrade or remove contaminants present in wastewater effluents. Oxidants including hydrogen peroxide (H_2O_2), free chlorine (HOCl), and monochloramine (NH_2Cl) are added during UV-AOP to produce radicals which degrade contaminants. Oxidant performance regarding specific contaminant removal has been compared in prior research, but there is no consensus on the overall comparative performance of these oxidants because the contaminants selected for each study are usually different. To address this, I investigated oxidant performance by considering a broader fraction of contaminants including known compounds and unknown/unidentified compounds via nontarget analysis and bioassays. Based on greater destruction of organic compounds, reduced transformation products, and a lack of oxidative stress induction, H_2O_2 was the most suitable oxidant tested for ultraviolet advanced oxidation in water reuse.

Disinfection byproducts form when precursor chemicals are oxidized by disinfectants to new hazardous products. *N*-nitrosodimethylamine (NDMA), a carcinogenic disinfection byproduct, has been regulated with 10 ng/L drinking water notification level. Controlling specific regulated contaminants such as *N*-nitrosodimethylamine (NDMA) is also crucial for regulatory compliance, improving potable reuse water quality, and public acceptance. Its precursors can persist through advanced treatment trains including RO and UV-AOP

contributing to NDMA formation during conveyance, and these precursors are not yet identified, making them difficult to treat. Dimethylamine (DMA) is a model NDMA precursor, which is usually present in wastewater that serves as potable reuse influent. DMA has been used extensively by others in bench-scale experiments to understand NDMA formation pathways but it has also been thought that it is not an important NDMA precursor in treated wastewater and surface water due to its low yield combined with relatively low concentrations in drinking water and wastewater samples. However, its occurrence in water reuse facilities has not been investigated. Samples from one pilot plant and four full-scale water reclamation facilities were collected to study DMA occurrence in FAT facilities. The median DMA concentrations in product and finished waters were 0.4 μg/L across six sampling events. DMA accounted for 5%-43% of the total NDMA precursor pool of the UV-AOP product water at one facility, and up to 40 of ng/L of NDMA at another.

Although DMA substantially contributed to NDMA formation in potable reuse facilities, the complete NDMA precursor pool that enters typical surface water treatment plants has not been identified. Further, it is commonly thought that most NDMA precursors present in drinking water intakes originate from wastewater-derived anthropogenic chemicals but no study has conclusively determined the contribution from anthropogenic vs. naturally occurring precursors due to the difficulty in finding an appropriate environmental system to conduct such an experiment. The only study which attempted to answer whether the dominant surface water NDMA precursors are anthropogenic or environmental in origin compared NDMA precursor concentrations in wastewater effluents, a eutrophic water,

stormwater/agricultural runoff, and a pristine river source. Wastewater effluents tended to contain relatively high concentrations of NDMA precursors but it was not clear how much they contributed to NDMA formation after dilution into the river systems. Although region-specific relationships between NDMA precursors and sucralose (one anthropogenic pharmaceutical) have also been reported, suggesting NDMA precursor sources are anthropogenic, the relationship is highly watershed specific, and does not lend itself to applications outside of the watershed where the relationship was original derived. To determine if the dominant NDMA precursor sources are wastewater effluents (anthropogenic source), I investigated NDMA precursors in Truckee River, which has only one anthropogenic point source. The background of NDMA precursors in the Truckee River is relatively low, and an apparent increase was observed downstream of wastewater effluents, suggesting that anthropogenic sources dominate NDMA precursor loading within the limited length from wastewater effluent in the Truckee River.

Keywords: monochloramine, free chlorine, hydrogen peroxide, disinfection byproduct, NDMA, DMA, NDMA precursor source

ACKNOWLEDGEMENT

First and foremost, I would like to thank my advisor, Dr. David Hanigan, for his support, guidance, and patience. His advice and guidance have always been helpful. I would also like to thank him for offering the opportunities for both my husband and me in his research group.

I would also like to thank my doctoral committee members, Dr. Yu Yang, Dr. Eric Marchand, Dr. Sage Hiibel, and Dr. Kerri Jean Ormerod for their valuable suggestions and time. A huge appreciation goes to my first friend, Elizabeth Mckenna, for acclimating me to America. Lin Li – thanks for being my stress reliever. I would also like thank my lab mates - Utsav Thapa, Ibrahim Abusallout, Priyamvada Sharma, and Kevin Stewart. It was great to work with you.

I am grateful to the financial support from the National Science Foundation under Grant No. 1804255, the Water Research Foundation (Project #5005, managed by Djanette Khiari and Katie Spahr), and scholarships from Air & Waste Management Association, Nevada Water Reuse Association, and Nevada Water Resources Association.

Finally, I would like to thank my husband, Junli Wang. Your love is the most valuable power for me to overcome every challenge. I also want to say thank you to my parents their strong support as always.

TABLE OF CONTENTS

LIST OF TABLES

LIST OF FIGURES

LIST OF IMPORTANT ABBREVIATIONS

AWPF	Advanced Water Purification Facility
CDMA	Chlorinated Dimethylamine
DBPs	Disinfection Byproducts
DMA	Dimethylamine
FAT	Full Advanced Treatment
FPW	Finished Product Water
GC-MS/MS	Gas Chromatography-tandem Mass Spectrometry
MF	Microfiltration
NDMA	*N*-nitrosodimethylamine
NDMA FP	*N*-nitrosodimethylamine Formation Potential
NTA	Non-target Analysis
OCWD	Orange County Water District
RO	Reverse Osmosis
ROF	Ultraviolet Feed
ROP	Reverse Osmosis Permeate
SPE	Solid-phase Extraction
UF	Ultrafiltration
UV/ambient	Ultraviolet/Ambient Chloramines

UV-AOP	Ultraviolet Advanced Oxidation Process
UVF	Ultraviolet Feed
UV/H_2O_2	Ultraviolet/Hydrogen Peroxide
UV/HOCl	Ultraviolet /Free Chlorine
UV/NH_2Cl	Ultraviolet /Monochloramine
UVP	Ultraviolet Product
WWRF	Wastewater Reclamation Facility

1. INTRODUCTION

1.1. Overview of the Research Gaps

The lack of drinking-water resources is of growing concern and attracts public attention.[1-2] In response to the water scarcity, highly-treated municipal wastewater effluents are considered as a reliable supply of potable water.[3] In order to produce potable reuse water which meets drinking water quality standards, full advanced treatment (FAT) defined by California State Water Resources Control Board is often considered the standard treatment train for potable reuse[4-5] to degrade or remove contaminants present in municipal wastewater effluents. FAT trains consist of secondary or tertiary wastewater treatment followed by microfiltration (MF) or ultrafiltration (UF), reverse osmosis (RO) as a broad-screen physical removal process and an ultraviolet-advanced oxidation process (UV-AOP) to destroy poorly rejected organic contaminants.

Many studies have been conducted to investigate the most suitable UV-AOP in FAT trains by comparing the UV-AOP oxidant performance (UV-AOP with chlorine [UV/HOCl], or hydrogen peroxide [UV/H_2O_2], or monochloramine [UV/NH_2Cl]). However, the conclusions drawn from the individual published studies are inconsistent due to differences in the selected target compounds. In terms of 1,4 dioxane, the removal by the three common oxidants was UV/HOCl > UV/H_2O_2 >> UV/NH_2Cl.[6] However, *N*-nitrosodimethylamine (NDMA) was destroyed by UV/H_2O_2 better than UV/HOCl.[7] Overall, there is a need to evaluate the three oxidants' performance in UV-AOPs considering both known target contaminants and unknown organics present in the treatment trains.

In addition to broadly destroying or controlling organic contaminants, controlling specific contaminants which have regulatory guidelines is important for improving social acceptance of potable reuse water. *N*-nitrosodimethylamine (NDMA) is a probable human carcinogen disinfection byproducts commonly observed in potable reuse facilities.[8-10] Several U.S. states including California and Massachusetts have set a 10 ng/L drinking water Notification Level.[11-12] In addition to states in U.S., the World Health Organization, Canada, and Australia have guidelines at 40-100 ng/L.[13-15] In FAT trains at potable reuse facilities, NDMA is formed via the reaction with wastewater organic matter and chloramines added to prevent biofouling of the RO membranes[16-17] Formed NDMA is poorly rejected by RO,[18] but effectively destroyed by photolysis during UV-AOP.[19] Although NDMA concentrations are reduced to below detection limits (< 2 ng/L) by UV-AOP, NDMA sometimes "rebounds" to low ng/L concentrations during conveyance.[20-21] It is not clear what the reactive precursors are that pass the RO membranes and UV-AOP. In order to mitigate NDMA formation in the finished water, identifying NDMA precursors and destroying or removing them beforehand is important for potable water security.

1.2. Research Objectives and Layout

This dissertation focuses on improving potable reuse water quality by evaluating destruction, formation, and toxicity of a broader fraction of organics and understanding the formation of one specific contaminant, NDMA. The dissertation is organized into six chapters:

Chapter 2 – Introduce the removal and toxicity of trace organic contaminants in UV-AOPs and NDMA formation background and provide an up-to date understanding of NDMA precursors. Research gaps are provided.

Chapter 3 - Evaluate the performance, in terms of the number of compounds destroyed or formed and the toxic potential of the treated water, of three oxidants used during UV-AOP (H_2O_2, HOCl, and NH_2Cl). Suspect and nontarget screening and bioassays were utilized to compare three oxidants' performance.

Chapter 4 - Determine the occurrence of NDMA precursor, dimethylamine (DMA), and its contribution to NDMA formation at RO water reclamation facilities. DMA occurrence in one pilot-scale and four full-scale water reclamation facilities using RO and UV-AOP was measured. Experiments were conducted to determine DMA contribution to NDMA formation.

Chapter 5 - Investigate the origins of NDMA precursors in surface water serving as drinking water treatment plant sources. NDMA precursor concentrations along ~ 100 miles of Truckee River, and diurnal changes in precursor loading in a stream which directly receives reclaimed wastewater, were measured to understand precursor loading and the contribution of wastewater effluent compared to natural precursor sources.

Chapter 6 – Provides broad conclusions and provides recommendations for future research.

2. LITERATURE REVIEW

2.1. Introduction

The pressures on existing drinking-water resources are increasing due to population growth, climate variability, and economic development.[1-2] Planned potable reuse using highly treated municipal wastewater effluents has garnered interest to meet increasing drinking water demands.[3, 5] Direct potable reuse (DPR) and indirect potable reuse (IPR) are two categories of potable reuse.[1-3] DPR represents the introduction of the highly treated municipal wastewater directly into drinking water supplies, whereas IPR represents the planned addition of highly treated municipal wastewater into an environmental buffer including rivers, lakes, reservoirs, and aquifers.

Trace organic contaminants includes pharmaceuticals and personal care products,[22-23] endocrine disrupting compounds,[22] synthetic compounds,[24] and disinfection byproducts (DBPs)[25]. Some trace organic contaminants are incompletely removed by the conventional wastewater treatment plants, [22-24, 26] and DBPs are formed unintentionally during the disinfection process of the wastewater treatment plants.[8, 27] Therefore, trace organic contaminants are commonly observed in wastewater effluents or effluent-dominated rivers.[24, 27] Although trace organic contaminants are usually detected in only ng/L to μg/L range, they have been reported to potentially affect human health with prolonged exposure.[28-30]

In order to ensure adequate removal of trace organic contaminants, wastewater effluents (i.e., secondary or tertiary effluents) are further treated by a full advanced treatment (FAT) train in potable reuse treatment systems. FAT trains commonly consist of a broad-screen

physical removal process including microfiltration (MF) or ultrafiltration (UF), and reverse osmosis (RO) and an ultraviolet/hydrogen peroxide (UV/H_2O_2) advanced oxidation process (AOP) to destroy poorly rejected organic contaminants.

N-nitrosodimethylamine (NDMA) has been indicated as a key concern for potable reuse treatment systems by National Research Council.[3] It is a carcinogenic DBP and 0.7 ng/L in drinking water is associated with a 10^{-6} life time excess cancer risk.[9] Accordingly, California has set a 10 ng/L drinking water Notification Level,[11] and a 3 ng/L public health goal.[31] Similar to California, Massachusetts, another state in the U.S., set a 10 ng/L drinking water guideline.[12] In addition, the World Health Organization, Canada, and Australia have guidelines at 40-100 ng/L.[13-15] Therefore, it is crucial to control NDMA formation.

This review aims to introduce the removal and toxicity of trace organic contaminant in UV-AOPs and NDMA formation background and up-to date understanding of NDMA precursors. In the end, knowledge gaps are proposed, which is the motivation of the dissertation.

2.2. UV-AOP Performance

2.2.1. UV-AOP oxidants

H_2O_2 is the most widely implemented oxidant in UV-AOP for potable reuse,[5] because hydroxyl radical (▪OH) can be generated under UV light to react with organic contaminants with nearly diffusion-controlled rate constants.[32] The redox potential of ▪OH ranged from 1.9 to 2.7 V depending on pH,[33] meaning is a strong oxidant. The quantum yield under UV light at 254 nm is 0.5,[34] and the molar absorption coefficients is ~19 $M^{-1}cm^{-1}$, which two

decide ▪OH production efficiency. There is growing interest in other UV-AOP oxidants with higher radical production efficiency and rate constant with organic contaminants.

Chlorine-based disinfectants including free chlorine (HOCl), monochloramine (NH_2Cl), and chlorine dioxide (ClO_2) are considered as alternatives because 1) it is easy to retrofit into existing treatment train for portable utilities; 2) they can be used for residual protection for DPR without additional quenching or removal, and 3) relatively higher radical production efficiency. HOCl or hypochlorite ion (OCl^-) can generate two radicals, ▪OH and chlorine radical (▪Cl), by UV photolysis, and ▪Cl will react with chloride ions to form $▪Cl_2^-$.[35] Both ▪Cl and $▪Cl_2^-$ are strong oxidants with redox potential of 2.4 V and 2.0 V, respectively.[36-37] The UV photolysis of NH_2Cl generates ▪Cl and amidogen radical ($▪NH_2$). Although $▪NH_2$ is less reactive,[35, 38] ▪Cl could degrade organic contaminants directly or form ▪OH. The UV photolysis of ClO_2 produces ▪Cl and chlorine oxide radical (▪ClO). Compared to H_2O_2, HOCl, NH_2Cl and ClO_2 has comparable or slightly higher quantum yields (~1 for HOCl, 0.35 for NH_2Cl, and 1.4 for ClO_2) and relatively high molar absorption coefficients (59 $M^{-1}cm^{-1}$ for HOCl, 66 $M^{-1}cm^{-1}$ for OCl^-, 371 $M^{-1}cm^{-1}$ for NH_2Cl, and 61 $M^{-1}cm^{-1}$ for ClO_2) under UV light of 254 nm [35, 39-44] suggesting more efficient radical production and thus a reduced energy required for organic contaminant degradation. However, there is one drawback for HOCl, NH_2Cl, and ClO_2 compared to H_2O_2. Radical scavenging rates ($k_{•OH}$) of HOCl (1.21×10^9 $M^{-1}s^{-1}$ for HOCl, and 6.37×10^9 $M^{-1}s^{-1}$ for OCl^-), NH_2Cl (1.02×10^9 $M^{-1}s^{-1}$), and ClO_2 (4×10^9 $M^{-1}s^{-1}$) are orders of magnitude greater than H_2O_2 (2.7×10^7 $M^{-1}s^{-1}$),[32, 45-46] suggesting the steady-state radical concentrations of HOCl,

NH_2Cl, and ClO_2 would be lower than expected, although they have a high radical production efficiency.

In addition to disinfectants utilized as UV-AOP oxidants, peroxydisulfate (PDS), peroxymonosulfate (PMS), and chlorinated cyanurates received some attentions as alternatives due to enhanced steady-state concentrations of reactive radicals. Photoactivation of PDS and PMS with UV irradiation at 254 nm generates sulfate radical ($\cdot SO_4^-$), a strong radical with a redox potential of 2.5-3.1 V.[33] Under UV photolysis at 254 nm, the molar absorption coefficients of PDS and PMS are 21.1 and 14, respectively, and the quantum yields are 0.7 and 0.52 under UV/PDS and UV/PMS, respectively, suggesting a slightly greater or comparable radical production efficiency compared to UV/H_2O_2.[47] Photolysis of chlorinated cyanurates forms ▪Cl by Cl-N cleavage.[48] Its molar absorption coefficients are 202-214 $M^{-1}cm^{-1}$ at 254 nm, approximately 3-fold higher than that for HOCl or OCl^-.[35] $k_{\cdot OH}$ of chlorinated cyanurates is $<1.95\times10^9$ $M^{-1}s^{-1}$, around 1 to 2-orders of magnitude lower than that for HOCl or 30% lower than thar for H_2O_2.[48] Based on the greater radical production efficiency and the lower radical scavenging rate, the steady-state radical concentrations from UV photolysis of chlorinated cyanurates are enhanced. However, these oxidants are not utilized in current potable reuse facilities, and thus would increase the costs on modification on existing treatment trains.

2.2.2. Trace organic contaminant removal

The performance of UV-AOP oxidants mentioned above was investigated with respect to the kinetics and removal efficiency of specific trace organic contaminant, but the conclusion drawn from each research is not consistent due to the difference of target

organic contaminants. The performance of H_2O_2, HOCl, and NH_2Cl was compared in terms of 1,4 dioxane, one trace organic contaminant, by Zhang et al,[6] where UV/HOCl performed better than UV/H_2O_2, followed by UV/NH_2Cl. In terms of ipamidol photodegradation, the removal efficiency ranked in descending order of UV/HOCl > UV/H_2O_2 > UV/NH_2Cl > UV/ClO_2.[49] Comparison of UV/H_2O_2, UV/HOCl, and UV/PDS was conducted with eight trace organic contaminants, and the performance followed the order of UV/HOCl > UV/H_2O_2 ≈ UV/PDS.[50] However, UV/H_2O_2 was reported to have higher degradation efficiency for NDMA than the UV/HOCl under the comparable experimental conditions.[7] In another study, the performance of UV/NH_2Cl was comparable to UV/H_2O_2 for degradation of benzoate and carbamazepine.[45] In terms of naphthenic acids and atrazine degradation, UV/PDS performed better than UV/H_2O_2.[47, 51] Therefore, there is a need to assess the performance of the common utilized UV-AOP oxidants considering a greater fraction of trace organic contaminants present in the UV-AOP effluents.

2.2.3. Toxicity

Byproduct-associated additive toxicity was considered to assess the oxidant performance. The byproduct-associated additive toxicity is calculated by a toxicity weighting method, where organic or inorganic contaminant concentrations divided by their individual toxicity indices are summed.[10, 52-53] However, the byproduct-associated toxicity of product water from UV-AOP with various oxidants under same condition was different because of the different byproducts considered. For example, from the same batch experiment, the organic by-product-associated toxicity followed the order of UV/HOCl > UV/NH_2Cl > UV/ClO_2, while the inorganic byproduct-associated toxicity followed the

order of UV/ClO_2 > UV/HOCl > UV/NH_2Cl.[52] Similarly, the fact that the omission or inclusion of certain DBPs over others is equivalent to statistical sampling bias which biases the conclusions was also reported.[53] Therefore, using an approach which can comprehensively assess the risk from a greater fraction of the organic matter present rather than individual DBPs is crucial to evaluate oxidant performance and thus select the best oxidant.

2.3. Control of a Regulated Contaminant: NDMA

N-nitrosodimethylamine (NDMA), a well-documented carcinogen, has been indicated as a key concern for potable reuse treatment systems by National Research Council because its concentrations in the treated wastewater are close to levels of potential human health concern.[3, 9] NDMA is the most commonly detected nitrosamine.[27] In the largest drinking water occurrence study in USA, NDMA was detected in 34% of chloramine plant effluents and 3% of chlorination plant effluents.[54] The regulatory limits, guideline, or notification level of NDMA is in the low ng/L range (3-100 ng/L).[11-15, 31] One obvious approach to control NDMA in the finished water of potable reuse facilities is to destroy or remove the existing NDMA by FAT trains. Nevertheless, mitigating NDMA formation by destroying or removing NDMA precursors is more suitable because NDMA can “rebound” to nearly 10 ng/L at distribution system after complete removal of NDMA itself.[20-21] Therefore, understanding NDMA formation pathways and its precursors is crucial to control NDMA in potable reuse facilities.

2.3.1. Formation mechanisms

Chloramination is the generally accepted mechanism of NDMA formation.[8, 27] Initially, NDMA was proposed to be formed between the reaction NH_2Cl and organic amine precursors.[55] However, the mechanism was revisited by a follow-up research,[17] where dichloramine ($NHCl_2$), coexisting with NH_2Cl (i.e., ~5%) under typical chloramine conditions, was pointed to contribute nearly 100% of NDMA formation. Briefly, unprotonated secondary amines (i.e., dimethylamine) react with $NHCl_2$ forms a chlorinated unsymmetrical dialkylhydrazine intermediate (i.e., Cl-UDMH), which is then oxidized by dissolved oxygen to the corresponding nitrosamine.[8, 17] Because secondary amines are usually at neutral (unprotonated) at high pH, nitrosamine formation increases with pH.[17] Additional studies indicated low pH promotes the conversion of NH_2Cl to $NHCl_2$, ultimately promoting NDMA formation once pH is increased.[56]

Tertiary and quaternary amines are degraded to secondary amines with exposure to chloramines or chlorine, resulting in NDMA formation. [27, 57-59] The NDMA molar yields from secondary and tertiary amines are around 2%, which is one order of magnitude greater than that of quaternary amines (0.2%).[57-58] However, there is one exception for tertiary amines containing β-aromatic rings, from which NDMA yields can reach up to 90%.[60-61]

Updated reaction pathway regarding the contribution of reactive nitrogen species to NDMA formation was reported by Pham et al.[62] In brief, reactive nitrogen species formed during $NHCl_2$ decomposition including nitroxyl/nitroxyl anion and peroxynitrous acid/peroxynitrite anion, which would react with dimethylamine or Cl-UDMH to from NDMA.

2.3.2. NDMA precursors

Many nitrogen-containing organics have been proved to be NDMA precursors according to the formation mechanisms discussed. They includes pharmaceuticals [63-64] and personal care products, [65] herbicides, [66] pesticides, [67] fungicides, [68] amine-based water treatment polymers, [59] and anion exchange resins[69]. Although some NDMA precursors with high yield rates (> 75%) were identified [70], their occurrence in surface water serving as the influent of drinking water treatment plants is low,[71] indicating they only account for a small fraction of the NDMA precursor pool. In addition, NDMA was reported to rebound to nearly 10 ng/L at distribution system after complete removal of NDMA at potable reuse facilities, and the precursors contributing to the reformation remains unkown.[20-21] Thus, identifying specific NDMA precursors that make up the total NDMA precursor pool is not complete.

Efforts were also made to identify the major source of NDMA precursors. One single study simply compared NDMA formation potentials (FPs) of source waters within a watershed, and indicated wastewater effluents were the primary NDMA precursor source.[72] Region-specific relationships between NDMA FPs and sucralose (one anthropogenic pharmaceutical) were developed by Prescott, et al. [73], suggesting that NDMA precursor sources in drinking water intakes are associated with sucralose (i.e., mostly from upstream wastewater inputs). However, surface waters with high NDMA FP and low sucralose concentrations have also been reported.[73] Therefore, the dominant source of NDMA precursors is not yet known.

2.4. Research Gaps

Three research gaps were identified through conducting the literature review:

1) The performance of oxidants utilized in UV-AOPs has not been comprehensively assessed by considering a broad fraction of organic contaminants.
2) The primary NDMA precursors contributing to NDMA rebound during conveyance after potable reuse treatment remain unknown.
3) The dominant source of NDMA precursors present in drinking water intakes is not yet known.

3. COMPARISON OF OXIDANTS USED IN ADVANCED OXIDATION FOR POTABLE REUSE: NON-TARGET ANALYSIS AND BIOASSAYS

Mingrui Song,[1] Elizabeth Mckenna,[1,£] E. Michael Thurman,[2] Imma Ferrer,[2] Lizbeth Taylor-Edmonds,[3] Ronald Hofmann,[3] Kenneth P. Ishida,[4] Shannon L. Roback,[5] Megan H. Plumlee,[4] David Hanigan[1*]

[1]Department of Civil and Environmental Engineering, University of Nevada, Reno, NV 89557-0258

[2]Center for Environmental Mass Spectrometry, University of Colorado, Boulder, Boulder, CO

[3]Department of Civil Engineering, University of Toronto, 35 St. George Street, Toronto, ON M5S 1A4, Canada

[4]Research & Development Department, Orange County Water District, Fountain Valley, CA 92708

[5]Department of Health Science, California State University, Dominguez Hills, Carson, CA 90747

[£] Currently at Corona Environmental Consulting LLC

*Corresponding author: DHanigan@unr.edu

Keywords: monochloramine, free chlorine, hydrogen peroxide, disinfection byproduct, indirect potable reuse, bioassays, nontarget

This manuscript has been submitted to *Environmental Science & Technology: Water* and is currently in review. I contributed ~90% of the original text.

3.1. Abstract

Free chlorine (HOCl) and monochloramine (NH_2Cl) are less-used oxidants than hydrogen peroxide (H_2O_2) in ultraviolet advanced oxidation processes (UV-AOPs) but have garnered interest from the water reuse industry and scientific community because they can be more cost effective than H_2O_2 and provide a protective disinfectant residual. The destruction of organic compounds, creation of UV-AOP byproducts, and change in toxicity during UV-AOP with H_2O_2, HOCl, NH_2Cl, or ambient residual chloramine were evaluated in recycled wastewater by suspect and non-target screening, and bioanalytical tests (bioassays). Ten (10) compounds were identified in reverse osmosis (RO) permeate via suspect screening with removal near 100% by UV/H_2O_2 and UV/HOCl, greater than decomposition by UV/NH_2Cl and UV/ambient (~60%), based on suspect screening mass spectrometry peak area. Non-target analysis based on organic features in mixed-mode cation exchange cartridge extracts indicated UV/H_2O_2 destroyed a similar or slightly greater fraction of organic compounds, formed fewer transformation products, and reduced the summed peak area of non-target features to the greatest extent. Fewer chlorinated byproducts were produced from the RO permeate treated by UV/H_2O_2 than exposure to the chlorine-containing oxidants. Addition of NH_2Cl to RO permeate resulted in a slight increase in the bioassay oxidative stress response but dropped below the response limit for all samples after UV-AOP for all oxidants.

3.2. Introduction

Planned potable reuse has been employed for decades to relieve water scarcity.[74-75] Various treatment trains based on the combinations of ozone, soil aquifer treatment,

biological activated carbon, membranes, and ultraviolet advanced oxidation process (UV-AOP) are designed with the intent to degrade or remove contaminants present in conventional wastewater effluents.[5] Full-advanced treatment (FAT) defined by California State Water Resources Control Board,[4-5] is a common treatment train and consists of ultrafiltration (UF) or microfiltration (MF) followed by reverse osmosis (RO) as a broad-screen physical removal process. An ultraviolet advanced oxidation process (UV-AOP) is then employed to provide disinfection and destruction of remaining organic compounds that are incompletely rejected by RO.

Hydrogen peroxide (H_2O_2) is a commonly added oxidant for UV-AOP because it produces highly reactive hydroxyl radicals when exposed to UV light.[5] Free chlorine (HOCl) is an alternative oxidant that may be coupled with UV that has garnered interest from the water reuse industry and scientific community due to certain practical advantages over H_2O_2: the low cost of sodium hypochlorite and the ability to avoid quenching the H_2O_2 residual in the finished water when removal is required prior to distribution. Another advantage is the on-site availability and familiarity of hypochlorite, since it is often used to form chloramines to control membrane biofouling[76] and disinfect the finished water while providing a protective residual for distribution.[77]

Chloramines for control of biofouling are readily formed when sodium hypochlorite is added to the secondary- or tertiary-treated wastewater effluent containing residual ammonia. Chloramines are poorly rejected by RO,[6] and therefore UV/H_2O_2 is *de facto* UV/H_2O_2/chloramine AOP. Photolysis of monochloramine (NH_2Cl) and dichloramine ($NHCl_2$) produces reactive chlorine, amine, and peroxide radicals which degrade organic

compounds.[41, 78-79] However, during UV-AOP, residual chloramines from upstream treatment also compete with added H_2O_2 or free chlorine for photons and scavenge hydroxyl radicals, decreasing AOP efficiency.[76-77] Nevertheless, because NH_2Cl is already present in the source water, use of supplemental NH_2Cl as a primary UV-AOP oxidant may reduce costs and has therefore received some attention from UV-AOP system operators and scientists.[78]

Certain pharmaceuticals have been shown to be poorly degraded by UV-AOP with H_2O_2, including metformin, cyclophosphamide, and ifosfamide,[80] and incomplete compound elimination during UV-AOP may result in transformation products, which, in some instances, are more toxic than the parent compounds.[81-83] Precursors of *N*-nitrosodimethylamine (NDMA), a carcinogenic disinfection by-product, are only partially removed by UV-AOP and their rejection by RO has been shown to decrease with increasing RO membrane age, increasing the potential for NDMA to form in potable reuse water after FAT.[20, 84] At higher concentrations, these incompletely removed compounds may pose a threat to human health [80, 85] and, even at low concentrations, they diminish social acceptance of the finished water.

Most studies that have investigated the degradation of organic compounds during potable reuse have focused on measuring or detecting preselected "target" organic compounds[48, 78, 86] such as pharmaceuticals and individual DBP precursors. However, unknown and previously unmonitored organic compounds may also be present with the potential to cause unanticipated adverse effects.[87-88] The availability of analytical methods may lead to over-emphasis of the importance of a particular organic compound, including

the benchmarking and ranking of treatment technologies against one another based on their performance for removal of somewhat arbitrary compounds—the proverbial "tail that wags the dog". Thus, improved methods are needed to meaningfully assess water quality and subsequent determination of their potential impact on public health through further studies.

Liquid chromatography (LC) or gas chromatography (GC) coupled to high-resolution mass spectrometry (HRMS) provides simultaneous detection of thousands of compounds, including known and unknown chemicals. is conducted by searching of a chemical database (prior information) for molecular weight, fragmentation pattern, and potential retention time matches to identify contaminants. Non-target analysis (NTA) is a separate method of identifying unknown chemicals by their mass to charge alone, without prior information.[89] Some studies have utilized NTA to investigate the occurrence of organic contaminants at potable reuse facilities.[84, 90-93] However, there are few NTA studies that have sought to investigate the fraction of organic compounds that persist through potable reuse, and thus the composition of these recalcitrant organic compounds is relatively unknown. In addition to chemical analysis, *in vitro* bioassays have been proposed to assess water quality.[94] Bioassays produce dose-response curves, which can be used to benchmark bulk water quality as a compliment to chemical analysis which only detects target compounds or, for NTA, only detects those organic molecules that are measurable by mass spectrometry.[95] Studies using bioassays have emphasized the agonistic and antagonistic effects of mixtures of compounds, including contributions from unidentified organic compounds,[96-99] and these effects are not directly captured by HRMS approaches. Further,

there is currently no consensus which bioassay(s) is an appropriate surrogate for risk to human health.

To determine the relative performance of HOCl, H_2O_2, and NH_2Cl oxidants during UV-AOP, we utilized suspect screening and non-target analysis, and *in vitro* bioassays. These tools were applied to the subset of organic matter recovered from product water of a pilot UV-AOP system operated at the Orange County Water District (OCWD) Groundwater Replenishment System (GWRS) Advanced Water Purification Facility (AWPF) that treated RO permeate from the full-scale plant. The reuse facility is broadly representative of many FAT plants that treat secondary and tertiary wastewater by MF/UF and RO. Our objectives were to (1) determine which suspect compounds are present in the treated wastewater, i.e., RO permeate, and the extent to which they are degraded with various radical forming oxidants during UV-AOP, (2) compare the removal of non-target features based on the type of oxidant and the generation of new UV-AOP byproducts, and (3) assess the changes to bioassay-measured toxicity before and after UV-AOP with various oxidants.

3.3. Materials and Methods

3.3.1. Chemicals and reagents

HPLC-grade solvents (methanol, acetonitrile, and methylene chloride) and ascorbic acid were purchased from Fisher Scientific (Pittsburgh, PA). Hydrogen peroxide (30% w/w), sodium hypochlorite (10–15%), and ammonium hydroxide were purchased from Sigma-Aldrich (St. Louis, MO). Reagent water was either ≥18.2 MΩ-cm (Milli-Q) or HPLC-grade (Fisher Scientific). Two types of solid phase extraction (SPE) cartridges commonly utilized for recovering organics were used to produce isolates: mixed-mode cation exchange (MCX)

6 mL/500 mg for nontarget analysis and hydrophilic-lipophilic balance (HLB) 6 mL/200 mg (Oasis, Waters Corporation, MA) for bioassay analysis. The SPE isolates are representative of subsets of the organic matter pool. In these experiments, the MCX sorbent was selected for mass spectrometry experiments because we previously demonstrated that organic bases, which are a large subset of compounds amenable to positive electrospray ionization (i.e., cations, polar compounds, moderately polar compounds, etc.), are captured and recovered well by MCX resin via cation exchange but not by the HLB resin.[100] Further, MCX resins are "mixed mode" and capture bases in addition to nonpolar compounds and we have previously demonstrated good recovery of compounds which are of broad importance to potable reuse utilities (NDMA precursors).[100] The HLB sorbent was used to capture a broad range of organic compounds and recover extracts for bioassay experiments. An important limitation of the methods is that all extraction methods of organic matter result in potential biases of the conclusion related to the inadvertent fractionation of organic matter (sorbent affinity, ionization efficiency, etc.). Sulfuric acid (Fisher Scientific) was used to adjust sample pH.

3.3.2. Sample collection and extraction

Samples were collected on two occasions (August 2018 and September 2019) from a pilot UV-AOP reactor fed with reverse osmosis permeate (ROP) from the full-scale GWRS AWPF in Fountain Valley, California. The AWPF treats secondary wastewater effluent from the Orange County Sanitation District (OC San) by MF or UF (installed in different, parallel cells), RO, and UV-AOP to produce high purity water for groundwater recharge via spreading (percolation) ponds, mid-basin injection wells, and injection into a coastal

seawater intrusion barrier. Ultimately, this groundwater augmentation is pumped by local water retailers via production wells for drinking water use, i.e., indirect potable reuse.

Sampling locations for ROP, UV feed (UVF), and UV product (UVP) are shown in Figure A-1. The pilot UV system was composed of a 9.7 L stainless steel reactor with a 257 W low-pressure high-output mercury amalgam lamp (Trojan Technologies, London, Ontario, Canada). The flow rate through the reactor was 22.7 L/min (6 gpm) with a residence time in contact with the oxidant (inline mixer injection point to UVF) of ~3 s and UV exposure (between UVF and UVP) of 26 s. The operation of the pilot UV reactor and preparation of oxidant solutions are described in detail in Zhang et al.[6] Working solutions of HOCl, H_2O_2, and NH_2Cl were delivered by peristaltic pump into the ROP through an inline static mixer (Koflo, Cary, IL) to achieve the target dose.

Grab samples (1-L) of the ROP, UVF and UVP were collected in 2018 and 2019 during separate UV-AOP pilot trials. In 2018 UV-AOP pilot trials, either no additional oxidant was added to the ROP, or one of three individual oxidants (HOCl, H_2O_2, or NH_2Cl) were added to the ROP prior to exposure to UV light, producing four sets of UV-AOP samples. We refer to these combinations of oxidants as UV/HOCl, UV/H_2O_2, UV/NH_2Cl, and UV/ambient, where "UV/ambient" refers to UV-AOP with only the residual chloramines in the ROP as the oxidant and "UV/NH_2Cl" refers to supplemental addition of NH_2Cl to the ROP. Residual chloramines for biofouling control are always present in the ROP and therefore also present when supplemental oxidant is added to form the UVF to the reactor. In 2019 UV-AOP pilot trials, only HOCl and H_2O_2 were dosed into the ROP to validate the more promising oxidants from the 2018. A summary of the sample information and

general water quality data is provided in Table A-1. The pH of ROP was 5.8 ± 0.2, which is near the optimal pH for UV/HOCl.[101] Although there are some studies investigating the effect of pH on organic degradation for UV/NH_2Cl, the suggested optimal pH is variable.[102-103] Hence, we made the reasonable and economical (for full-scale design) decision to leave the pH unchanged.

Residual total chlorine (Hach Co., Method 10070) in the grab samples was measured immediately and quenched with a 1.2 molar excess of ascorbic acid. The hydrogen peroxide and residual chloramines were quenched with 100 mg ascorbic acid added to each bottle prior to sample collection. In addition, free chlorine (Hach Co., Method 10241), monochloramine (Hach Co., Method 10171), ammonia (Hach Co., Method 10200), UV transmittance (UVT) at 254 nm, and pH were measured. Samples and field blanks (consisting of a new bottle of Burdick & Jackson LC-MS grade water opened and poured into 1-L sample bottles on site) were immediately shipped on ice to the University of Nevada, Reno (UNR). The field blanks or blanks of Milli-Q water (≥18 MΩ-cm) were extracted to assess potential contamination from reagent water. Samples were extracted at UNR with MCX cartridges by previous established methods[100] and sent to University of Colorado, Boulder (CU) overnight on ice. As is typical in suspect screening and nontarget analysis, a surrogate standard was not added to account for recovery because no individual standard (or even multiple standards) will appropriately account for recovery of the thousands of compounds which were to be measured. Further, it is not possible to know what will be discovered during the analysis, and thus it is not possible to anticipate which surrogate may be appropriate to add. Further details are provided in the Supporting

Information Text A-1. Water parameters including DOC and anions are not provided due to the low concentrations after RO treatment and the difficulty measuring such low concentrations.

Samples collected for bioassays were quenched with a 2.5 molar excess of ascorbic acid and shipped to the University of Toronto. The usage of quenching agents was in accordance with standard procedures for each individual lab. SPE was conducted on duplicate aliquots with 200 mg HLB cartridges. Two liters of acidified sample (pH 2) were loaded on the cartridge, eluted with 10 mL of acetone, and evaporated under a gentle ultra-high purity nitrogen stream. Samples were reconstituted in 60 μL dimethyl sulfoxide for subsequent cellular testing. Detailed procedures can be found in Zheng et al.[104] For comparison of bioanalytical activity to a typical finished drinking water, Otonobee River water was collected after coagulation, flocculation, and filtration from a conventional drinking water treatment plant and subjected to bench chlorination (5 mg/L as Cl_2 for 24 hr at room temperature). The chlorine dose mimicked the upper limit disinfection dose of the full-scale plant. Chlorine was quenched after 24 hr with ascorbic acid and the samples were extracted.

3.3.3. Instrumental analysis

Extracts from MCX cartridges were analyzed by an LC system consisting of a vacuum degasser, thermostatted autosampler, column compartment, and binary pump (Agilent Series 1290, Agilent Technologies, Santa Clara, CA, USA) coupled to an Agilent 6545 ultra-high definition quadrupole time-of-flight mass spectrometer (qTOF/MS, Agilent Technologies, Santa Clara, CA, USA) with electrospray Jet Stream Technology. Isolates

were diluted 10-fold into Milli-Q water prior to injection to facilitate chromatographic separation by a reversed-phase C8 analytical column (150 mm × 4.6 mm) with 3.5 µm particle size (Zorbax Eclipse XDB-C8). For quality assurance and control, stability of mass accuracy was checked daily and if values were above 2 ppm error, the instrument was re-calibrated. Further details regarding operation parameters and mass stability check are provided in the Supporting Information Text A-1.

3.3.4. Data analysis

Mass Hunter software was initially utilized to conduct suspect screening with LC-qTOF/MS data. Suspect screening was conducted by matching the retention time, accurate mass, fragmentation pattern, and the isotope abundance ratios to two in-house databases at CU; one containing over 100 pharmaceuticals and pesticides, and another containing approximately 60 known *N*-nitrosamine precursors. In prior experiments with this instrument, molecular features with high scores (> 80, full score 100) were nearly always a correct hit. Matches with a score of <80 were disregarded.

Raw data files were converted into a centroided mzML format by MSConvert software (ProetoWizard, Palo Alto, CA). Processing non-target features included construction of extracted ion chromatograms (EIC) and peak detection performed by the automated data analysis pipeline within MZmine 2.[105] Other non-target feature processing such as grouping and retention time algorithms were conducted using methods described by Verkh et al.[106] Preprocessing parameters of peak detection, EIC building, and peak picking for all data files is summarized in Table A-2. Only features (i.e., unique peaks) present in samples with peak area at least three times greater than those present in the field and Milli-Q blanks

are reported. Summed peak area of the non-target features was obtained by summing the peak area of all qualified features in the sample.

Molecular formulae were assigned by MZmine 2.[107] The ionization type was $[M+H]^+$ with a charge of +1, and the mass tolerance was 0.005 *m/z*. The possible ranges of each element in formulae were: $C_{1\text{-}80}$, $H_{1\text{-}100}$, $O_{1\text{-}30}$, $N_{0\text{-}3}$, $S_{0\text{-}2}$, $Cl_{0\text{-}4}$. Element count heuristics and ring double bond equivalent restrictions of 0–40 were applied during formula prediction. All results were exported to csv format by MZmine 2. Blank subtraction was performed in R Studio.[108]

3.3.5. Bioassays

Bioassays (Table A-3) were selected to provide a broad-spectrum screening of various adaptive stress response pathways that are relevant to drinking water treatment including general cellular stress (p53), oxidative stress (ARE-Nrf2), and genotoxicity (SOS Chromotest™). Cytotoxicity was measured by conversion of dye-based cytotoxicity assay (MTT); the detailed procedure is presented in Sun et al.[109] The human cell-based ARE-Nrf2 assay targets the activation of the oxidative stress response pathway. Detailed methods are described by Sun et al.[109] Activation of the DNA repair pathway mediated by the SOS-response pathway was performed to measure DNA damage, using the SOS-Chromotest™ (EBPI Inc) assay. Detailed methods are described in Zheng et al.[104] p53 activation was also assayed as this pathway is a sensitive indicator for chemicals with genotoxic properties. Methods are described in Sun et al.[109]

For the luciferase reporter assays fused to ARE-Nrf2 and p53 response element operons, activation of the protectives pathways is expressed as an induction ratio (IR) of treated cells

compared to control, where an IR ≥ 1.5 was considered a positive response. For positive samples, effect concentrations (EC) for IRs of 1.5 were derived from the linear slopes of the dose-response curves, where the concentrations correspond to the relative enrichment factor.[110] Thus, $EC_{IR1.5}$ corresponds to how many times the sample must be concentrated or diluted to elicit an IR of 1.5. Further details are presented in Escher et al.[110] The results are expressed as $1/EC_{IR1.5}$ and referred to as Toxicity Units (TU); a higher TU represents a greater toxic effect. The bioassay limit of detection (LOD) is 0.018 TU.

Similarly, the SOS-Chromotest™ response was determined as the induction ratio of the ß-galactosidase (ß-gal) reporter gene fused to the bacterial SOS operon. In addition, general protein synthesis was measured and corrected for using the photometric quantification of alkaline phosphatase (AP). The induction of ß-gal is indicative of the DNA damage and was expressed as the ratio of ß-gal activity to AP activity, which is referred to as the induction factor (IF). An IF ≥ 1.5 was considered positive in the genotoxicity assay. For cytotoxicity, samples with cell viability greater than 80% were considered for toxicity bioassay assessment.

3.4. Results and Discussion

3.4.1. Suspect compounds

Across 28 water samples spanning the full treatment train (ROP, UVF, and UVP) over two sampling events, and including 4 field blanks, a total of 10 compounds were identified via suspect screening from a mass spectrometry library of over 160 compounds (Table A-4). The compounds of the in-house library are provided in previous work by our team.[84, 111-113] Six of the 10 compounds were detected in samples from both 2018 and 2019:

benzotriazole and two methylated benzotriazoles (anti-corrosion agents), atenolol and metoprolol (blood pressure medications), and lamotrigine (anti-seizure medication). Three compounds were identified only in samples from 2018: phthalic acid (plasticizer), and thiabendazole and carbendazim (fungicide). Sucralose (artificial sweetener) was only identified in samples from 2019.

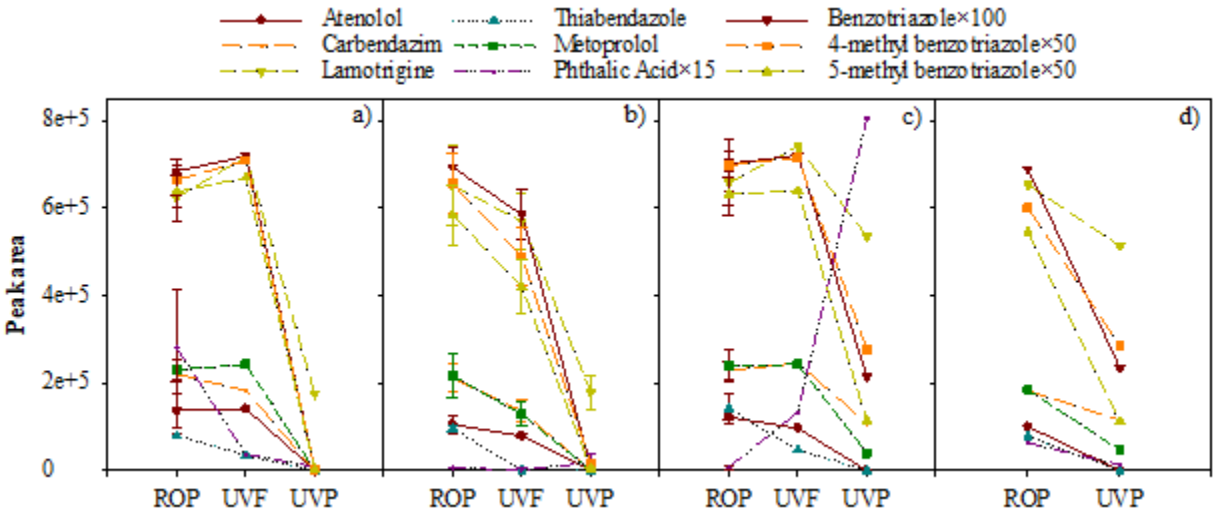

Figure 3-1. Peak area of suspect compounds in MCX extracts of samples from 2018 ROP, UVF, and UVP treated by a) UV/HOCl, b) UV/H_2O_2, c) UV/NH_2Cl, and d) UV/ambient.

The peak areas of suspect compounds that were present in the ROP, UVF, and UVP samples under varying oxidant conditions are shown in Figure 3-1 for the 2018 UV-AOP pilot sampling event. Although peak area is subject to ionization matrix effects (and no surrogates were added to the samples prior to extraction to correct for this) and is thus comparisons between samples are only semi-quantitative, we have previously shown that the matrix effects are minimal in similar extracts as salts are removed during the MCX extraction and most organic matter is removed by the RO membranes.[84] As is typical in

suspect screening and nontarget analysis, a surrogate standard was not added to account for recovery because no individual standard (or even multiple standards) will appropriately account for recovery of the thousands of compounds which were to be measured. Further, it is not possible to know what will be discovered during the analysis, and thus it is not possible to anticipate which surrogate may be appropriate to add. Trends from 2018 were similar to 2019 (Figure A-2), except that fewer suspect compounds were detected in 2019. Rapid oxidation by H_2O_2 prior to exposure to UV light was somewhat greater than other oxidants. After ~3 s exposure to 2.9 mg/L H_2O_2 (2018) and 2.8 mg/L (2019), the summed peak area of the suspect compounds in ROP dropped 21% and 8%, respectively, while less than a 2% reduction in summed peak area (Table A-5) was observed by exposure to 2.0 mg/L HOCl (2018), 2.3 mg/L (2019) HOCl, and 2.2 mg/L NH_2Cl (2018). These oxidant doses represent likely concentrations used in water reuse plants with UV-AOP.

For UV/HOCl and UV/NH_2Cl, the peak areas of atenolol, lamotrigine, metoprolol, benzotriazole, and two methylated benzotriazoles detected in ROP were unchanged by exposure to HOCl and NH_2Cl, indicating that these compounds were recalcitrant to rapid oxidation by low concentrations of these oxidants (Figure 3-1a, 3-1c, and Figure A-2a). This trend was consistent with the results of similar studies, where atenolol, metoprolol, and benzotriazole were poorly degraded by chlorination.[114-116]

For the 2018 sampling event, the summed peak area of all suspect compounds recovered from ROP was reduced 99%, 98%, 66%, and 61% by UV/HOCl, UV/H_2O_2, UV/ambient, and UV/NH_2Cl, respectively (Table A-5). The percent reduction of the summed peak areas for both UV/HOCl and UV/H_2O_2 were similar for the 2019 sampling event (Figure A-2).

Other studies have also reported that degradation of the relatively recalcitrant organic compounds 1,4-dioxane and iopamidol by UV/HOCl and UV/H_2O_2 is greater than UV/NH_2Cl.[6, 49] Notably, the peak area of phthalic acid increased ~5× across the UV/H_2O_2 (Figure 3-1b) and UV/NH_2Cl (Figure 3-1c). Because the peak area of phthalic acid was small in UVF samples, which are taken after oxidant addition, the phthalic acid was not from the oxidant solutions. It was likely produced via the oxidation or photolysis of phthalates[117] and this phenomenon highlights that some compounds are not removed completely but are transformed to new oxidation products. Overall, UV/HOCl and UV/H_2O_2 were the most effective in terms of removal of these suspect compounds over the two sampling events, and this agrees with the literature for difficult-to-degrade organic compounds.

3.4.2. Production and persistence of nontarget features

Non-target analysis was only conducted on samples processed from the 2018 event because the travel blank during 2019 was lost during shipment, making the necessary blank subtraction impossible. Bar plots of the number and summed peak areas of the non-target features from the ROP, UVF, and UVP samples are shown in Figure 3-2. UV/ambient conditions are only represented by ROP and UVP samples as no supplemental oxidant was added to the ROP prior to UV exposure. Samples were extracted with Oasis MCX cartridges and the data is therefore representative of a large subset of the organic matter pool that is amenable to cation exchange and positive electrospray ionization (cations, polar compounds, moderately polar compounds, etc).[100, 118]

The total number of non-target features (i.e., unique peaks measured by mass spectrometry) in the feed water (ROP) ranged from 3114 to 7203. ROP samples before UV/H_2O_2 and UV/NH_2Cl were comparable (~3200) and less than UV/HOCl and UV/ambient, ~4100 and ~7200, respectively. Although the number of non-target features varied, the summed peak areas in the ROP before UV/HOCl, UV/H_2O_2, and UV/NH_2Cl were comparable ($4.6–5.5\times10^8$), although the UV/ambient was 2–2.5 times greater in total peak area (1.13×10^9). Variability in the number and peak area of features detected in the ROP samples is attributable to the natural variation in wastewater chemistry throughout the day in which the experiments were conducted. Thus, it is important to consider both the raw number (i.e., count) of features, their summed peak areas, and their percent removal/formation across the treatment train.

Across all oxidants, the number of non-target features in the UVF (ROP + oxidant, prior to UV exposure) was similar or greater than in the ROP, suggesting formation of decomposition products by reactions with the oxidant. For example, for the UV/H_2O_2 treatment, there were 3246 non-target features present in the ROP sample (Figure 3-2a). Comparing the features in the sample after contact with H_2O_2, we find that 48% increase (yellow plus green) in unique features compared to the ROP sample (i.e., products of oxidation products). For HOCl and NH_2Cl, the number of features in the UVF which were not present in the ROP sample was 67% increase and nearly 100% increase, respectively. In terms of the summed peak area of all features, after NH_2Cl oxidation the area increased by 62% (from 4.6×10^8 to 7.5×10^8), but was comparable ($\leq$ 2% difference) for HOCl and H_2O_2 (Figure 3-2b). It is not clear why the number of nontarget features increased but the

summed peak area did not, but this may reflect that the number of compounds changed but the total mass of organic material did not change substantially, and/or that the formation products from HOCl and H_2O_2 are compounds which ionize poorly, reflecting the semi-quantitative nature of this approach.

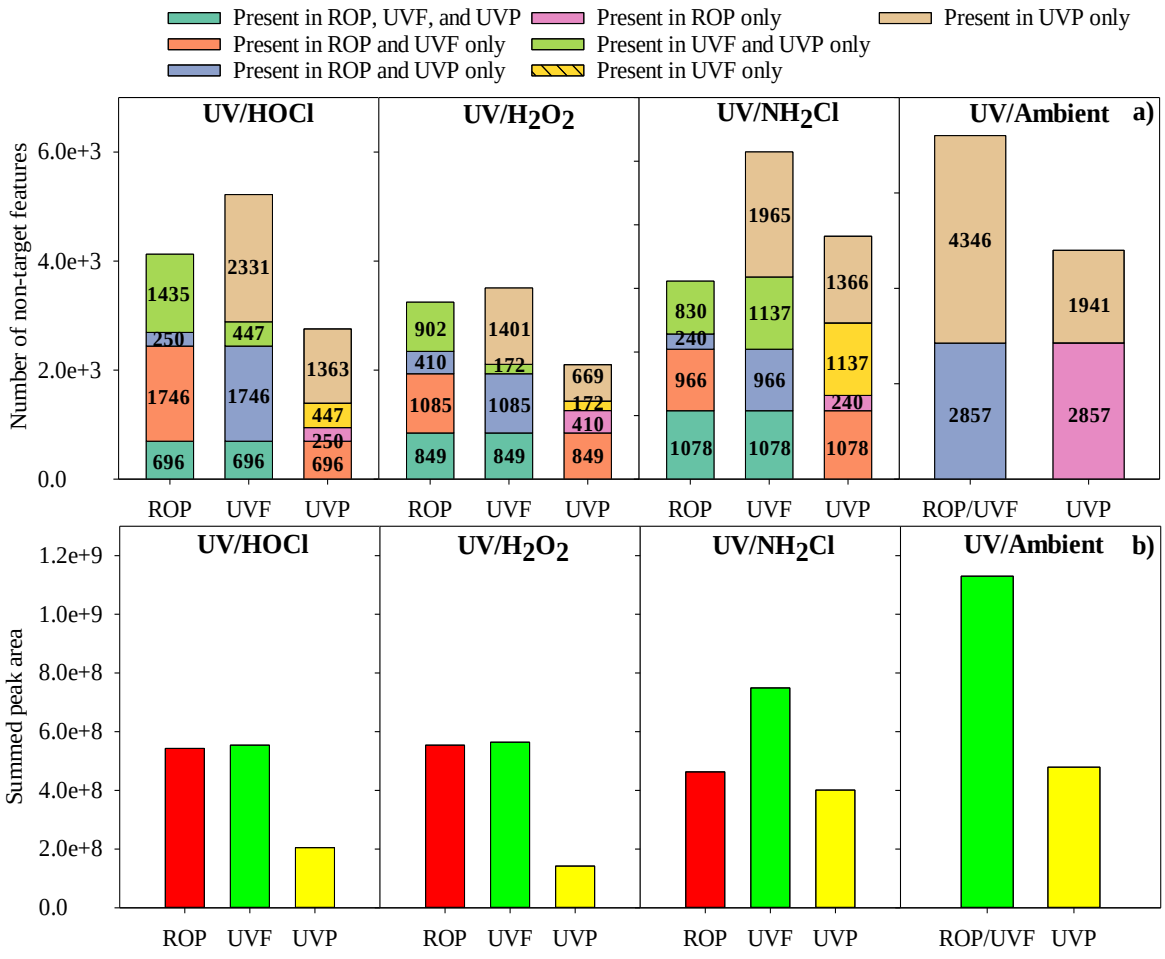

Figure 3-2. Plots of a) number and b) summed peak area of all non-target features across the pilot-scale UV-AOP in 2018.

Notably, a substantial portion of the features present in the ROP samples persisted after supplemental oxidant was applied (see Figure 3-2, dark green plus orange). A total of 2442 (59%) features were still detected in the UVF after HOCl addition, and 1934 (60%) and 2044 (66%) of features were still detectable after H_2O_2 and NH_2Cl exposure, respectively. Therefore, based on feature (i.e., compound) count, brief exposure to HOCl and H_2O_2 oxidation resulted in decomposition of a comparable fraction of non-target features, and H_2O_2 oxidation resulted in the least number/fraction of transformation products (albeit noting the fewer number of features in the ROF at that time for H_2O_2), followed by HOCl and NH_2Cl. In terms of summed peak area of non-target features, NH_2Cl oxidation increased the peak area the most (62%), followed by HOCl and H_2O_2 ($\leq$ 2%).

After UV-AOP (from UVF to UVP), there was a reduction in the number of features regardless of the supplemented oxidant. The total number of non-target features in the UVF samples ranged from 3507–5220, which was reduced to 2100–3821 in the UVP (Figure 3-2a). There were 1143, 1021, and 2215 non-target features that persisted from UVF to UVP under UV-AOP conditions when HOCl, H_2O_2, and NH_2Cl were added, respectively, and 2857 when no oxidant was added (ambient residual chloramines), accounting for 22%, 29%, 43%, and 40% of features in the corresponding UVF samples that were not completely removed by the UV-AOP. Stated differently, UV-AOP with HOCl, H_2O_2, NH_2Cl, and ambient NH_2Cl removed/decomposed 78%, 71%, 57%, and 60% of features from the UVF, respectively. The summed peak area from UVF to UVP of non-target features was reduced 63%, 75%, 46%, and 58% by UV/HOCl, UV/H_2O_2, UV/NH_2Cl, and UV/ambient, respectively. This suggests that UV-AOP with H_2O_2 or HOCl perform

comparably (i.e., in this study, feature count was reduced to a greater extent by HOCl, but more summed peak area was removed by H_2O_2), and better than residual chloramine or supplemental NH_2Cl.

UV-AOP transformation products (new non-target features in the UVP, which were not present in UVF) were also evaluated. There were 1613, 1079, 1606 newly formed non-target features after UV/HOCl, UV/H_2O_2, UV/NH_2Cl, equivalent to ~31% new features regardless of which oxidant was added. UV/ambient formed 1941 new features, or 27% new features. Note that UV/ambient formed the greatest number of UV-AOP transformation products but the corresponding fractional increase in new features was the lowest of the four scenarios. This was likely caused by the greater number of non-target features in the corresponding UVF sample and demonstrates that percent changes are somewhat affected by the water quality of UVF samples.

In terms of the overall reduction of the total count of non-target features across the pilot system from ROP to UVP, UV/HOCl, UV/H_2O_2, and UV/ambient performed similarly; the total number of non-target features was reduced 33%, 35%, and 33% by UV/H_2O_2, UV/HOCl, and UV/ambient, respectively (Figure 3-2). The equivalent performance of UV/ambient compared to the added oxidants H_2O_2 and HOCl is initially surprising. However, this is due to the net increase in feature count from ROP to UVF for H_2O_2 and HOCl. In other words, the use of strong oxidants appears to create (transform) additional detectable compounds, of which, the majority are subsequently destroyed by UV-AOP (89% for H_2O_2 and 84% for HOCl per Figure 3-2). In the case of UV/NH_2Cl, the total number of non-target features in the UVP sample was greater than that in the ROP sample, indicating

worse performance of UV/NH_2Cl in terms of overall reduction of non-target features counts (Figure 3-2a).

In terms of the summed peak area of non-target features from ROP to UVP, 62%, 74%, 13%, and 58% of the summed peak area was reduced by UV/HOCl, UV/H_2O_2, UV/NH_2Cl, and UV/ambient, respectively (Figure 3-2b). Compared to the trend from non-target features counts, where UV/HOCl and UV/H_2O_2 performed similarly, the total peak area removal observations suggest that UV/H_2O_2 reduced non-target feature counts to a greater extent.

Transformation products formed across the pilot system (non-target features in UVP which were not present in ROP were also investigated (tan plus bright green in Figure 3-2a). There were 1810, 841, 2503, and 1941 non-target features formed across the pilot system with UV/HOCl, UV/H_2O_2, UV/NH_2Cl, and UV/ambient, respectively. 44%, 26%, 80%, and 27% new products were formed when compared to the corresponding ROP samples, suggesting UV/H_2O_2 generated the least new products, relative to the initial feed water.

In summary, samples were taken at three different points in the treatment train (prior to oxidant addition, after oxidant addition, and after UV-AOP) and UV/H_2O_2 was the most favorable AOP with respect to the number of non-target features and their summed peak areas. UV/H_2O_2 formed the least new transformation products upon oxidant addition based on number and percent formation (i.e., UVF compared to ROP) and had greater or similar performance to other oxidants with respect to non-target features removed and formed

during UV-AOP (i.e., UVP compared to ROP or UVF). UV/H_2O_2 also reduced the summed peak area to the greatest extent across the full treatment train.

3.4.3. Element composition of assigned organic compounds

Molecular formulae were assigned by MZmine 2 based on elemental compositions that result in the measured accurate mass. Molecular formulae were assignable to 84%, 87%, 84%, and 72% of the non-target features in MCX extracts of samples collected in 2018 under UV/HOCl, UV/H_2O_2, UV/NH_2Cl, and UV/ambient conditions, respectively (Figure A-3). Features for which no formulae were assigned are likely those which have elemental ratios outside of the assigned tolerances. The number of formulae across five classifications based on heteroatoms, including Cl-containing compounds, is depicted in Figure A-4. Compounds containing only CHO or CHON were the most abundant of those classified, similar to other studies of organic matter occurring in drinking water and wastewater.[119-121] The transformations of organic compounds across ROP to UVP are depicted as van Krevelen diagrams in Figure 3-3. In terms of the non-target features where formulae were assigned, UV/HOCl, UV/H_2O_2, and UV/ambient had similar removal (30–33%, the grey circle and cross) but UV/NH_2Cl increased the number of compounds with assigned formulae by 35%. This may be an artifact of the ~30% of the features that were not assigned a formula in the UV/ambient sample.

Of the degraded compounds across all oxidation conditions, olefins were decomposed to the greatest extent, likely due to the greater reactivity of unsaturated bonds, while aromatics tended to be decomposed the least (Figure A-5a). Cl-containing compounds tended to be mostly aliphatic (over 44% over all treatments), followed by condensed

aromatics (from 31–46%). There were 90, 77, 48, and 111 Cl-containing compounds decomposed by UV/HOCl, UV/H_2O_2, UV/NH_2Cl, and UV/ambient, accounting for 66%, 68%, 41%, and 43% Cl-containing compounds in the corresponding ROP samples. In the terms of summed peak area of Cl-containing compounds, UV/H_2O_2 reduced the summed peak area to the greatest extent (74%), followed by UV/HOCl (46%) and UV/ambient (38%). The summed peak area increased when NH_2Cl was added as an oxidant due to increased Cl substitution (Figure A-6). UV/H_2O_2 produced the fewest number (52) of Cl-containing compounds in the UVP overall (however, noting that the ROP at that time featured overall smaller feature count), followed by UV/HOCl (86), UV/NH_2Cl (136), and UV/ambient (192). Together, these findings are highly relevant as Cl-containing compounds are thought to be responsible for a significant portion of the total toxic burden of disinfected waters, particularly when iodine concentrations are low.[122]

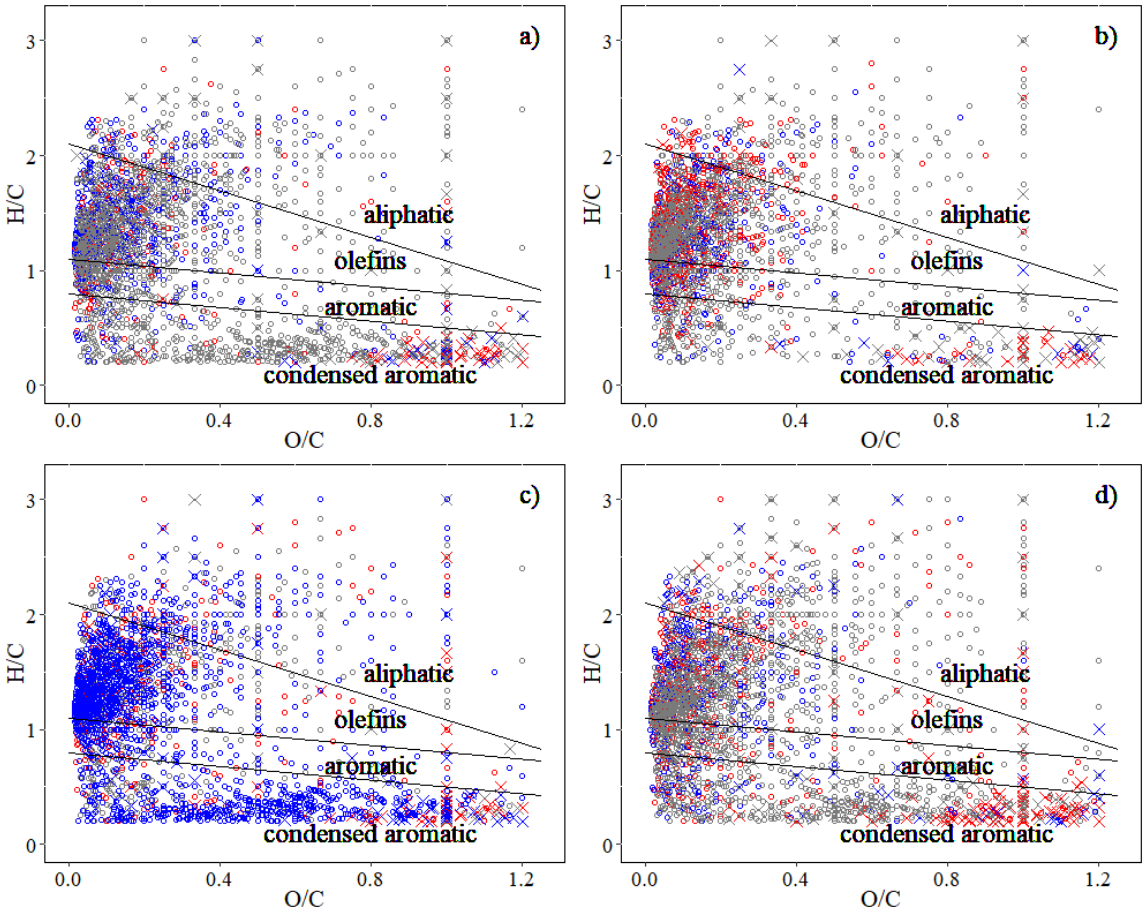

Figure 3-3. Van Krevelen diagrams of molecular formulae identified by LC-qTOF/MS during sampling conducted in 2018: a) UV/HOCl, b) UV/H_2O_2, c) UV/NH_2Cl, and d) UV/ambient. Red indicates persistent compounds (found in both ROP and UVP), blue indicates newly formed compounds (found in UVP but not in ROP), and gray indicates decomposed compounds (found in ROP but not in UVP). Circles indicate compounds without Cl and crosses indicate Cl-containing compounds. Cl-containing compounds include any combination of C, H, N, O, or S, and at least one Cl. The stoichiometric ranges used to establish the category boundaries are described in the Supporting Information.[123-124]

The molecular composition of transformation products (i.e., those features present in UVP, but not in ROP) was also evaluated. Similar to the conclusion regarding decomposed compounds, UV/H_2O_2 generated the least fraction of transformation products (40% in UVP), nearly the same as the fraction generated when there was no supplemental oxidant

(UV/ambient, 41%), compared to UV/NH_2Cl (~66%) and UV/HOCl (~70%). Of the transformation products, olefins were the largest group across all oxidant conditions (Figure A-5b). UV/HOCl and UV/H_2O_2 formed the least condensed aromatics, but aromatics were formed the least with UV/NH_2Cl and UV/ambient. Cl-containing transformation products tended to be condensed aromatics, followed by aliphatics. Similar to decomposed formulae, the least Cl-containing compounds were formed when H_2O_2 was the oxidant (13% increase in Cl-containing compounds compared to UVP from ROP), followed by UV/ambient (18%), UV/HOCl (28%), and UV/NH_2Cl (59%). Overall, UV/H_2O_2 formed the least Cl-containing transformation products and decomposed the greatest Cl-containing compounds present in the feed water to the UV-AOP.

3.4.4. Bioassays

Bioassays have been proposed for use in tandem with non-target analysis as an approach to assess potable reuse water quality once both methods become more standardized for water facility use.[125] A suite of bioassays (MTT, p53, SOS Chromotest™, and ARE- Nrf2 assay, see Table S3 for details) were used to assess water quality before and after UV-AOP. HLB was used intentionally, rather than MCX used for NTA analysis, in an attempt to independently validate the conclusions from NTA. Finished drinking water from a conventional drinking water treatment plant was also assayed and is presented for comparison. The MTT, p53, and SOS Chromotest™ assays did not elicit a toxicological response for any extract, indicating the concentrations of toxic compounds was low in the HLB extracts. Further, concentration of the extracts tends to lead to precipitation of organic matter and thus no further experimentation with these assays was conducted.

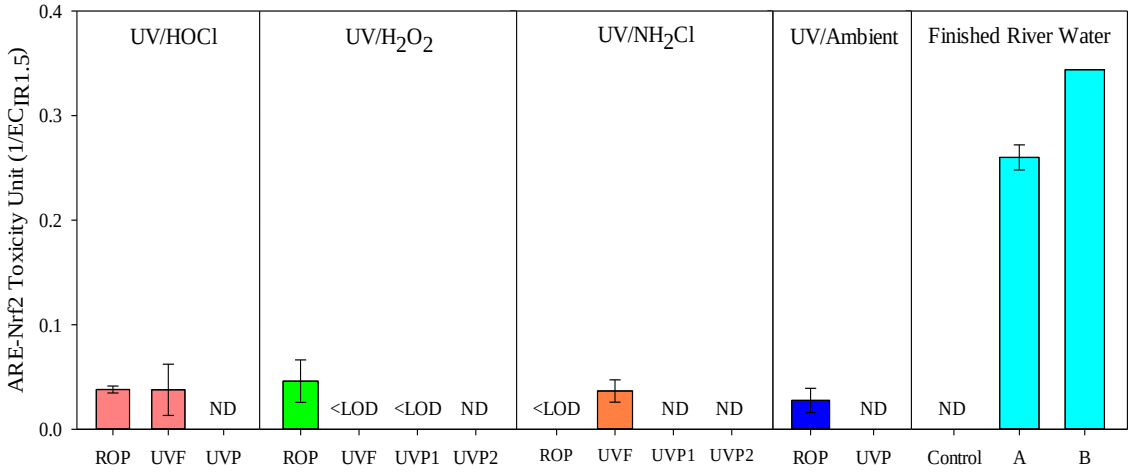

Figure 3-4. Oxidative stress response (ARE-Nrf2) of samples collected in 2018. Finished river water from a conventional drinking water plant (A) is presented alongside finished river water from Australia (B).[94] UVP1 and UVP2 indicates 0-day-hold UVP and 5-day-hold UVP, respectively.

Extracts that elicited a response in the ARE-Nrf2 assay (the human cell-based assay targeting the activation of the oxidative stress response pathway) are presented in Figure 3-4 as unitless toxicity units ($1/EC_{IR1.5}$). Based on the lack of response in the p53 and SOS bioassays, extracts that elicited an oxidative stress response via the ARE-NRf2 assay did not have a significant impact on DNA. Three of the four ROP extracts elicited a response in the oxidative stress pathway (0.046, 0.038 and 0.028 TU). Based on comparison of ROP and UVF (i.e., after oxidant addition before UV treatment), for UV/H_2O_2, the application of H_2O_2 attenuated the toxic response (0.046 TU to <LOD). For UV/HOCl, the response was comparable after HOCl addition (~ 0.038 TU). For UV/NH_2Cl, the ROP that was initially non-reactive but increased to detectable levels in the ARE-Nrf2 bioassay upon monochloramine addition (<LOD to 0.037 TU).

In all treatment scenarios, application of UV with any oxidant attenuated the oxidative stress response (Figure 3-4). This suggests that UV-AOP is effective at decomposing potentially-toxic compounds that may be produced by oxidants during oxidant addition prior to UV and agrees well with the other findings in this study suggesting that the oxidant addition prior to UV-AOP may create additional transformation products which are then decomposed during UV-AOP.

Filter effluent grab samples of river water treated with conventional treatment were disinfected in the laboratory by spiking with chlorine at a concentration mimicking the upper limit disinfection doses at full-scale (5 mg Cl_2/L, quenched after 24 hr) and then were used for comparison. The ARE-Nrf2 assay again had a positive response (0.26 TU) which agreed with literature values for conventionally treated surface waters in Australia (0.344 TU[94]). Other assays did not elicit a response. Notably, the highest RO permeate responses (0.046 TU) in the present study are 86% less reactive than finished treated "conventional" river waters from Australia. Many reporter gene assays are very sensitive and can detect an effect in clean water samples, including highly treated drinking water and bottled water [126-127]. Therefore, a response in an assay does not mean that the water quality is necessarily unacceptable, but the responses can be compared to literature values for qualitative comparison.

3.5. Conclusions

Oxidants outside of traditional H_2O_2 have recently been proposed as effective alternatives during UV-AOP. The performance of four different oxidant scenarios in terms of organic compound removal, organic compound production (transformation products),

and bioassay-indicated toxicity were investigated in extracts produced from a UV-AOP pilot system at the Orange County Water District Advanced Water Purification Facility. Based on the results:

- Suspect compounds recovered by MCX cartridges from RO permeate that matched an in-house LC-qTOF/MS library were degraded more efficiently by UV/HOCl and UV/H_2O_2 compared to UV/NH_2Cl and UV/ambient chloramines.
- Based on the compounds present in MCX extracts and ionizable in ESI+ mode, as measured by non-target analysis, UV/H_2O_2 appears to be the most favorable AOP since it formed the least number and percentage of new transformation products in the UV feed water upon oxidant addition to the RO permeate (i.e., before UV exposure), had better or similar performance to other AOPs with respect to non-target features removed/formed across UV-AOP, and reduced the summed peak area the greatest extent across the treatment train.
- Olefins were decomposed to the greatest extent, and aromatics were decomposed the most poorly. UV/H_2O_2 formed the least Cl-containing transformation products and decomposed the greatest fraction of Cl-containing compounds.
- UV-AOP with any of the studied oxidants (HOCl, H_2O_2, and NH_2Cl) produced water with lower oxidative stress response (ARE-Nrf2) than conventionally treated drinking water (river water). The oxidative stress response in pre-AOP samples was mitigated to below the assay response limit after UV-AOP. Samples which were positive in the ARE-Nrf2 assay did not elicit a response in

four other assays measuring genetic stress or repair, indicating that the oxidative stress did not significantly impact the genetic material or induce cell death.

- Recognizing that feed water quality varies, reproduction of these results in additional experiments will advance the comparative assessment of oxidants used during AOP.
- It is important to consider these conclusions with recognition that extraction of organic matter results in the potential for biased conclusions as no sorbent perfectly extracts all organic matter present. The non-target results presented here are biased towards organic bases (cation exchange extraction) because organic bases ionize well during electrospray positive. Further experimentation examining organic acids and neutrals should be conducted to improve our understanding of how these treatment methods affect the organic matter pool.

3.6. Acknowledgments

This research was supported by the National Science Foundation under Grant No. 1804255, the Water Research Foundation (Project #5005, managed by Djanette Khiari and Katie Spahr) and the United States Bureau of Reclamation Desalination and Water Purification Research Program.[128]

4. CONTRIBUTION OF DIMETHYLAMINE TO N-NITROSODIMETHYLAMINE FORMATION AT REVERSE OSMOSIS WATER RECLAMATION FACILITIES

Mingrui Song,[1] Shannon L. Roback,[2] Kenneth P. Ishida,[3] Junli Wang,[1] Megan H. Plumlee,[3] David Hanigan[1*]

[1]Department of Civil and Environmental Engineering, University of Nevada, Reno, NV 89557-0258

[2]Department of Health Science, California State University, Dominguez Hills, Carson, CA 90747

[3]Orange County Water District, Fountain Valley, CA 92708

*Corresponding author: DHanigan@unr.edu

Keywords: NDMA, precursor, disinfection byproduct, wastewater reclamation, potable reuse.

This manuscript has been published on *Environmental Science and Technology: Letters* and is currently in review. I contributed ~90% of the original text and conducted all experiments.

4.1. Abstract

N-nitrosodimethylamine (NDMA) is a disinfection byproduct formed from reactions between dichloramine and nitrogenous precursors. At water reuse facilities with reverse osmosis (RO) and ultraviolet-advanced oxidation processes (UV-AOP), NDMA is typically reduced to <2 ng/L. However, in some cases, NDMA "rebounds" to low ng/L concentrations during conveyance. The precursors evading RO and UV-AOP are currently unknown. Dimethylamine (DMA) does not substantially contribute to the NDMA precursor pool in treated wastewater or surface water, but DMA occurrence in reuse facilities has not been evaluated. We measured DMA and its chlorinated analogue (CDMA) in four full-scale water reclamation facilities utilizing RO and UV-AOP, and one at pilot-scale. The median sum of DMA and CDMA concentration in UV-AOP product and finished waters was 0.4 µg/L across six sampling events. At one reclamation facility sampled three times over one year, finished water DMA/CDMA ranged from 0.4 to 1.4 µg/L. DMA/CDMA accounted for 5%-43% of the total NDMA precursor pool of the UV-AOP product water at one facility, and up to ~40 of ng/L of NDMA. These findings enable treatment strategies which will result in reduced NDMA formation, thereby strengthen the future of potable reuse.

4.2. Introduction

Drought has rapidly decreased the availability of conventional water sources driving the urgent need for planned potable water reuse. Full advanced treatment (FAT) is utilized at wastewater reclamation facilities to produce potable water for reuse. FAT consists of secondary or tertiary wastewater treatment followed by microfiltration (MF) or

ultrafiltration (UF), reverse osmosis (RO) and an advanced oxidation process (AOP). The most commonly utilized AOP is ultraviolet-advanced oxidation process (UV-AOP) with hydrogen peroxide (UV/H_2O_2) or chlorine (UV/HOCl). *N*-nitrosodimethylamine (NDMA) currently stands as a barrier to many potable reuse projects because the concentrations at which it tends to occur in the treated water for reuse are similar or greater to regulatory values (e.g., 10 ng/L California Notification Level).[3, 9, 129]. It is a carcinogenic disinfection by-product[9] formed by reactions between dichloramine and nitrogenous precursors.[16-17, 130] Chloramines, including dichloramine, are formed upstream of membrane processes via addition of chlorine for biofouling control, which reacts with residual ammonia to form chloramines. Massachusetts, Canada, Australia, and World Health Organization have established guidelines for NDMA in drinking water.[12-15] California has a public health goal of 3 ng/L for NDMA[31] and has currently set the drinking water notification level (NL) to 10 ng/L.[11] Exceeding this NL in potable waters triggers increased monitoring and corrective actions.[129]

NDMA is poorly removed by RO with reported rejections between 14–78%.[18, 131-132] However, it is effectively destroyed by ultraviolet (UV) light during UV-AOP.[19] Although NDMA concentrations are reduced to below the detection limit (<2 ng/L) by UV-AOP, NDMA can "rebound" to low ng/L concentrations (~2 to 10 ng/L) during conveyance.[20-21] Past studies have shown that NDMA formation is promoted as a result of the reduction in pH (~5.5) that occurs across RO treatment.[56, 130] Consequently, an approach to rapidly shift to a more basic pH after RO has been proposed to reduce the formation of NDMA,[56] but a follow-up study found that increasing the pH to ~8.5 via the addition of lime decreased the

NDMA destruction from 90% to 64% by UV/H_2O_2 due to the lower NDMA quantum yield at higher pH.[133] Another approach is to mitigate NDMA formation in the finished water by removing or destroying the precursors prior to distribution. However, the identity of precursors is not yet known.

Dimethylamine (DMA) is one of the most studied model NDMA precursors despite prior studies demonstrating that DMA is not a predominant precursor in secondary municipal wastewater[134] or surface water.[135] However, DMA is present in wastewater at up to µg/L concentrations,[134, 136] and if only 0.6 µg/L DMA were to pass the RO membranes and UV-AOP, the resulting NDMA formation could be as high as 10 ng/L NDMA assuming a 1% molar yield.[17, 137-139] Such formation is meaningful in terms of potable reuse because 10 ng/L NDMA is near or above many regulatory guidelines. While DMA rejection by pristine RO membranes has varied at bench-scale from 88% to >98%,[140-142] DMA rejection by in-service, full-scale RO membranes that have been subject to repeated chemical cleanings has not been reported, but it has been reported that NDMA precursor rejection by RO membranes worsens over time.[20] Chlorinated dimethylamine (CDMA), another NDMA precursor with somewhat lower yield,[141] forms rapidly from reactions between HOCl or monochloramine (NH_2Cl) and DMA.[55, 139, 143] CDMA is neutral and thus likely to pass RO membranes.[141]

DMA and CDMA are relatively small molecules present in wastewater that serve as potable reuse influent.[137, 144-145] Additionally, CDMA is likely recalcitrant to reactions with hydroxyl radicals during AOP (although no published rate constants are available). For these reasons, we hypothesized that DMA/CDMA may pass through RO membranes and

endure UV-AOP unaffected, at concentrations great enough to substantially contribute to the NDMA precursor pool in finished FAT water. To investigate the importance of DMA/CDMA as a NDMA precursor at potable reuse facilities, an optimized solid-phase extraction (SPE) gas chromatography-tandem mass spectrometry (GC-MS/MS) method with reduced organic solvent usage for measuring DMA/CDMA was developed to improve upon literature methods reported 20 years ago.[145-146] Using this method, DMA/CDMA were quantified at four full-scale treatment plants. The yield of NDMA from DMA or CDMA in UV-AOP product was determined through standard addition experiments. Pilot-scale UV-AOP experiments were performed to validate full-scale results.

4.3. Materials and Methods

4.3.1. Chemicals and materials

Details of chemicals and solvents are described in the Supporting Information (Text B-1). SPE cartridges including EPA 521 activated carbon (2 g/6 mL) and Sep-Pak C_{18} (1 g/6 mL) were utilized for NDMA and DMA analysis, respectively. Further details are provided in Text B-1.

4.3.2. Sample collection

Samples were collected from four potable reuse facilities in California: Orange County Water District (OCWD) Advanced Water Purification Facility (AWPF) and three other water reclamation facilities utilizing RO and UV-AOP. At the AWPF, samples of the RO feed (ROF), RO permeate (ROP), UV-AOP feed (UVF), UV-AOP product (UVP), and the finished product water (FPW) were collected on three occasions over an approximately one-year period (January 2020, September 2020, and February 2021). The rationale for the

sampling plan is provided in Text B-2. OCWD AWPF sampling sites are shown in Figure B-1. ROF, UVF, and UVP samples from the other three RO-based water reclamation facilities were collected in December 2020, January 2021, and February 2021. Total residual chlorine was measured and immediately quenched with 100 mg/L sodium sulfite. Samples were shipped overnight on ice to the University of Nevada, Reno and stored at 4 °C prior to analysis.

The pilot-scale experiments were conducted at OCWD in April and October 2021. In April, RO permeate from the AWPF was fed to a pilot-scale low-pressure UV reactor with H_2O_2 or HOCl as an oxidant and in October a second pilot-scale experiment utilized 20 μg/L NDMA spiked to deionized (DI) water as the feed solution with H_2O_2 as the oxidant. Pilot UVF and UVP were collected and shipped on ice to University of Nevada, Reno for analysis. Further details about the pilot UV-AOP reactor are provided in the Supporting Information (Text B-2).

4.3.3. DMA quantification

DMA was analyzed by a modified SPE method[146] and a published GC-MS/MS method.[145] The modifications to the extraction method were made to improve the detection limit and to reduce solvent use. Multiple variables were optimized and the optimized method is described in Text B-3. Note that because CDMA is reduced to DMA by the quenching agents employed in the present study at full- and pilot-scale,[141] both DMA and CDMA were captured by the analytical method and are referred to as DMA/CDMA.

GC-MS/MS (Shimadzu TQ8040, Japan) was conducted in electron impact positive ionization mode using a capillary column (DB 1701P, 30 m×0.25 mm×0.25 μm). The

instrument conditions for DMA analysis are summarized in Table B-1. DMA and DMA-d6 were quantified using the 215 *m/z* parent ion and 215 *m/z* daughter ion for DMA and the 221 *m/z* parent ion and 221 *m/z* daughter ion for DMA-d6, similar to GC-MS/MS of DMA conducted by others.[145] The fragmentation of interfering compounds that make it past the first mass filter was the goal of this type of MS/MS, where in other MS approaches the collision cell is used to fragment the target. The Pearson coefficient for the calibration curve with a range of DMA concentrations from 1–100 μg/L was > 0.99 (Figure B-3). The calibration range provided is for samples injected into the GC-MS/MS, after 50× concentration by SPE, corresponding to a range of 0.2-2 μg/L in the samples prior to extraction. Method validation was conducted with recoveries of DMA spiked into tap water and Milli-Q water between 92-113% and the method detection limit (MDL) was 0.15 μg/L. Further method validation details are provided in Text B-4.

4.3.4. NDMA formation potential and NDMA analysis

NDMA formation potential (FP) tests were conducted with 500 mL samples in 1-L amber bottles as described elsewhere.[100, 147] Briefly, samples were buffered at pH 8.0 with a borate solution and dosed with 18 mg-Cl_2/L freshly prepared monochloramine. NDMA FP tests with 18 mg-Cl_2/L NH_2Cl were chosen over uniform formation condition (UFC) tests for two reasons: 1) the low concentrations of NDMA formed from UFC tests would result in substantial variability in NDMA measurement, and 2) UFC and FP tests tend to be well correlated.[8] Samples were allowed to react in the dark at room temperature for 72 h. Residual monochloramine always >4.5 mg-Cl_2/L before quenching with 5 mL of 0.5 M ascorbic acid. The quenching agents used by respective sampling and lab experimental

teams were based on their on-site availability and familiarity. 1 mL of 100 μg/L isotopically labeled NDMA was added and samples were stored in the dark at 4 °C before analysis. NDMA was quantified by a modified U.S. EPA Method 521.[100, 148] Further details regarding NDMA analysis are described in Text B-5.

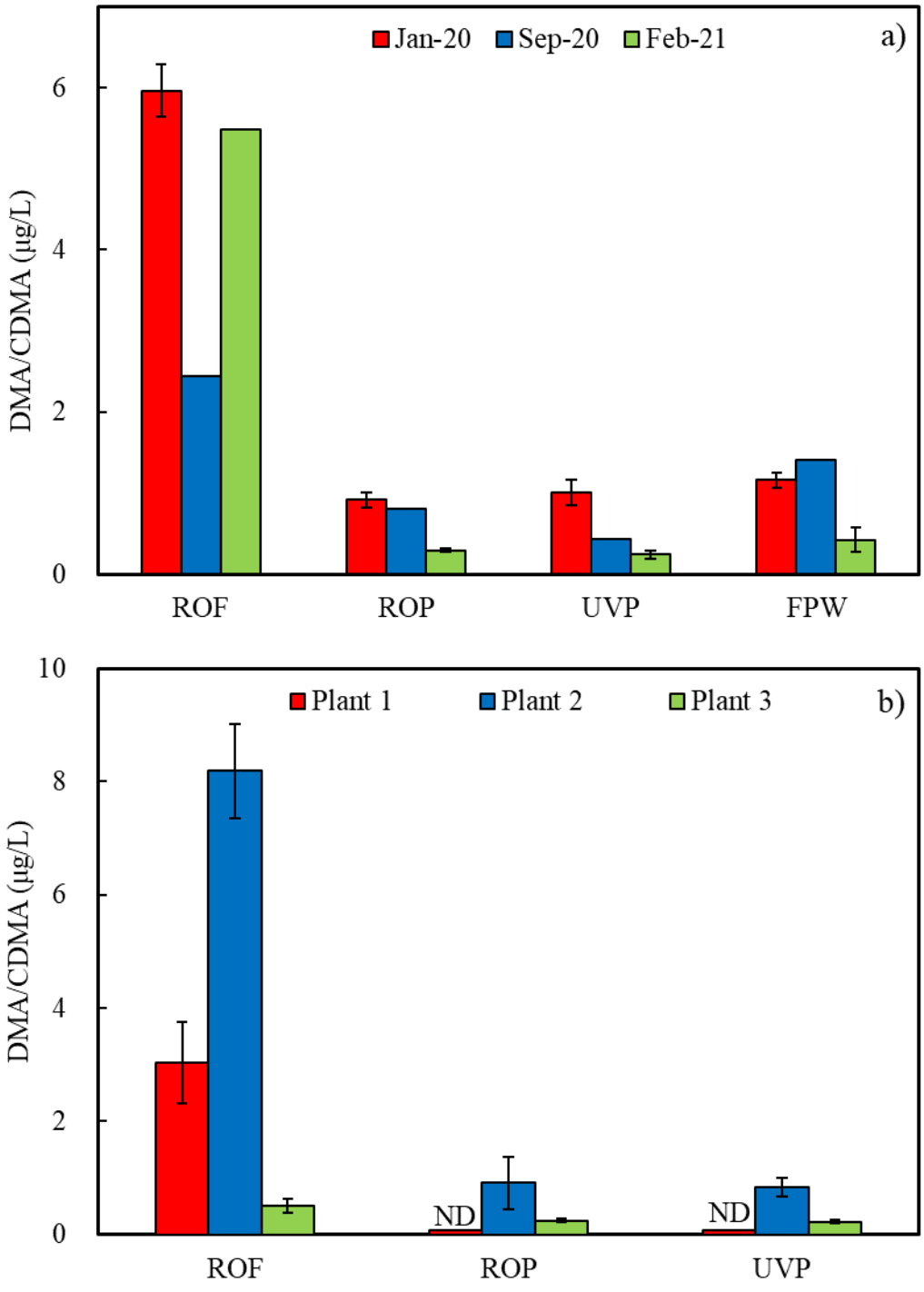

Figure 4-1. DMA/CDMA concentrations in source waters from a) the OCWD AWPF on three occasions and b) three additional RO potable reuse facilities in California. Non-detect DMA/CDMA concentrations (ND) in ROP and UVP at Plant 1 are plotted as one-half the MDL (0.15 µg/L).

4.4. Results and Discussion

4.4.1. Occurrence of DMA/CDMA in potable reuse facilities

DMA/CDMA was measured at four facilities that produce potable water for reuse to understand if DMA passes through full-scale RO and UV-AOP treatment processes. Available water quality data is provided in Table B-4. DMA/CDMA in the ROF samples ranged from 0.5 to 8.1 μg/L (Figure 4-1), consistent with previous studies where DMA concentrations in the secondary effluents ranged from <0.9 to 13 μg/L.[134] DMA/CDMA concentrations in the ROP samples were reduced to <0.15 to 0.9 μg/L, corresponding to DMACDMA rejection by the RO membranes of 52% to ≥95% (MDL of 0.15 μg/L used to calculate the rejection for ROP where the DMA was below the detection limit). Rejection measured at bench-scale by prior research utilizing virgin membranes varied less. For example, two studies reported >98% rejection of DMA,[140, 142] while a third study observed 71% and 88% rejection of CDMA and DMA, respectively.[141] The variability in full-scale DMA/CDMA rejection in this study may be attributable to variable RO membrane age and feed water chemistry. Factors such as plant operational history (e.g., frequency and aggressiveness of membrane cleanings). Increased salt and trace organic compound permeability, including unidentified NDMA precursors, has been observed with aging of the membrane from continuous use and repeated chemical cleanings.[20, 149] The contribution from CDMA is likely another factor influencing permeability, because CDMA is neutral, compared to DMA, which is ionized at this pH.[141] The dominant factor affecting DMA/CDMA rejections needs further study, likely batch-scale. DMA/CDMA

concentrations in UVP samples from the four facilities ranged from <0.15 to 1.0 μg/L. DMA/CDMA concentrations were generally comparable between ROP and UVP (i.e., across UV-AOP) for all treatment plants and all sampling dates suggesting that DMA/CDMA is not well removed or destroyed by UV-AOP (Figure 4-1).

At OCWD AWPF, the UVP water is stabilized to minimize corrosion of the cement mortar conveyance pipeline. The pH of UVP is adjusted from 5.5 to 8.5 by partial decarbonation and addition of saturated lime supernatant,[150] resulting in FPW. FPW samples contained from 0.4 to 1.4 μg/L DMA/CDMA, similar or slightly greater than concentrations in the UVP samples in the three sampling events, although not significantly different (t-test, $p>0.05$). Overall, at the four potable reuse facilities, DMA concentrations in the UVP and FPW samples fell within the narrow range of 0.2 to 1.4 μg/L when detected. In some cases, DMA/CDMA was rejected well by RO membranes (95%), but in most cases, rejection was poor (52%-89%). UV-AOP had minimal or no additional impact on DMA/CDMA removal.

4.4.2. Contribution of DMA/CDMA formation to NDMA formation

In order to assess the contribution of DMA/CDMA to NDMA formation, we conducted experiments to determine DMA and CDMA yield in forming NDMA. We sampled AWPF UVP an additional time (March 2021) and spiked DMA at varying concentrations to determine NDMA yield from DMA in the RO permeate matrix (i.e., standard addition, Figure B-2a).The slope indicates the NDMA mass yield from DMA, equivalent to a molar yield of 1.73%, which is comparable to published yields ranging from 1 to 3%[137-139] and indicates that the low level of background organic matter in UVP water had no effect on

NDMA formation. NDMA yield from 1 to 100 µg/L CDMA was investigated in DI water because of the negligible impact from the matrix demonstrated for DMA and because of the large volume of shipped water required to conduct the experiments in ROP. The CDMA to NDMA molar yield was 0.09% (Figure B-2b). The molar yield is somewhat greater than a previously published yield (~0.01%),[141] reflective of the lower oxidant concentration used in prior study. Finally, because UV treatment of CDMA may alter the NDMA yield,[141, 151] the NDMA molar yield was investigated exposing CDMA to 1000 mJ/cm^2 of 254 nm light (experiment details are provided in Text B-6), followed by chloramination, and the NDMA molar yield was 0.32%. (Figure B-3).

The potential contribution to NDMA formation in the UVP and FPW samples were calculated from the measured DMA/CDMA multiplied by the range of NDMA molar yields expected from DMA, CDMA, and UV irradiated CDMA (Table 1). Because of the limited volume of water sampled, NDMA FP was only directly measured in one UVP sample collected from the AWPF. Measured DMA/CDMA and NDMA FP in this UVP sample were 0.6 µg/L and 36.5 ng/L, respectively. Comparing the expected NDMA FP from these three precursors and their respective yields to the NDMA FP observed in the sample results in the finding that DMA/CDMA contributed 5% to 43% of the precursor loading. DMA/CDMA concentrations in UVP or FPW samples at the other four facilities ranged from <MDL to 1.4 µg/L, corresponding to NDMA FP of up to ~40 ng/L, assuming only DMA present, substantially greater than NL of 10 ng/L in California, although treatment plants are likely to use a substantially lower dose of oxidant. If only CDMA was present, or only irradiated CDMA, the expected NDMA FP would be 1.2 ng/L or 4.2 ng/L,

respectively, similar to what is observed at full-scale facilities. DMA/CDMA is therefore an important or primary contributor to the precursor pool in finished full advanced treated water.

Table 4-1. Calculated NDMA FPs in UVP and FPW samples based on varying NDMA molar yields from DMA, CDMA, and UV irradiated CDMA.

Sample information		Measured DMA/CDMA (µg/L)	Potential NDMA FP (ng/L) from possible precursors		
Location	Date		DMA[a]	CDMA[b]	UV irradiated CDMA[c]
UVP at OCWD	Jan-20	1	28.4	0.8	3.0
FPW at OCWD		1.2	34.1	1.0	3.6
UVP at OCWD	Sep-20	0.4	11.4	0.3	1.2
FPW at OCWD		1.4	39.8	1.2	4.2
UVP at OCWD	Feb-21	0.2	5.7	0.2	0.6
FPW at OCWD		0.4	11.4	0.3	1.2
UVP at OCWD	Mar-21	0.6	15.9	0.5	1.8
UVP at Plant 1	Jan-21	/	/	/	/
UVP at Plant 2	Feb-21	0.8	22.8	0.7	2.4
UVP at Plant 3	Dec-20	0.2	5.7	0.2	0.6

a: assuming only DMA present, 1.73% NDMA molar yield;
b: assuming only CDMA present, 0.09% NDMA molar yield;
c: assuming only CDMA present, 0.32% NDMA molar yield.

If NDMA rebound in finished water is observed to be significant at a particular facility,[21] whether resulting from DMA occurrence or a combination of DMA and other NDMA precursors, the resulting NDMA concentration could impede implementation of

direct potable reuse depending on state regulatory thresholds or guidance values. Treatment facilities with short residence time environmental buffers or no environmental buffer will particularly benefit from an understanding of DMA/CMDA as a precursor. In the case of groundwater augmentation, which is a form of indirect potable reuse practiced by OCWD in the present study in California, NDMA rebound may not be as great of a concern since drinking water regulatory thresholds apply later at the production well (groundwater) where NDMA concentrations may have been reduced due to various factors (e.g., photolysis in recharge ponds,[133] blending, and limited soil aquifer treatment).

4.4.3. Pilot-scale destruction of DMA/CDMA and NDMA

HOCl addition prior to UV-AOP (rather than H_2O_2) was investigated because it is being considered as an alternative by many utilities due to its perceived potential to destroy trace organic contaminants better than advanced oxidation with H_2O_2. ROP from the OCWD AWPF was fed to the pilot UV-AOP reactor (Figure B-4) at a dose of 2.6 mg/L H_2O_2 or 2 mg-Cl_2/L HOCl, and UVF and UVP samples were grabbed. The water quality data is provided in Table B-5. A control experiment was conducted without dosing an oxidant into the ROP feed that contained 2.0–2.3 mg/L total chlorine (chloramines). DMA/CDMA concentrations of ROP ranged from 0.7 to 1.0 μg/L, comparable with that of ROP measured on the three occasions at the AWPF. DMA/CDMA concentrations decreased from 0.7–1.0 μg/L to 0.5 μg/L independent of the applied oxidant (H_2O_2 or HOCl). In the presence of UV light with no added oxidant (and residual chloramines), the concentration of DMA/CDMA increased from 0.7 to 1.0 μg/L, suggesting that some precursors, including NDMA,[144, 152] may be decomposed to DMA/CDMA by UV photolysis. Therefore, HOCl

did not perform substantially better as an oxidant for UV-AOP (similar reduction in DMA/CDMA when either H_2O_2 or HOCl was the oxidant) and is not a viable alternative to reduce NDMA formation from DMA/CDMA based on results from this limited study.

To understand the mass balance of DMA in the system, including its potential to form as a photolytic decomposition product during UV-AOP, DI water free of measurable NDMA was spiked with 20 μg/L NDMA and then treated by UV/H_2O_2 or only UV at pilot-scale (Figure B-5). Although the photolysis of NDMA to DMA is well known,[144, 152] there has not yet been any experimentation to demonstrate that is a negligible precursor during conveyance of FAT-treated waters (i.e., "reformation" of NDMA from its photolytic decomposition product). For control samples (DI water), no DMA was detected with or without oxidant addition. We refer here to DMA as measured by the analytical method, which captures both DMA and CDMA as DMA, because there is no chlorine present in the system and thus DMA will not be oxidized to CDMA. With UV only and DI water spiked with NDMA, the DMA concentrations increased from below the MDL to 0.2 μg/L, indicating some DMA is produced from NDMA photolysis. With H_2O_2 addition, 1.0 μg/L DMA was formed across the UV-AOP system, equivalent to a DMA molar yield of 14%. NDMA concentrations in ROP from the OCWD AWPF have been reported between 9–30 ng/L,[153] suggesting that only 0.8–2.5 ng/L DMA would be produced from NDMA photolysis. Thus, since DMA/CDMA present in the ROP is not well destroyed by UV-AOP, and because NDMA is not present at concentrations high enough in ROP to account for the DMA/CDMA detected in the UVP, the primary source of DMA/CDMA within the water reclamation facility that results in the formation of NDMA downstream of the

treatment process is likely to be the wastewater effluent rather than in-system production via photolysis (i.e., “reformation”).

4.5. Implication

DMA/CDMA present in the treated wastewater influent is likely to contribute significantly to the total NDMA precursor pool and is at least partially or primarily responsible for observed NDMA “rebound” downstream of full advanced treatment potable reuse facilities in the presence of residual chloramines in the finished product water. Such NDMA rebound could hinder implementation or approval of direct potable reuse of full advanced treated water in regions where NDMA regulatory limits or response levels are set low. Potable reuse is increasingly being adopted in the U.S. and throughout the world to improve drought resilience and to adapt to climate change. To this end, reliable treatment strategies outside of RO membranes and UV-AOPs are needed to effectively remove (i.e., sorption) or degrade DMA to mitigate NDMA formation during conveyance and strengthen the future of potable reuse. Expanded sampling campaigns that are outside the scope of this research will help to understand the contribution of DMA/CDMA to individual treatment plants’ NDMA precursor pools, the temporal variability of DMA/CDMA, and the potential to be rejected by in use RO membranes.

4.6. Acknowledgements

This research was supported by the National Science Foundation under Grant No. 1804255 and the Water Research Foundation (Project #5005), managed by Djanette Khiari and Katie Spahr. We are grateful to the anonymous utilities who provided samples.

5. NATURAL VS. ANTHROPOGENIC SOURCES OF *N*-NITROSODIMETHYLAMINE PRECURSORS IN SURFACE WATER

Mingrui Song,[1] Junli Wang,[1] Michael Denicola,[1] Priyamvada Sharma,[1] Ibrahim Abusallout,[1] Utsav Thapa,[1] David Hanigan[1*]

[1]Department of Civil and Environmental Engineering, University of Nevada, Reno, NV 89557-0258

*Corresponding author: DHanigan@unr.edu

Keywords: NDMA, disinfection byproduct, wastewater reclamation, water treatment.

I plan to submit this manuscript to *Science of Total Environment*. I contributed ~90% of the original text, conducted all experiments, and collected ~90% of the source water samples.

5.1. Abstract

N-nitrosodimethylamine (NDMA) is a disinfection byproduct with a 0.7 ng/L concentration in drinking water associated with 10^{-6} lifetime cancer risk. It is unclear that the dominant NDMA precursors come from anthropogenic or natural sources. Because the Truckee River has few anthropogenic contaminant sources and a single point source release of wastewater effluent, it is an ideal water system to better understand the relative importance of wastewater-associated NDMA precursors (anthropogenic) source in surface water. Three separate Lagrangian sampling events were conducted to investigate the profile of NDMA formation potential (FP) in Truckee River and NDMA FP was monitored in the Truckee River along a ~100 mile reach, and NDMA FPs were 11 ng/L (median concentration) at upstream of the Truckee River, reached 25 ng/L immediately downstream of the WWRF effluent in the Truckee River, and decreased to 20 ng/L along the downstream of the Truckee River (~4 miles from WWRF), suggesting the dominant NDMA precursor source is WWRF effluent within the limited length from WWRF effluent in the Truckee River. Two 24-hour continuous sampling events were conducted to understand how changes in reclaimed wastewater loading affect NDMA precursor loading in the environment. NDMA precursor contributions of WWRF loading to the surface water ranged from 10% to ~100% and varied with the changes of the WWRF flowrate contributions.

5.2. Introduction

N-nitrosodimethylamine (NDMA) is a disinfection byproduct that forms via reactions between dichloramine and precursors containing organic nitrogen [16-17]. NDMA has been

identified as a human carcinogen with 0.7 ng/L in drinking water associated with 10^{-6} lifetime cancer risk by the U.S. Environmental Protection Agency [9]. Several U.S. states including California and Massachusetts have set a 10 ng/L drinking water Notification Level [11-12]. In addition to states in U.S., the World Health Organization, Canada, and Australia have guidelines at 40-100 ng/L [13-15].

Natural organic matter (NOM) has been demonstrated to form NDMA in natural waters [135, 154], and one study reported that NOM concentrate accounts for nearly 90% of NDMA precursors in natural waters. Wastewater effluents, algal blooms and agricultural or stormwater runoff were regarded as important NDMA precursor sources [27, 72, 155] as well. In a single study, wastewater effluents have been pointed out to be the primary NDMA precursor source by comparing NDMA formation potentials (NDMA FPs) of different source waters including wastewater effluents, eutrophic water, stormwater or agricultural runoff and headwater [72]. Region-specific relationships between NDMA FPs, streamflow, and sucralose (one anthropogenic pharmaceutical) were developed by Prescott, et al. [73]), suggesting that NDMA precursor sources in drinking water intakes are same as sucralose (i.e., upstream wastewater inputs).

Many anthropogenic nitrogen containing substances have been identified as NDMA precursors, including pharmaceuticals [63-64] and personal care products [65], herbicides [66], pesticides [67], fungicides [68], amine-based water treatment polymers [59] and anion exchange resins [69]. Although some NDMA precursors with high yields (> 75%) were identified [70], their occurrence in surface water serving as the influent to drinking water treatment plants is low or unknown [71], indicating they may only account for a small fraction of NDMA

precursor pool. For example, Methadone has been reported to have a molar yield ranging from 23% to 70% with relatively high occurrence rates, but it was only responsible for up to 62% NDMA precursor pool in wastewater, mostly between 1% and 10% [63]. Thus, it is still not clear if the dominant NDMA precursors come from anthropogenic or natural sources.

Because nearly all surface water systems have some impacts from wastewater effluent, there is little opportunity to distinguish between wastewater or anthropogenic precursors and natural precursors. The Truckee River is the sole outlet of Lake Tahoe, which doesn't directly receive any wastewater, and empties into Pyramid Lake, providing 85% of drinking water for Reno/Sparks metropolitan area[156]. There is only one wastewater reclamation facility (WWRF) discharging directly into the Truckee River. Since the Truckee River has few contaminant sources and a single point source release of wastewater effluent, it is an ideal water system to better understand the relative importance of wastewater-associated NDMA precursor source in surface water.

In this work, we investigated the NDMA precursor sources in a river which has relatively few point sources of anthropogenic input. We first monitored NDMA FP along a ~100 mile reach, including both upstream and downstream of the sole WWRF input, to understand the background NDMA precursor loading and degradation in the Truckee River. We then measured the flow normalized diurnal changes in NDMA precursors present in a stream and the Truckee River which receives reclaimed wastewater to better understand how changes in reclaimed water loading affect precursor loadings in the environment.

5.3. Materials and Methods

5.3.1. Chemicals and materials

An EPA 521 nitrosamine mix was purchased from Sigma-Aldrich (St. Louis, MO) and used as NDMA standard. The isotopically labeled NDMA standard (NDMA-d6, 98%) was from Cambridge Isotopes (Tewksbury, MA, USA). HPLC grade methanol and dichloromethane (DCM), sodium hypochlorite (NaOCl, 5.65-6%), ammonium chloride (NH_4Cl), borax, boric acid, and ascorbic acid were purchased from Fisher Scientific (Waltham, MA, USA). Dionex seven anion standard was from Thermo Fisher Scientific (Waltham, MA, USA). Total organic carbon (TOC) calibration standard was from NSI Lab Solurions (Raleigh, North Carolina, USA). Milli-Q water with electric resistance of ≥ 18.2 MΩ-cm was used. EPA 521 activated carbon solid phase extraction (SPE) cartridges (2 g/6 mL) for NDMA analysis were from Restek (Bellefonte, PA, USA). Sodium sulfate drying cartridges were from Agilent Technologies (Santa Clara, CA, USA). Monochloramine and free chlorine were analyzed with indophenol colorimetric Monochlor F reagent and DPD free chlorine reagent, respectively, from Hach (Loveland, CO, USA). Glass microfiber filters (GF/F, 0.45 μm pore size) from Advantec MFS, Inc. (Dublin, CA) were previously combusted and used for filtering samples.

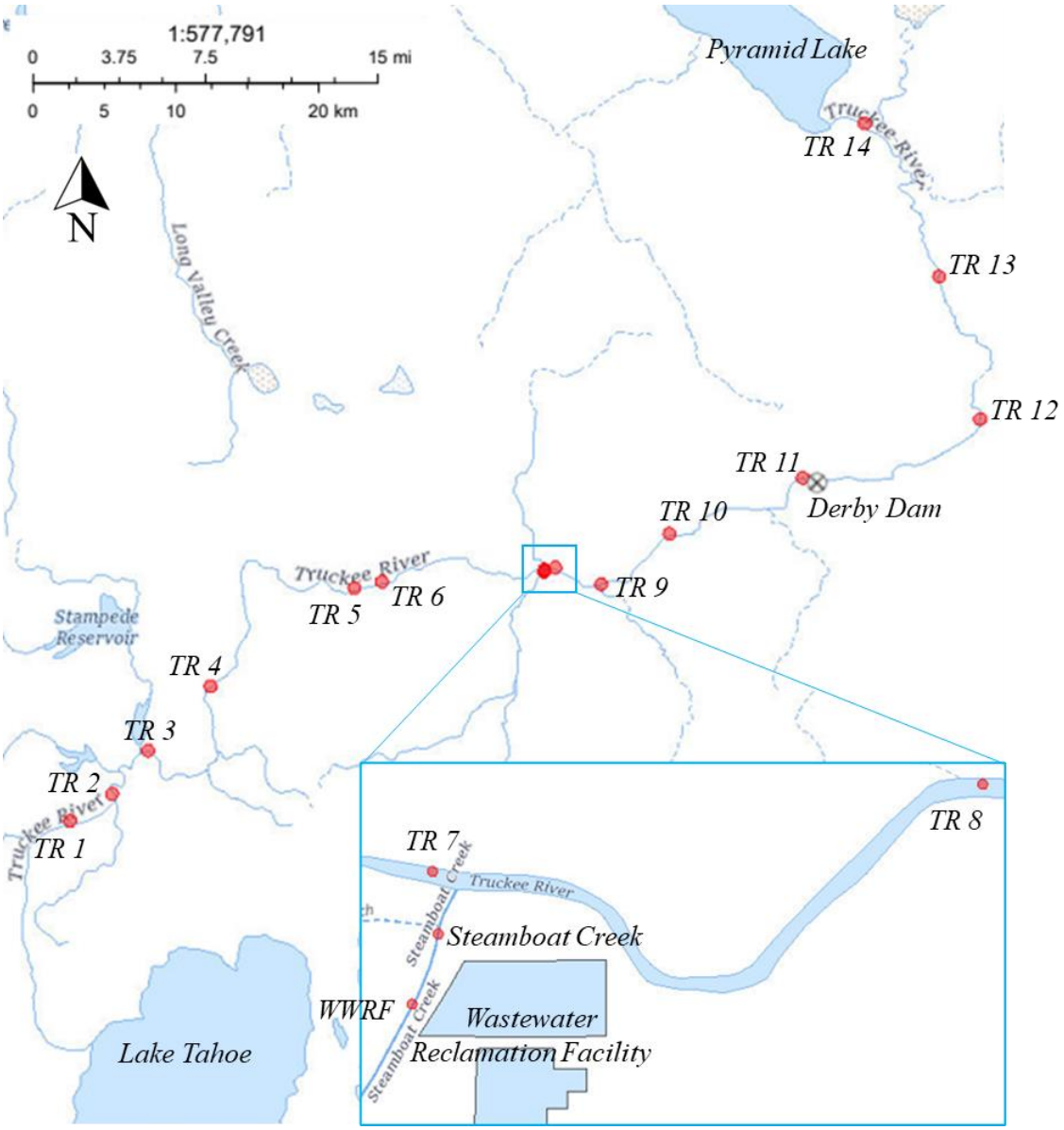

Figure 5-1. Map of Truckee River with sampling sites indicated. Map was generated by USGS National Map.[157] WWRF and SC indicates WWRF final effluent and its downstream at Steamboat Creek.

5.3.2. Site description and sample collection

Surface water was collected at multiple locations from the Truckee River and Steamboat Creek. Steamboat Creek is a stream receiving WWRF effluent and empties into the

Truckee River. Of these sampling locations, locations from TR1 to TR 7 are located at upstream of the WWRF. WWRF is at WWRF effluent outfall, the WWRF effluent which goes directly into Steamboat Creek, and Steamboat Creek is the downstream of WWRF effluent at Steamboat Creek, before the Truckee River. Locations from TR 8 to TR 14 are located at the downstream of the Truckee River (received WWRF discharge). Detailed sampling locations are shown in Figure 5-1 and coordinates for all locations are provided in Table C-1.

Lagrangian sampling was conducted on three occasions (September 2020, October 2021, and June 2022). The flowrates of the Truckee River across every sampling location were obtained from USGS gage data [158-159], which were provided in Table S2. Travel time between every two sampling sites was predicted based on the Truckee River flowrates and previous tracer studies [160-161]. Sampling time of each sampling event based on travel time is also provided in Table S2. In order to investigate background of NDMA precursor loading in the Truckee River, four 2-L samples (TR 1-2, TR 6-7) and six 4-L samples (TR 1-5 and TR7) were collected in September 2020 and October 2021, respectively. Samples were collected from WWRF effluent, Steamboat Creek downstream after receiving WWRF discharge and downstream of the Truckee River (WWRF, Steamboat Creek, and TR 8-9) in September 2020 and October 2021 to study the effects of WWRF discharge on the Truckee River. One more batch sample was collected from TR 9-14 at downstream of the Truckee River to study the change of NDMA precursors. Samples were collected in 1-L pre-combusted glass amber bottles. Because of the difficulties of samplings (i.e., sampling

overnight, sampling permission, etc.), samples were not collected from all sampling sites by the three sampling events.

In a separate sampling campaign, 24-hour continuous sampling was conducted with autosamplers (Teledyne ISCO 6712, St. Lincoln, NE, USA) on two occasions (May and June 2022). In May, one auto-sampler was placed at Steamboat Creek and a total of 24 samples were collected every hour during one day. In June 2022, auto-samplers were placed at WWRF effluent and TR 8, respectively. Sampling time and flowrates during these continuous 24-hr sampling are described in Table S3-4. 1-L polypropylene plastic bottles were used in the sampler. Samples were transported on ice into University of Nevada, Reno, and stored in the dark at 4 ℃ until further use.

5.3.3. NDMA formation potential

NDMA precursors were analyzed by NDMA FP test, which was conducted with 500 mL samples in 1-L glass amber bottles following previous studies [100, 147]. Monochloramine was prepared freshly before each experiment by dropwise addition of NaOCl solution to 10 mM borate buffered NH_4Cl (pH 8) solution at $N:Cl_2$ molar ratio of 1.2 with rapidly stirring. Fresh monochloramine of 18 mg Cl_2/L was dosed to each borate buffered sample (pH=8). After monochloramine addition, samples were allowed to react in the dark at room temperature for 72 hr. Residual monochloramine was measured by indophenol colorimetric Monochlor F method and quenched with 5 mL of 0.5 M ascorbic acid. All samples were spiked with 1 mL of 100 μg/L NDMA-d6 and kept in the dark at 4 °C before analysis.

5.3.4. NDMA and water quality parameter analysis

NDMA concentrations were measured following the U.S. EPA method 521 with some modifications [100]. Samples were extracted with Dionex AutoTrace 280 SPE instrument (Thermo Scientific). EPA 521 cartridges were first conditioned with DCM, methanol, and Milli-Q water and then loaded with 500 mL sample with NDMA-d6 at a rate of 5 mL/min. After loading, cartridges were dried with ultra high purity (UPH) nitrogen gas for 30 min and then eluted with 5 mL DCM. The extracts were dried with sodium sulfate drying cartridges and then evaporated to 1 mL under UPH nitrogen gas at 40 ℃. The extracts were analyzed by gas chromatography-tandem mass spectrometry (GC-MS/MS, Shimadzu TQ8040, Japan) with a capillary column (Stabilwax-MS, 30 m × 0.25 mm × 0.25 μm). Further details regarding GC-MS/MS conditions are provide in supporting information Text C-1. The method detection limits (MDL) were 1 ng/L based on a Signal: Noise ratio of 5.

Water quality parameters including total dissolved nitrogen (TDN), dissolved organic nitrogen (DON), dissolved organic carbon (DOC), ammonia (NH_4^+-N) and chloride (Cl^-), nitrate (NO_3^-), nitrite (NO_2^-), and sulfate (SO_4^{2-}) were analyzed. Anions were analyzed by an ion chromatography (IC, Dionex ICS-6000 SP, Thermo Scientific) with a Dionex Ionpac AS-19 analytical column (2 mm × 250 mm × 4 μm) at 0.25 mL/min flow rate. NH_4^+-N was measured by a spectrophotometric method (EPA Hach Method 10205). A Shimadzu TOC analyzer (TOC-L) was utilized to measure DOC and TDN. DON was obtained by subtracting NH_4^+-N, NO_3^-, NO_2^- and from TDN.

5.3.5. NDMA FP prediction

NDMA FPs at downstream of WWRF in Truckee River are subject to two hydrologic fates between two sampling sites: 1) mass removal between travel sites, and 2) dilution due to inflow from upstream water, tributaries, and groundwater.[162] Assume no degradation within Truckee River, the mass balance loading equation for downstream sampling site is

$$NDMA\ FP_{downstream} \times Q_{downstream} = NDMA\ FP_{upstream} \times Q_{upstream} + NDMA\ FP_{tributary} \times Q_{tributary}.$$

where NDMA $FP_{downstream}$ and NDMA $FP_{upstream}$ represent NDMA FPs of two contiguous sampling sites, and NDMA $FP_{tributary}$ represents tributary NDMA FP. $Q_{downstream}$, $Q_{upstream}$, and $Q_{tributary}$ represent flowrates of downstream, upstream, and tributary, respectively. For NDMA FP prediction at SC (downstream of Steamboat Creek after receiving WWRF effluent), NDMA FP of WWRF effluent is the tributary. Because samples were not collected at upstream of Steamboat Creek (before WWRF effluent) and it should be low compared to NDMA FP of WWRF effluent, NDMA FP at SC was predicted with measured NDMA FP of WWRF effluent. For TR 8, water originates from upstream Truckee River (TR 7) and Steamboat Creek (SC), so NDMA FP at TR 8 was predicted with NDMA FP and flowrate at TR 7 and SC. Since there were no tributaries at downstream of Truckee River (TR 9-14), NDMA FPs of TR 9-14 were predicted with last sampling point in Truckee River.

Table 5-1. Summary of water quality parameters for all sampling events.

Parameters	TDN (mg-N/L)	DON (mg-N/L)	DOC (mg-C/L)	NH_4^+-N (mg-N/L)	NO_3^- (mg-N/L)	NO_2^- (mg-N/L)	Cl^- (mg-Cl/L)	SO_4^{2-} (mg/L)
TR 1	0.08-0.11	0.07-0.09	0.43-0.94	ND-0.01	ND	ND-0.02	3.40-15.56	2.40-9.61
TR 2	0.13-0.20	ND-0.13	0.60-1.05	ND-0.01	ND-0.20	ND-0.02	7.00-24.14	3.40-10.81
TR 3	0.2	0.2	1.34	0.01	ND	ND	12.01	6.55
TR 4	ND	ND	1.27	ND	ND	ND	11.14	7.16
TR 5	0.11	ND	1.54	ND	0.11	ND	13.41	41.13
TR 6	0.13	0.13	1.13	ND	ND	ND	4.30	4.10
TR 7	0.11-0.14	0.11-0.13	1.20-2.15	ND	ND	ND	4.80-20.85	7.90-62.65
WWRF	1.23-1.74	0.88-1.32	6.82-10.27	0.01-0.31	ND-0.29	ND-0.02	63.03-105.40	49.20-87.43
SC	1.12-4.33	ND-1.12	5.53-9.43	0.06-2.82	ND-1.21	ND-0.09	67.28-318.20	37.70-92.69
TR 8	0.06-0.73	0.06-0.58	1.45-6.07	ND-0.04	ND-0.08	ND-0.03	10.98-73.73	14.65-84.26
TR 9	0.36-0.85	0.32-0.65	2.44-6.36	0.04-0.07	ND-0.11	ND-0.02	22.56-80.34	22.42-88.60
TR 10	0.17	0.17	5.72	ND	ND	ND	17.53	20.42
TR 11	0.21	0.20	6.87	0.01	ND	ND	16.73	19.46
TR 12	0.16	0.16	4.14	0.01	ND	ND	16.39	19.33
TR 13	0.15	0.10	3.54	0.05	ND	ND	20.07	22.98
TR 14	0.15	0.15	5.05	ND	ND	ND	30.12	24.89

5.4. Results and Discussion

5.4.1. Water quality parameters

A summary of water quality parameters for all sampling events is provided in Table 5-1. The concentrations of TDN, DON, and DOC were ND to 4.33 mg-N/L, ND to 1.32 mg-N/L, and 0.43 to 10.27 mg-C/L, respectively. NH_4^+-N, NO_3^-, NO_2^- concentrations were less than 0.3 mg-N/L, except one sampling at Steamboat Creek in May 2022 with NH_4^+-N concentrations greater than 1 mg-N/L (data not shown), which is likely from incomplete nitrogen removal at WWRF. Cl^- and SO_4^{2-} concentrations ranged between 3.40 and 318.20 mg/L and between 2.40 and 92.69 mg/L. The highest concentration of the whole river sampling across all sampling campaigns was usually found at WWRF and Steamboat Creek (WWRF effluents and downstream of Steamboat Creek receiving WWRF effluents). For all detected water quality parameters including TDN, DON, DOC, Cl^-, and SO_4^{2-}, concentrations were relatively low at the upstream of the Truckee River (TR 1-7) and increased after receiving WWRF discharge (TR 8-9), suggesting water quality in Truckee River is mainly affected by WWRF discharge (the anthropogenic pollution source). This has expected because on the days of sampling, WWRF effluents contributed to 11.5% and 38.3% the total river flow. Notably, some parameter concentrations, including DOC, Cl^-, and SO_4^{2-}, at Steamboat Creek is greater than that at WWRF, meaning that the background (upstream) concentrations at Steamboat Creek is higher than WWRF effluent concentrations.

5.4.2. NDMA and its precursor loading in Truckee River

To understand the potential for NDMA to contribute to measurements of NDMA precursors (i.e., NDMA FP), NDMA samples were collected from all sampling locations in October 2021 and June 2022, and the results are shown in Figure C-1. NDMA concentrations ranged from <MDL to 8 ng/L with a median concentration of 2 ng/L. It is comparable to prior studies where <10 ng/L NDMA were usually detected in river waters [163-167]. The highest concentration of 8 ng/L was observed at WWRF and decreased to <MDL after ~1.4 miles at TR 8 [160]. The rapid NDMA loss could attribute to a combined effect of direct photolysis of NDMA [168] and dilution by the upstream river flow [165]. Generally, NDMA contributed little to measurements of NDMA FP.

NDMA precursor loading in the Truckee River was investigated by analyzing NDMA FP with chloramination of water samples collected on three occasions (September 2020, October 2021, and June 2022), and the results are shown in Figure 5-2. NDMA FPs of all sampling occasions ranged from 2 to 280 ng/L, with a median of 15 ng/L (Figure 5-2). NDMA FPs ranged from 2 to 28 ng/L with a median concentration of 11 ng/L at the upstream of the Truckee River. For the downstream of the Truckee River, NDMA FPs ranged from 8 to 31 ng/L with a median concentration of 13 ng/L. Similar NDMA FPs were observed in worldwide rivers which were impacted by wastewater effluents. For example, NDMA FPs in Santa Ana River, the largest river entirely within Southern California in the U.S., were between 34 and 90 ng/L [163]. In addition, NDMA FPs in Tokyo rivers ranged from 11 to 185 ng/L [167], and in Llobregat River, 90-270 ng/L NDMA FPs were measured [165].

For upstream the Truckee River (TR 1-7), NDMA FPs in September 2020 ranged from 17 to 28 ng/L with a median concentration of 23 ng/L (Figure 5-2a), whereas NDMA FPs of 2 to 13 ng/L with a median concentration of 7 ng/L were observed in October 2021 (Figure 5-2b). Notably, there are little anthropogenic sources at upstream of the Truckee River, which can be supported by the concentration changes of DOC and Cl^- (low at upstream and high at downstream, Table 1). Therefore, the NDMA FPs ranging from 2 to 28 ng/L represents the natural background of NDMA precursors in this system. The upstream flowrates of 195-262 cfs in September 2020 were higher than that in October 2021 (18-102 cfs), meaning travel time of NDMA precursors across the upstream in October 2021 was longer [161].

The highest NDMA FPs were found at WWRF (WWRF effluents, Figure 5-2). NDMA FPs at WWRF in September 2020 and October 2021 were 280 ng/L and 232 ng/L, respectively. NDMA FPs in wastewater effluents were at least 2 times greater than NDMA FP measured in the Truckee River. Similar results were reported by previous study where NDMA FPs in wastewater effluents were at least 3 times greater than that measured in the Quinnipiac River [162]. At TR 9 in the Truckee River 4 miles downstream of WWRF, NDMA FP decreased to 27 ng/L and 12 ng/L in September 2020 and October 2021, respectively.

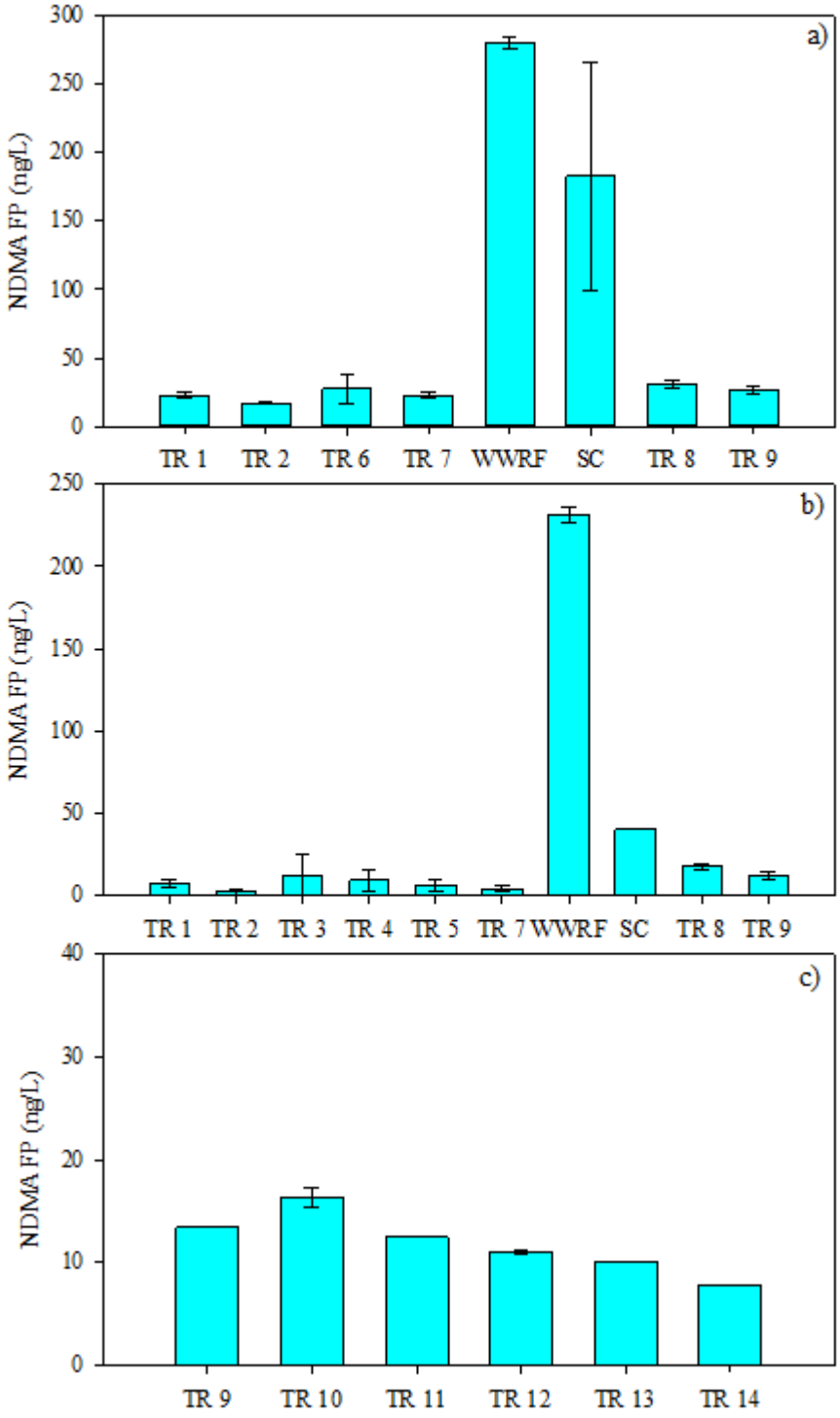

Figure 5-2. NDMA precursor loading and flowrates in Truckee River on three sampling occasions: a) September 2020, b) October 2021, and c) June 2022. The flowrates of every

sampling location were obtained from USGS gage data.[158-159] SC indicates Steamboat Creek.

NDMA FP decreased from WWRF to TR 9 correspond to 90% and 95% NDMA FP degradation in September 2020 and October 2021, respectively which were higher than prior study where 50% NDMA precursors was degraded along 24 mile of the Santa Cruz River in Summer [166]. One reason for the degradation difference might be little dilution effects in the river because the concentrations of Cl^- and SO_4^{2-}, the conservative ions, were remain the same [166]. In order to investigate the neat degradation of NDMA precursors in addition to dilution effects, NDMA FPs in downstream sampling sites (Steam boat Creek, TR8, and TR 9) were predicted by mass balance loading equation described in section 2.5. Since no degradation within the Truckee River was assumed for the mass balance loading equation, any significant decrease in measured NDMA FP compared to predictions would indicate the NDMA precursor degradation in the river (Figure 5-3). Predicted NDMA FP and measured NDMA FP at TR 9 in 2020 sampling were 50 ng/L and 27ng/L, respectively, meaning 46% NDMA FP was degraded (95% confidence level, p value <0.02). Similarly, NDMA FP at TR 9 in 2021sampling was 88 ng/L, suggesting an 86% decrease compared to measured NDMA FP of 12 ng/L. Higher degradation in 2021 sampling may be caused by longer travel time (Table S1), which brings longer photolysis time by sunlight.

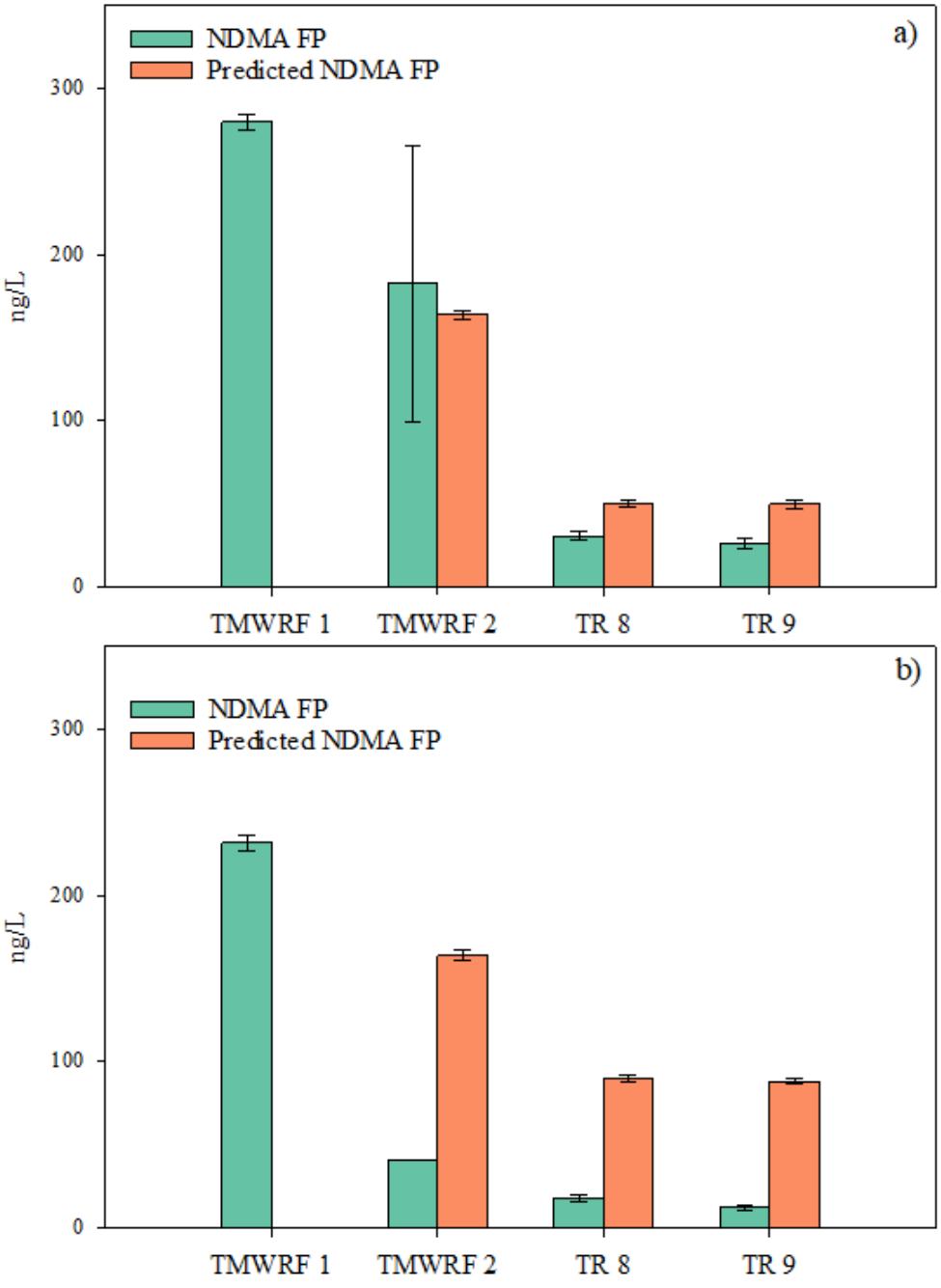

Figure 5-3. NDMA FP and predicted NDMA FP based on conservation of precursors and change in flow from the prior site to the current site after WWRF discharge in a) September 2020 and b) October 2021. SC indicates Steamboat Creek.

Samples were also collected at downstream of the Truckee River (TR 9-TR14) to investigate NDMMA FP degradation for a long distance (~ 50 miles). NDMA FPs at downstream of the Truckee River were consistent and ranged from 8 to 14 ng/L at first glance. However, approximately 42% NDMA precursors were decreased from TR 9 to TR 14 based on the measured NDMA FP values at each site. The flowrates at TR 9 and TR 10 were around 480 cfs, whereas it decreased to approximately 200 cfs, resulting from Derby Dam (near TR 11 in Figure 5-1), which diverts water into Truckee Canal for irrigation. Similar to the last two sampling, predicted NDMA FP, which can indicate neat NDMA precursor degradation compared to measured NDMA FP, were also calculated based on the mass balance loading equation, and the results were described in Figure C-2. Since no samples were collected in Truckee Canal, predicted NDMA FP at TR 11 was not calculated and NDMA FPs of following sampling sites were calculated based on measured NDMA FP at TR11. At TR 14 about 35 miles after TR 11, predicted NDMA FP was 12 ng/L, indicating 33% NDMA precursor degradation. The neat NDMA precursor degradation is similar to the decrease (38%) of measured NDMA FP, which can be explained by limitted dilution effect (the constant river flow from TR 11 to TR 14). Therefore, it is better to consider dilution effects caused by flowrate change when investigating NDMA precursor degradation in surface waters.

5.4.3. Flow normalized diurnal change in NDMA precursors

In order to understand how changes in reclaimed wastewater loading affect NDMA precursor loading in the environment, a total of 24 samples were collected every hour during one day at Steamboat Creek, a stream which directly receives reclaimed wastewater

and NDMA FPs were analyzed by NDMA FP tests (Figure 5-4). NDMA FPs ranged from 24 to 98 ng/L with a median concentration of 32 ng/L during day time (from 5:32 to 20:25, May 2022), while at night time NDMA FPs were 18 to 34 ng/L with a lower median concentration of 23 ng/L. Based on the flowrates of WWRF final effluents and Steamboat Creek (Table S3), the percent flowrate contribution of WWRF final effluent to Steamboat Creek was calculated and described in Figure 5-4. The median flowrate contribution from reclaimed wastewater was 40% during day time, which was higher than 38% at night. The same trends between NDMA FP and percentage flowrate contribution during day and night suggests NDMA precursor loading may be affected by the percentage flowrate contribution from reclaimed wastewater. Similar finding was reported by a previous study [169], where NDMA FP levels increased as the ratio of waste water treatment plant discharge to river discharge increase from 1% to 2%.

The exact NDMA precursor contribution of reclaimed wastewater loading to the surface water was further investigated by analyzing the flowrate and NDMA FP in WWRF and downstream of the Truckee River receiving WWRF final effluents (TR 8), and the results were shown in Figure 5-5. The flowrate ratios of WWRF to TR 8 indicated the flowrate contributions of reclaimed wastewater to the surface water, ranging from 2% to 7% during day time and from 4% to 6% at night. NDMA FPs were 41-138 ng/L and 3-15 ng/L at WWRF and TR 8, respectively. NDMA FP ratios of WWRF to TR 8 indicated the NDMA precursor contributions of reclaimed wastewater loading to the surface water, which ranged from 10% to ~100%. As shown in Figure 5-5, NDMA FP contributions from reclaimed wastewater usually had the same trends as flowrate contributions from reclaimed

wastewater (i.e., both decreased from 2:20 to 7:20, and increased from 7:20 to 10:20), supporting the previous finding that NDMA precursor loading may be affected by the percentage flowrate contribution from reclaimed wastewater.

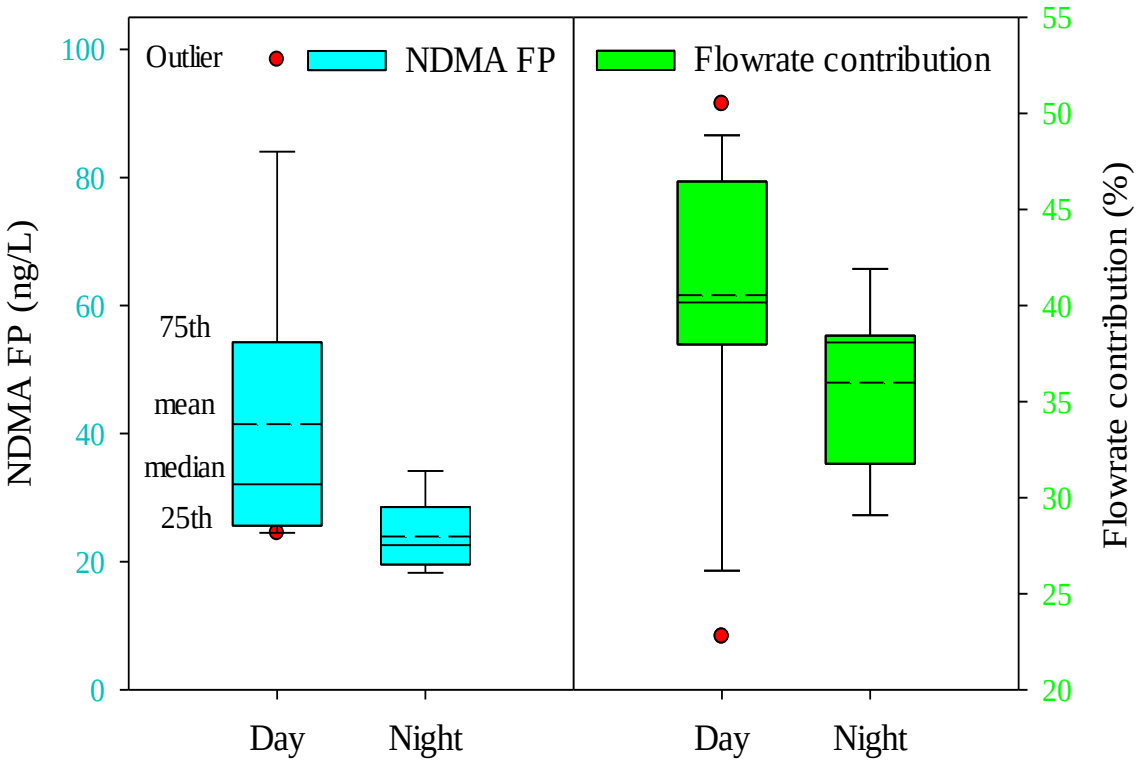

Figure 5-4. Boxplot of NDMA FP and percent flowrate contribution (the ratio of WWRF final effluent flowrate to total Steamboat Creek flowrate) at Steamboat Creek, directly receiving reclaimed wastewater. Day time is from 5:31 to 20:25 based on the sunrise and sunset time at Reno. For the boxplots, the ends of the boxes define the 25th and 75th percentiles, with a solid line at the median and a dash line indicating mean value.

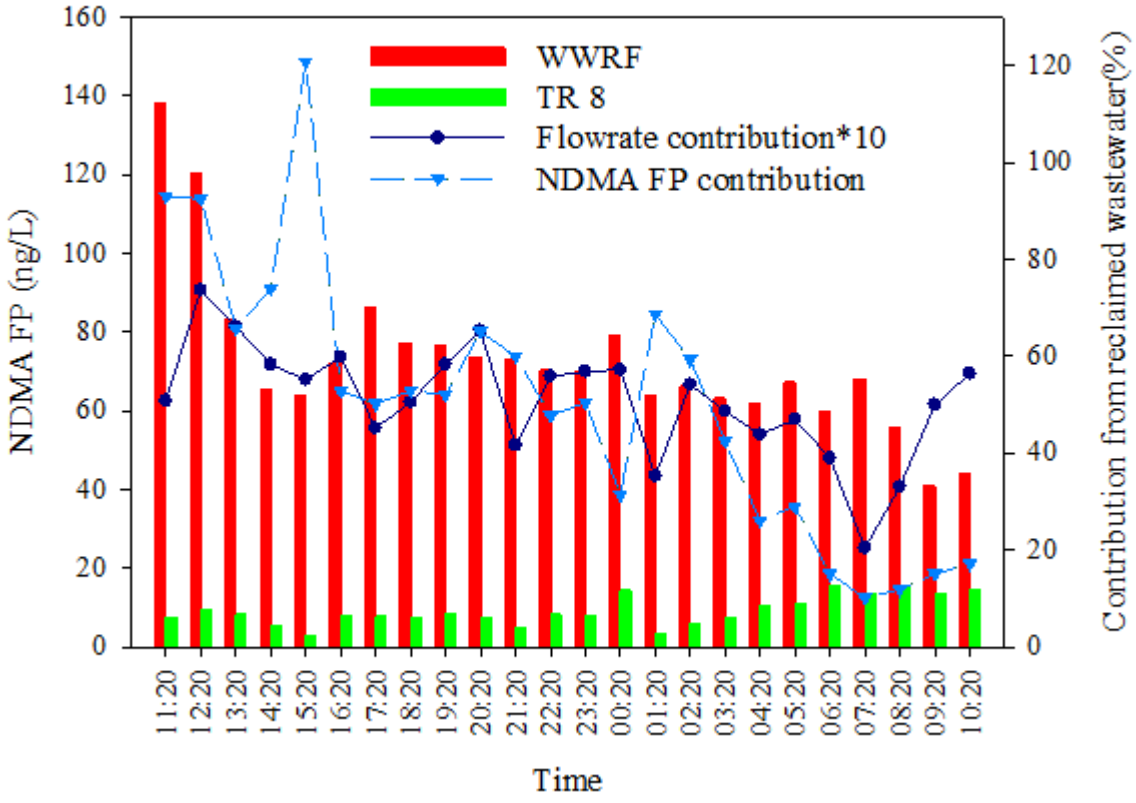

Figure 5-5. NDMA FP, flowrate contribution from reclaimed wastewater (the ratio of WWRF final effluent flowrate (WWRF) to total Truckee River flowrate [TR 8]), and NDMA FP contribution from reclaimed wastewater (the ratio of NDMA FP at WWRF to NDMA FP at TR 8) during continuous 24-hr sampling in June 2022.

The medians of NDMA FP and flowrate contributions from reclaimed wastewater during continuous 24-hr sampling in June were shown in Figure C-3. The medians of the NDMA FP contributions from reclaimed wastewater were 53% and 48% during day time and at night, respectively. The medians of the reclaimed wastewater flowrate contribution were 6% during the day time and 5% at night. The same trend between the two medians

was observed as well, further supporting the finding that NDMA precursor loading is affected by the percentage flowrate contribution from reclaimed wastewater.

5.5. Conclusions

In the study, we used Truckee River as the model of surface water environment to investigate the background, degradation, and source of NDMA precursor in surface water. Based on the on three lagrandian sampling events and two 24-hour continuous sampling events, we found:

- NDMA FPs were usually low in the upper reaches of the Truckee River, were greatest immediately downstream of the WWRF effluent, and decreased to near background concentrations ~4 miles from WWRF, suggesting the dominant NDMA precursor source of Truckee River is reclaimed wastewater effluent within a limited length.
- Dilution effects caused by flowrate change need to be considered when investigating NDMA precursor degradation in surface water environment. NDMA precursors were removed by 46% (~ 350 cfs flowrate) and 86% (~ 100 cfs flowrate) between WWRF final effluents and TR 9 (4-mile travel from WWRF final effluent).
- NDMA precursor loading in surface water may be affected by the percentage flowrate contribution from reclaimed wastewater.
- NDMA precursor contributions of reclaimed wastewater loading to the surface water ranged from 10% to ~100% and varied with the changes of the reclaimed wastewater flowrate contributions.

5.6. Acknowledgements

This research was supported by the National Science Foundation under Grant No. 1804255 and the Water Research Foundation (Project #5005, managed by Djanette Khiari).

6. CONCLUSIONS AND RECOMMENDATIONS FOR FUTURE RESEARCH

The overarching goal of this dissertation was to improve potable reuse water quality by evaluating destruction and toxicity of a broad fraction of organics and understanding the formation of one specific contaminant, NDMA. The following summarizes the finding and conclusions in this dissertation.

6.1. Conclusions

Chapter 3: Comparison of Oxidants Used in Advanced Oxidation for Potable Reuse: Non-Target Analysis of Organic Compounds and Bioassays.

- Suspect compounds recovered by MCX cartridges from RO permeate that matched an in-house LC-qTOF/MS library were degraded more efficiently by UV/HOCl and UV/H_2O_2 compared to UV/NH_2Cl and UV/ambient chloramines.
- Based on the compounds present in MCX extracts and ionizable in ESI+ mode, as measured by non-target analysis, UV/H_2O_2 appears to be the most favorable AOP since it formed the least number and percentage of new transformation products in the UV feed water upon oxidant addition to the RO permeate (i.e., before UV exposure), had better or similar performance to other AOPs with respect to non-target features removed/formed across UV-AOP, and reduced the summed peak area the greatest extent across the treatment train.
- Olefins were decomposed to the greatest extent, and aromatics were decomposed the most poorly. UV/H_2O_2 formed the least Cl-containing transformation products and decomposed the greatest fraction of Cl-containing compounds.

- UV-AOP with any of the studied oxidants (HOCl, H_2O_2, and NH_2Cl) produced water with lower oxidative stress response (ARE-Nrf2) than conventionally treated drinking water (river water). The oxidative stress response in pre-AOP samples was mitigated to below the assay response limit after UV-AOP. Samples which were positive in the ARE-Nrf2 assay did not elicit a response in four other assays measuring genetic stress or repair, indicating that the oxidative stress did not significantly impact the genetic material or induce cell death.

Chapter 4: Contribution of Dimethylamine to *N*-nitrosodimethylamine Formation at Reverse Osmosis Water Reclamation Facilities.

- The median DMA concentration in UV-AOP product and finished waters was 0.4 µg/L across six sampling events. At one reclamation facility sampled three times over one year, finished water DMA ranged from 0.4 to 1.4 µg/L.
- DMA rejection by the RO membranes varied from 52% to ≥95%.
- UV-AOP had minimal to no impact on DMA destruction.
- Given the DMA occurrence and molar yields for NDMA, DMA accounted for 5%-43% of the total NDMA precursor pool of the UV-AOP product water at one facility, and up to 40 ng/L of NDMA.

Chapter 5: Dominant Source of *N*-nitrosodimethylamine precursors in surface water.

- NDMA FPs were usually low in the upper reaches of the Truckee River, were greatest immediately downstream of the WWRF effluent, and decreased to near background concentrations ~4 miles from WWRF, suggesting the dominant

NDMA precursor source of Truckee River is reclaimed wastewater effluent within a limited length.

- Dilution effects caused by flowrate changes need to be considered when investigating NDMA precursor degradation in surface water environment. NDMA precursors were removed by 46% (~ 350 cfs flowrate) and 86% (~ 100 cfs flowrate) between WWRF final effluents and TR 9 (4-mile travel from WWRF final effluent).
- NDMA precursor loading in surface water may be affected by the percentage flowrate contribution from reclaimed wastewater.
- NDMA precursor contributions of reclaimed wastewater loading to the surface water ranged from 10% to ~100% and varied with the changes of the reclaimed wastewater flowrate contributions.

6.2. Recommendations for Future Research

During the research, several opportunities for future research became apparent.

1. I believed that UV/H_2O_2 was the most suitable oxidant for ultraviolet advanced oxidation in water reuse, compared to HOCl and NH_2Cl, based on destruction of organic compounds, reduced transformation products, and lack of oxidative stress induction. However, feed water quality varied during the experiment. Reproduction of these results in additional experiments will advance the comparative assessment of oxidants used during AOP.

2. I found DMA rejections by RO membranes varied over time, likely due to the age and type of RO membranes used in the potable reuse facilities. Also, I inferred the

formation of chlorinated DMA in presence of HOCl but there are not currently available methods which distinguish between Cl-DMA and DMA. Further batch-scale experiments are needed to confirm these inferences.

3. To my knowledge, the current DMA analytical method cannot differentiate DMA and chlorinated DMA because chlorinated DMA could be converted to DMA by quenching agents. A novel analytical method for chlorinated DMA with low detection limits (ng/L level) would be highly beneficial to understand DMA oxidation and its contribution to NDMA during potable reuse and in other situations where DMA is expected and an oxidant is used.

4. I found NDMA precursor contributions of reclaimed wastewater loading to the surface water ranged from 10% to ~100% based on one 24-hr continuous sampling event where WWRF effluents contributed to 2%-7% Truckee River flows. However, only one sampling event was only conducted in dry period. More sampling events will advance the NDMA precursor contributions of reclaimed wastewater loading to the surface water.

7. References

1. Fatta-Kassinos, D.; Dionysiou, D. D.; Kümmerer, K., *Wastewater reuse and current challenges*. Springer: 2016.
2. Organization, W. H., Potable reuse: Guidance for producing safe drinking-water. **2017**.
3. Council, N. R., *Water reuse: potential for expanding the nation's water supply through reuse of municipal wastewater*. National Academies Press: 2012.
4. Board, C. S. W. R. C., Terms and Definitions for Potable Reuse. Availalbe online from: https://www.waterboards.ca.gov/drinking_water/certlic/drinkingwater/documents/recharge/ag_draft_recom_app_b.pdf. 2016.
5. Gerrity, D.; Pecson, B.; Trussell, R. S.; Trussell, R. R., Potable reuse treatment trains throughout the world. *Journal of Water Supply: Research and Technology—AQUA* **2013,** *62* (6), 321-338.
6. Zhang, Z.; Chuang, Y. H.; Szczuka, A.; Ishida, K. P.; Roback, S.; Plumlee, M. H.; Mitch, W. A., Pilot-scale evaluation of oxidant speciation, 1,4-dioxane degradation and disinfection byproduct formation during UV/hydrogen peroxide, UV/free chlorine and UV/chloramines advanced oxidation process treatment for potable reuse. *Water Res* **2019,** *164*, 114939.
7. Chuang, Y. H.; Szczuka, A.; Shabani, F.; Munoz, J.; Aflaki, R.; Hammond, S. D.; Mitch, W. A., Pilot-scale comparison of microfiltration/reverse osmosis and ozone/biological activated carbon with UV/hydrogen peroxide or UV/free chlorine AOP treatment for controlling disinfection byproducts during wastewater reuse. *Water Res* **2019,** *152*, 215-225.
8. Krasner, S. W.; Mitch, W. A.; McCurry, D. L.; Hanigan, D.; Westerhoff, P., Formation, precursors, control, and occurrence of nitrosamines in drinking water: a review. *Water Res* **2013,** *47* (13), 4433-50.
9. Agency, U. S. E. P., Integrated Risk Information System (IRIS), N-nitrosodimethylamine. 2002.
10. Zeng, T.; Plewa, M. J.; Mitch, W. A., N-Nitrosamines and halogenated disinfection byproducts in U.S. Full Advanced Treatment trains for potable reuse. *Water Research* **2016,** *101*, 176-186.
11. CDPH, NDMA and Other Nitrosamines e Drinking Water Issues. **2009**.
12. Protection, M. D. o. E., Standards and Guidlines for Contaminants in Massachusetts Drinking Waters. Available online from https://www.mass.gov/guides/drinking-water-standards-and-guidelines#-guidelines- 2020.
13. Organization, W. H., *Guidelines for drinking-water quality: second addendum. Vol. 1, Recommendations*. World Health Organization: 2008.
14. Canada, H., Guidelines for Canadian Drinking WaterQuality: Guideline Technical Document: N-Nitrosodimethylamine (NDMA). 2011; Vol. No H128-1/11-662E.
15. Council, N. H. a. M. R., Australian drinking water guideline: NDMA, Commonwealth of Australia. **2011**.

16. Shah, A. D.; Mitch, W. A., Halonitroalkanes, halonitriles, haloamides, and N-nitrosamines: a critical review of nitrogenous disinfection byproduct formation pathways. *Environ Sci Technol* **2012,** *46* (1), 119-31.
17. Schreiber, I. M.; Mitch, W. A., Nitrosamine Formation Pathway Revisited: The Importance of Chloramine Speciation and Dissolved Oxygen. *Environmental Science & Technology* **2006,** *40* (19), 6007-6014.
18. Fujioka, T.; Khan, S. J.; McDonald, J. A.; Roux, A.; Poussade, Y.; Drewes, J. E.; Nghiem, L. D., N-nitrosamine rejection by reverse osmosis membranes: a full-scale study. *Water Res* **2013,** *47* (16), 6141-8.
19. Roback, S. L.; Ishida, K. P.; Chuang, Y.-H.; Zhang, Z.; Mitch, W. A.; Plumlee, M. H., Pilot UV-AOP Comparison of UV/Hydrogen Peroxide, UV/Free Chlorine, and UV/Monochloramine for the Removal of N-Nitrosodimethylamine (NDMA) and NDMA Precursors. *ACS ES&T Water* **2020**.
20. Roback, S. L.; Ishida, K. P.; Plumlee, M. H., Influence of reverse osmosis membrane age on rejection of NDMA precursors and formation of NDMA in finished water after full advanced treatment for potable reuse. *Chemosphere* **2019,** *233*, 120-131.
21. Sgroi, M.; Roccaro, P.; Oelker, G. L.; Snyder, S. A., N-nitrosodimethylamine (NDMA) formation at an indirect potable reuse facility. *Water Res* **2015,** *70*, 174-83.
22. Melvin, S. D.; Leusch, F. D. L., Removal of trace organic contaminants from domestic wastewater: A meta-analysis comparison of sewage treatment technologies. *Environment International* **2016,** *92-93*, 183-188.
23. Subedi, B.; Codru, N.; Dziewulski, D. M.; Wilson, L. R.; Xue, J.; Yun, S.; Braun-Howland, E.; Minihane, C.; Kannan, K., A pilot study on the assessment of trace organic contaminants including pharmaceuticals and personal care products from on-site wastewater treatment systems along Skaneateles Lake in New York State, USA. *Water Research* **2015,** *72*, 28-39.
24. Lenka, S. P.; Kah, M.; Padhye, L. P., A review of the occurrence, transformation, and removal of poly- and perfluoroalkyl substances (PFAS) in wastewater treatment plants. *Water Research* **2021,** *199*, 117187.
25. Glover, C. M.; Verdugo, E. M.; Trenholm, R. A.; Dickenson, E. R. V., N-nitrosomorpholine in potable reuse. *Water Research* **2019,** *148*, 306-313.
26. Liu, W.; Song, X.; Huda, N.; Xie, M.; Li, G.; Luo, W., Comparison between aerobic and anaerobic membrane bioreactors for trace organic contaminant removal in wastewater treatment. *Environmental Technology & Innovation* **2020,** *17*, 100564.
27. Sgroi, M.; Vagliasindi, F. G. A.; Snyder, S. A.; Roccaro, P., N-Nitrosodimethylamine (NDMA) and its precursors in water and wastewater: A review on formation and removal. *Chemosphere* **2018,** *191*, 685-703.
28. Adeel, M.; Song, X.; Wang, Y.; Francis, D.; Yang, Y., Environmental impact of estrogens on human, animal and plant life: A critical review. *Environment International* **2017,** *99*, 107-119.
29. Cancer, I. A. f. R. o., IARC monographs on the evaluation of the carcinogenic risk of chemicals to humans. Vol. 17. Some N-nitroso compounds. *IARC monographs on the evaluation of the carcinogenic risk of chemicals to humans. Vol. 17. Some N-nitroso compounds.* **1978**.

30. USEPA, Integrated risk information system (IRIS), N-nitrosodimethylamine (CASRN 62-75-9). **2002**.
31. COEHHA, Public Health Goal for Chemical in Drinking Water: N-nitrosodimethylamine. **2006**.
32. Buxton, G. V.; Greenstock, C. L.; Helman, W. P.; Ross, A. B., Critical review of rate constants for reactions of hydrated electrons, hydrogen atoms and hydroxyl radicals (· OH/· O− in aqueous solution. *Journal of physical and chemical reference data* **1988,** *17* (2), 513-886.
33. Yang, Q.; Choi, H.; Chen, Y.; Dionysiou, D. D., Heterogeneous activation of peroxymonosulfate by supported cobalt catalysts for the degradation of 2,4-dichlorophenol in water: The effect of support, cobalt precursor, and UV radiation. *Applied Catalysis B: Environmental* **2008,** *77* (3), 300-307.
34. Baxendale, J.; Wilson, J., The photolysis of hydrogen peroxide at high light intensities. *Transactions of the Faraday Society* **1957,** *53*, 344-356.
35. Fang, J.; Fu, Y.; Shang, C., The roles of reactive species in micropollutant degradation in the UV/free chlorine system. *Environ Sci Technol* **2014,** *48* (3), 1859-68.
36. Neta, P.; Huie, R. E.; Ross, A. B., Rate constants for reactions of inorganic radicals in aqueous solution. *Journal of Physical and Chemical Reference Data* **1988,** *17* (3), 1027-1284.
37. Beitz, T.; Bechmann, W.; Mitzner, R., Investigations of reactions of selected azaarenes with radicals in water. 2. Chlorine and bromine radicals. *The Journal of Physical Chemistry A* **1998,** *102* (34), 6766-6771.
38. Grebel, J. E.; Pignatello, J. J.; Mitch, W. A., Effect of Halide Ions and Carbonates on Organic Contaminant Degradation by Hydroxyl Radical-Based Advanced Oxidation Processes in Saline Waters. *Environmental Science & Technology* **2010,** *44* (17), 6822-6828.
39. Watts, M. J.; Linden, K. G., Chlorine photolysis and subsequent OH radical production during UV treatment of chlorinated water. *Water Res* **2007,** *41* (13), 2871-8.
40. Jin, J.; El-Din, M. G.; Bolton, J. R., Assessment of the UV/Chlorine process as an advanced oxidation process. *Water Research* **2011,** *45* (4), 1890-1896.
41. Zhang, Z.; Chuang, Y. H.; Huang, N.; Mitch, W. A., Predicting the Contribution of Chloramines to Contaminant Decay during Ultraviolet/Hydrogen Peroxide Advanced Oxidation Process Treatment for Potable Reuse. *Environ Sci Technol* **2019,** *53* (8), 4416-4425.
42. De Laat, J.; Boudiaf, N.; Dossier-Berne, F., Effect of dissolved oxygen on the photodecomposition of monochloramine and dichloramine in aqueous solution by UV irradiation at 253.7 nm. *Water Research* **2010,** *44* (10), 3261-3269.
43. Peng, J.; Yin, R.; Yang, X.; Shang, C., A Novel UVA/ClO2 Advanced Oxidation Process for the Degradation of Micropollutants in Water. *Environmental Science & Technology* **2022,** *56* (2), 1257-1266.
44. Cooper, W. J.; Jones, A. C.; Whitehead, R. F.; Zika, R. G., Sunlight-Induced Photochemical Decay of Oxidants in Natural Waters: Implications in Ballast Water Treatment. *Environmental Science & Technology* **2007,** *41* (10), 3728-3733.
45. Chuang, Y. H.; Chen, S.; Chinn, C. J.; Mitch, W. A., Comparing the UV/Monochloramine and UV/Free Chlorine Advanced Oxidation Processes (AOPs) to the

UV/Hydrogen Peroxide AOP Under Scenarios Relevant to Potable Reuse. *Environ Sci Technol* **2017,** *51* (23), 13859-13868.
46. Klaning, U. K.; Sehested, K.; Holcman, J., Standard Gibbs energy of formation of the hydroxyl radical in aqueous solution. Rate constants for the reaction chlorite (ClO2-) + ozone .dblarw. ozone(1-) + chlorine dioxide. *The Journal of Physical Chemistry* **1985,** *89* (5), 760-763.
47. Luo, C.; Ma, J.; Jiang, J.; Liu, Y.; Song, Y.; Yang, Y.; Guan, Y.; Wu, D., Simulation and comparative study on the oxidation kinetics of atrazine by UV/H2O2, UV/HSO5− and UV/S2O82−. *Water Research* **2015,** *80*, 99-108.
48. Chuang, Y.-H.; Shi, H.-J., UV/chlorinated cyanurates as an emerging advanced oxidation process for drinking water and potable reuse treatments. *Water Research* **2022,** *211*, 118075.
49. Tian, F. X.; Ye, W. K.; Xu, B.; Hu, X. J.; Ma, S. X.; Lai, F.; Gao, Y. Q.; Xing, H. B.; Xia, W. H.; Wang, B., Comparison of UV-induced AOPs (UV/Cl2, UV/NH2Cl, UV/ClO2 and UV/H2O2) in the degradation of iopamidol: Kinetics, energy requirements and DBPs-related toxicity in sequential disinfection processes. *Chem Eng J* **2020,** *398*, 125570.
50. Miklos, D. B.; Wang, W. L.; Linden, K. G.; Drewes, J. E.; Hübner, U., Comparison of UV-AOPs (UV/H2O2, UV/PDS and UV/Chlorine) for TOrC removal from municipal wastewater effluent and optical surrogate model evaluation. *Chemical Engineering Journal* **2019,** *362*, 537-547.
51. Fang, Z.; Huang, R.; Chelme-Ayala, P.; Shi, Q.; Xu, C.; Gamal El-Din, M., Comparison of UV/Persulfate and UV/H2O2 for the removal of naphthenic acids and acute toxicity towards Vibrio fischeri from petroleum production process water. *Science of The Total Environment* **2019,** *694*, 133686.
52. Zhao, J.; Peng, J.; Yin, R.; Fan, M.; Yang, X.; Shang, C., Multi-angle comparison of UV/chlorine, UV/monochloramine, and UV/chlorine dioxide processes for water treatment and reuse. *Water Research* **2022**, 118414.
53. McKenna, E.; Thompson, K. A.; Taylor-Edmonds, L.; McCurry, D. L.; Hanigan, D., Summation of disinfection by-product CHO cell relative toxicity indices: sampling bias, uncertainty, and a path forward. *Environ Sci Process Impacts* **2020,** *22* (3), 708-718.
54. Russell, C. G.; Blute, N. K.; Via, S.; Wu, X.; Chowdhury, Z., Nationwide assessment of nitrosamine occurrence and trends. *Journal - American Water Works Association* **2012,** *104* (3), E205-E217.
55. Mitch, W. A.; Sedlak, D. L., Formation of N-Nitrosodimethylamine (NDMA) from Dimethylamine during Chlorination. *Environmental Science & Technology* **2002,** *36* (4), 588-595.
56. McCurry, D. L.; Ishida, K. P.; Oelker, G. L.; Mitch, W. A., Reverse Osmosis Shifts Chloramine Speciation Causing Re-Formation of NDMA during Potable Reuse of Wastewater. *Environ Sci Technol* **2017,** *51* (15), 8589-8596.
57. Kemper, J. M.; Walse, S. S.; Mitch, W. A., Quaternary Amines As Nitrosamine Precursors: A Role for Consumer Products? *Environmental Science & Technology* **2010,** *44* (4), 1224-1231.
58. Mitch, W. A.; Schreiber, I. M., Degradation of Tertiary Alkylamines during Chlorination/Chloramination: Implications for Formation of Aldehydes, Nitriles,

Halonitroalkanes, and Nitrosamines. *Environmental Science & Technology* **2008,** *42* (13), 4811-4817.
59. Park, S.-H.; Wei, S.; Mizaikoff, B.; Taylor, A. E.; Favero, C.; Huang, C.-H., Degradation of Amine-Based Water Treatment Polymers during Chloramination as N-Nitrosodimethylamine (NDMA) Precursors. *Environmental Science & Technology* **2009,** *43* (5), 1360-1366.
60. Shen, R.; Andrews, S. A., NDMA formation kinetics from three pharmaceuticals in four water matrices. *Water Research* **2011,** *45* (17), 5687-5694.
61. Shen, R.; Andrews, S. A., Formation of NDMA from ranitidine and sumatriptan: The role of pH. *Water Research* **2013,** *47* (2), 802-810.
62. Pham, H. T.; Wahman, D. G.; Fairey, J. L., Updated Reaction Pathway for Dichloramine Decomposition: Formation of Reactive Nitrogen Species and N-Nitrosodimethylamine. *Environmental Science & Technology* **2021,** *55* (3), 1740-1749.
63. Hanigan, D.; Thurman, E. M.; Ferrer, I.; Zhao, Y.; Andrews, S.; Zhang, J.; Herckes, P.; Westerhoff, P., Methadone contributes to N-nitrosodimethylamine formation in surface waters and wastewaters during chloramination. *Environmental Science & Technology Letters* **2015,** *2* (6), 151-157.
64. Jasemizad, T.; Bromberg, L.; Hatton, T. A.; Padhye, L. P., Oxidation of betrixaban to yield N-nitrosodimethylamine by water disinfectants. *Water Res* **2020,** *186*, 116309.
65. Shen, R.; Andrews, S. A., Demonstration of 20 pharmaceuticals and personal care products (PPCPs) as nitrosamine precursors during chloramine disinfection. *Water Research* **2011,** *45* (2), 944-952.
66. Chen, W.-H.; Young, T. M., NDMA Formation during Chlorination and Chloramination of Aqueous Diuron Solutions. *Environmental Science & Technology* **2008,** *42* (4), 1072-1077.
67. Padhye, L. P.; Kim, J.-H.; Huang, C.-H., Oxidation of dithiocarbamates to yield N-nitrosamines by water disinfection oxidants. *Water Research* **2013,** *47* (2), 725-736.
68. Schmidt, C. K.; Brauch, H.-J., N,N-Dimethylsulfamide as Precursor for N-Nitrosodimethylamine (NDMA) Formation upon Ozonation and its Fate During Drinking Water Treatment. *Environmental Science & Technology* **2008,** *42* (17), 6340-6346.
69. Flowers, R. C.; Singer, P. C., Anion Exchange Resins as a Source of Nitrosamines and Nitrosamine Precursors. *Environmental Science & Technology* **2013,** *47* (13), 7365-7372.
70. Selbes, M.; Kim, D.; Ates, N.; Karanfil, T., The roles of tertiary amine structure, background organic matter and chloramine species on NDMA formation. *Water Res* **2013,** *47* (2), 945-53.
71. Kolpin, D. W.; Furlong, E. T.; Meyer, M. T.; Thurman, E. M.; Zaugg, S. D.; Barber, L. B.; Buxton, H. T., Pharmaceuticals, Hormones, and Other Organic Wastewater Contaminants in U.S. Streams, 1999−2000: A National Reconnaissance. *Environmental Science & Technology* **2002,** *36* (6), 1202-1211.
72. Zeng, T.; Glover, C. M.; Marti, E. J.; Woods-Chabane, G. C.; Karanfil, T.; Mitch, W. A.; Dickenson, E. R. V., Relative Importance of Different Water Categories as Sources of N-Nitrosamine Precursors. *Environmental Science & Technology* **2016,** *50* (24), 13239-13248.

73. Prescott, M.; Krasner, S. W.; Guo, Y. C., Estimation of NDMA precursor loading in source water via artificial sweetener monitoring. *Journal - American Water Works Association* **2017,** *109* (6), E243-E251.
74. Harris-Lovett, S. R.; Binz, C.; Sedlak, D. L.; Kiparsky, M.; Truffer, B., Beyond User Acceptance: A Legitimacy Framework for Potable Water Reuse in California. *Environ Sci Technol* **2015,** *49* (13), 7552-61.
75. Bixio, D.; Thoeye, C.; De Koning, J.; Joksimovic, D.; Savic, D.; Wintgens, T.; Melin, T., Wastewater reuse in Europe. *Desalination* **2006,** *187* (1), 89-101.
76. Farhat, N. M.; Loubineaud, E.; Prest, E. I. E. C.; El-Chakhtoura, J.; Salles, C.; Bucs, S. S.; Trampé, J.; Van den Broek, W. B. P.; Van Agtmaal, J. M. C.; Van Loosdrecht, M. C. M.; Kruithof, J. C.; Vrouwenvelder, J. S., Application of monochloramine for wastewater reuse: Effect on biostability during transport and biofouling in RO membranes. *Journal of Membrane Science* **2018,** *551*, 243-253.
77. Kwon, M.; Royce, A.; Gong, Y.; Ishida, K. P.; Stefan, M., UV/Chlorine vs. UV/H2O2 for water reuse at Orange County Water District, CA: A pilot study. *Environmental Science: Water Research & Technology* **2020**.
78. Cao, Z.; Yu, X.; Zheng, Y.; Aghdam, E.; Sun, B.; Song, M.; Wang, A.; Han, J.; Zhang, J., Micropollutant abatement by the UV/chloramine process in potable water reuse: A review. *J Hazard Mater* **2022,** *424* (Pt B), 127341.
79. Wu, Z.; Chen, C.; Zhu, B.-Z.; Huang, C.-H.; An, T.; Meng, F.; Fang, J., Reactive Nitrogen Species Are Also Involved in the Transformation of Micropollutants by the UV/Monochloramine Process. *Environmental Science & Technology* **2019,** *53* (19), 11142-11152.
80. Wols, B. A.; Hofman-Caris, C. H.; Harmsen, D. J.; Beerendonk, E. F., Degradation of 40 selected pharmaceuticals by UV/H2O2. *Water Res* **2013,** *47* (15), 5876-88.
81. Li, W.; Xu, E.; Schlenk, D.; Liu, H., Cyto- and geno-toxicity of 1,4-dioxane and its transformation products during ultraviolet-driven advanced oxidation processes. *Environmental Science: Water Research & Technology* **2018,** *4* (9), 1213-1218.
82. Mariani, M. L.; Romero, R. L.; Zalazar, C. S., Modeling of degradation kinetic and toxicity evaluation of herbicides mixtures in water using the UV/H2O2 process. *Photochem Photobiol Sci* **2015,** *14* (3), 608-17.
83. Sharma, A.; Ahmad, J.; Flora, S. J. S., Application of advanced oxidation processes and toxicity assessment of transformation products. *Environmental Research* **2018,** *167*, 223-233.
84. Roback, S. L.; Ferrer, I.; Thurman, E. M.; Ishida, K. P.; Plumlee, M. H.; Poustie, A.; Westerhoff, P.; Hanigan, D., Non-target mass spectrometry analysis of NDMA precursors in advanced treatment for potable reuse. *Environmental Science: Water Research & Technology* **2018,** *4* (12), 1944-1955.
85. Huang, Y.; Kong, M.; Coffin, S.; Cochran, K. H.; Westerman, D. C.; Schlenk, D.; Richardson, S. D.; Lei, L.; Dionysiou, D. D., Degradation of contaminants of emerging concern by UV/H2O2 for water reuse: Kinetics, mechanisms, and cytotoxicity analysis. *Water Res* **2020,** *174*, 115587.
86. Chuang, Y. H.; Wu, K. L.; Lin, W. C.; Shi, H. J., Photolysis of Chlorine Dioxide under UVA Irradiation: Radical Formation, Application in Treating Micropollutants,

Formation of Disinfection Byproducts, and Toxicity under Scenarios Relevant to Potable Reuse and Drinking Water. *Environ Sci Technol* **2022**.
87. Escher, B. I.; van Daele, C.; Dutt, M.; Tang, J. Y.; Altenburger, R., Most oxidative stress response in water samples comes from unknown chemicals: the need for effect-based water quality trigger values. *Environ Sci Technol* **2013,** *47* (13), 7002-11.
88. Hanigan, D.; Truong, L.; Simonich, M.; Tanguay, R.; Westerhoff, P., Zebrafish embryo toxicity of 15 chlorinated, brominated, and iodinated disinfection by-products. *J Environ Sci (China)* **2017,** *58*, 302-310.
89. Schymanski, E. L.; Singer, H. P.; Slobodnik, J.; Ipolyi, I. M.; Oswald, P.; Krauss, M.; Schulze, T.; Haglund, P.; Letzel, T.; Grosse, S.; Thomaidis, N. S.; Bletsou, A.; Zwiener, C.; Ibanez, M.; Portoles, T.; de Boer, R.; Reid, M. J.; Onghena, M.; Kunkel, U.; Schulz, W.; Guillon, A.; Noyon, N.; Leroy, G.; Bados, P.; Bogialli, S.; Stipanicev, D.; Rostkowski, P.; Hollender, J., Non-target screening with high-resolution mass spectrometry: critical review using a collaborative trial on water analysis. *Anal Bioanal Chem* **2015,** *407* (21), 6237-55.
90. Albergamo, V.; Escher, B. I.; Schymanski, E. L.; Helmus, R.; Dingemans, M. M. L.; Cornelissen, E. R.; Kraak, M. H. S.; Hollender, J.; de Voogt, P., Evaluation of reverse osmosis drinking water treatment of riverbank filtrate using bioanalytical tools and non-target screening. *Environmental Science: Water Research & Technology* **2020,** *6* (1), 103-116.
91. Soliman, M. A.; Pedersen, J. A.; Park, H.; Castaneda-Jimenez, A.; Stenstrom, M. K.; Suffet, I. H., Human pharmaceuticals, antioxidants, and plasticizers in wastewater treatment plant and water reclamation plant effluents. *Water Environ Res* **2007,** *79* (2), 156-67.
92. Ishida, K. P.; Luna, R. F.; Richardot, W. H.; Lopez-Galvez, N.; Plumlee, M. H.; Dodder, N. G.; Hoh, E., Nontargeted Analysis of Trace Organic Constituents in Reverse Osmosis and UV-AOP Product Waters of a Potable Reuse Facility. *ACS ES&T Water* **2021**.
93. Tang, J. Y. M.; Busetti, F.; Charrois, J. W. A.; Escher, B. I., Which chemicals drive biological effects in wastewater and recycled water? *Water Research* **2014,** *60*, 289-299.
94. Escher, B. I.; Allinson, M.; Altenburger, R.; Bain, P. A.; Balaguer, P.; Busch, W.; Crago, J.; Denslow, N. D.; Dopp, E.; Hilscherova, K.; Humpage, A. R.; Kumar, A.; Grimaldi, M.; Jayasinghe, B. S.; Jarosova, B.; Jia, A.; Makarov, S.; Maruya, K. A.; Medvedev, A.; Mehinto, A. C.; Mendez, J. E.; Poulsen, A.; Prochazka, E.; Richard, J.; Schifferli, A.; Schlenk, D.; Scholz, S.; Shiraishi, F.; Snyder, S.; Su, G.; Tang, J. Y.; van der Burg, B.; van der Linden, S. C.; Werner, I.; Westerheide, S. D.; Wong, C. K.; Yang, M.; Yeung, B. H.; Zhang, X.; Leusch, F. D., Benchmarking organic micropollutants in wastewater, recycled water and drinking water with in vitro bioassays. *Environ Sci Technol* **2014,** *48* (3), 1940-56.
95. Escher, B.; Leusch, F., *Bioanalytical tools in water quality assessment*. IWA publishing: 2011.
96. Neale, P. A.; Antony, A.; Bartkow, M. E.; Farre, M. J.; Heitz, A.; Kristiana, I.; Tang, J. Y.; Escher, B. I., Bioanalytical assessment of the formation of disinfection byproducts in a drinking water treatment plant. *Environ Sci Technol* **2012,** *46* (18), 10317-25.
97. McKenna, E.; Thompson, K. A.; Taylor-Edmonds, L.; McCurry, D. L.; Hanigan, D., Summation of disinfection by-product CHO cell relative toxicity indices: sampling bias,

uncertainty, and a path forward. *Environmental Science: Processes & Impacts* **2020,** *22* (3), 708-718.
98. Lau, S. S.; Wei, X.; Bokenkamp, K.; Wagner, E. D.; Plewa, M. J.; Mitch, W. A., Assessing Additivity of Cytotoxicity Associated with Disinfection Byproducts in Potable Reuse and Conventional Drinking Waters. *Environmental Science & Technology* **2020,** *54* (9), 5729-5736.
99. Liu, C.; Shin, Y. H.; Wei, X.; Ersan, M. S.; Wagner, E.; Plewa, M. J.; Amy, G.; Karanfil, T., Preferential Halogenation of Algal Organic Matter by Iodine over Chlorine and Bromine: Formation of Disinfection Byproducts and Correlation with Toxicity of Disinfected Waters. *Environ. Sci. Technol.* **2021**.
100. Hanigan, D.; Liao, X.; Zhang, J.; Herckes, P.; Westerhoff, P., Sorption and desorption of organic matter on solid-phase extraction media to isolate and identify N-nitrosodimethylamine precursors. *J Sep Sci* **2016,** *39* (14), 2796-805.
101. Mackey, E. D.; Hofmann, R.; Festger, A.; Vanyo, C. *UV-Chlorine AOP in Potable Reuse: A Guidance Manual to Assessment and Implementation (Report No. 5050)*; The Water Research Foundation, 2022.
102. Sun, P.; Meng, T.; Wang, Z.; Zhang, R.; Yao, H.; Yang, Y.; Zhao, L., Degradation of Organic Micropollutants in UV/NH(2)Cl Advanced Oxidation Process. *Environ Sci Technol* **2019,** *53* (15), 9024-9033.
103. Jiang, B.; Tian, Y.; Zhang, Z.; Yin, Z.; Feng, L.; Liu, Y.; Zhang, L., Degradation behaviors of Isopropylphenazone and Aminopyrine and their genetic toxicity variations during UV/chloramine treatment. *Water Res* **2020,** *170*, 115339.
104. Zheng, D.; Andrews, R. C.; Andrews, S. A.; Taylor-Edmonds, L., Effects of coagulation on the removal of natural organic matter, genotoxicity, and precursors to halogenated furanones. *Water Res* **2015,** *70*, 118-29.
105. Myers, O. D.; Sumner, S. J.; Li, S.; Barnes, S.; Du, X., One Step Forward for Reducing False Positive and False Negative Compound Identifications from Mass Spectrometry Metabolomics Data: New Algorithms for Constructing Extracted Ion Chromatograms and Detecting Chromatographic Peaks. *Anal Chem* **2017,** *89* (17), 8696-8703.
106. Verkh, Y.; Rozman, M.; Petrovic, M., Extraction and cleansing of data for a non-targeted analysis of high-resolution mass spectrometry data of wastewater. *MethodsX* **2018,** *5*, 395-402.
107. Pluskal, T. s.; Uehara, T.; Yanagida, M., Highly accurate chemical formula prediction tool utilizing high-resolution mass spectra, MS/MS fragmentation, heuristic rules, and isotope pattern matching. *Analytical chemistry* **2012,** *84* (10), 4396-4403.
108. R Core Team, R: A Language and Environment for Statistical Computing. R Foundation for Statistical Computing, Vienna, Austria. URL http://www.R-project.org. **2019**.
109. Sun, J.; Peng, H.; Alharbi, H. A.; Jones, P. D.; Giesy, J. P.; Wiseman, S. B., Identification of Chemicals that Cause Oxidative Stress in Oil Sands Process-Affected Water. *Environ Sci Technol* **2017,** *51* (15), 8773-8781.
110. Escher, B. I.; Dutt, M.; Maylin, E.; Tang, J. Y.; Toze, S.; Wolf, C. R.; Lang, M., Water quality assessment using the AREc32 reporter gene assay indicative of the oxidative stress response pathway. *Journal of Environmental Monitoring* **2012,** *14* (11), 2877-2885.

111. Hanigan, D.; Ferrer, I.; Thurman, E. M.; Herckes, P.; Westerhoff, P., LC/QTOF-MS fragmentation of N-nitrosodimethylamine precursors in drinking water supplies is predictable and aids their identification. *J Hazard Mater* **2017,** *323* (Pt A), 18-25.
112. Ferrer, I.; Thurman, E. M., Analysis of 100 pharmaceuticals and their degradates in water samples by liquid chromatography/quadrupole time-of-flight mass spectrometry. *J Chromatogr A* **2012,** *1259*, 148-57.
113. Ferrer, I.; Thurman, E. M., Multi-residue method for the analysis of 101 pesticides and their degradates in food and water samples by liquid chromatography/time-of-flight mass spectrometry. *J Chromatogr A* **2007,** *1175* (1), 24-37.
114. Gao, Y.-q.; Gao, N.-y.; Chen, J.-x.; Zhang, J.; Yin, D.-q., Oxidation of β-blocker atenolol by a combination of UV light and chlorine: Kinetics, degradation pathways and toxicity assessment. *Separation and Purification Technology* **2020,** *231*, 115927.
115. Yang, T.; Mai, J.; Wu, S.; Liu, C.; Tang, L.; Mo, Z.; Zhang, M.; Guo, L.; Liu, M.; Ma, J., UV/chlorine process for degradation of benzothiazole and benzotriazole in water: Efficiency, mechanism and toxicity evaluation. *Science of The Total Environment* **2021,** *760*.
116. Nam, S. W.; Yoon, Y.; Choi, D. J.; Zoh, K. D., Degradation characteristics of metoprolol during UV/chlorination reaction and a factorial design optimization. *J Hazard Mater* **2015,** *285*, 453-63.
117. Chen, C.-Y., The Oxidation of Di-(2-Ethylhexyl) Phthalate (DEHP) in Aqueous Solution by UV/H2O2 Photolysis. *Water, Air, & Soil Pollution* **2009,** *209* (1-4), 411-417.
118. Thurman, E. M.; Ferrer, I.; Barceló, D., Choosing between Atmospheric Pressure Chemical Ionization and Electrospray Ionization Interfaces for the HPLC/MS Analysis of Pesticides. *Analytical Chemistry* **2001,** *73* (22), 5441-5449.
119. Maizel, A. C.; Remucal, C. K., The effect of advanced secondary municipal wastewater treatment on the molecular composition of dissolved organic matter. *Water Res* **2017,** *122*, 42-52.
120. Qian, Y.; Chen, Y.; Hanigan, D.; Shi, Y.; Sun, S.; Hu, Y.; An, D., pH adjustment improves the removal of disinfection byproduct precursors from sedimentation sludge water. *Resources, Conservation and Recycling* **2022,** *179*.
121. Ishida, K. P.; Luna, R. F.; Richardot, W. H.; Lopez-Galvez, N.; Plumlee, M. H.; Dodder, N. G.; Hoh, E., Nontargeted Analysis of Trace Organic Constituents in Reverse Osmosis and UV-AOP Product Waters of a Potable Reuse Facility. *ACS ES&T Water* **2021,** *2* (1), 96-105.
122. Allen, J. M.; Plewa, M. J.; Wagner, E. D.; Wei, X.; Bokenkamp, K.; Hur, K.; Jia, A.; Liberatore, H. K.; Lee, C. T.; Shirkhani, R.; Krasner, S. W.; Richardson, S. D., Drivers of Disinfection Byproduct Cytotoxicity in U.S. Drinking Water: Should Other DBPs Be Considered for Regulation? *Environ. Sci. Technol.* **2021**.
123. Kellerman, A. M.; Dittmar, T.; Kothawala, D. N.; Tranvik, L. J., Chemodiversity of dissolved organic matter in lakes driven by climate and hydrology. *Nat Commun* **2014,** *5*, 3804.
124. Varanasi, L.; Coscarelli, E.; Khaksari, M.; Mazzoleni, L. R.; Minakata, D., Transformations of dissolved organic matter induced by UV photolysis, Hydroxyl radicals, chlorine radicals, and sulfate radicals in aqueous-phase UV-Based advanced oxidation processes. *Water Res* **2018,** *135*, 22-30.

125. Snyder, S. A., Emerging chemical contaminants: Looking for greater harmony. *Journal-American Water Works Association* **2014,** *106* (8), 38-52.
126. Neale, P. A.; Escher, B. I., In vitro bioassays to assess drinking water quality. *Current Opinion in Environmental Science & Health* **2019,** *7*, 1-7.
127. Hebert, A.; Feliers, C.; Lecarpentier, C.; Neale, P. A.; Schlichting, R.; Thibert, S.; Escher, B. I., Bioanalytical assessment of adaptive stress responses in drinking water: A predictive tool to differentiate between micropollutants and disinfection by-products. *Water Research* **2018,** *132*, 340-349.
128. Roback, S.; Plumlee, M. H.; Hanigan, D.; Song, M.; Mckenna, L. *Understanding the Formation of a Critical Disinfection Byproduct: NDMA and NDMA Precursors in Advanced Potable Reuse Treatment Plants (Report No. 222)*; Orange County Water District, CA. Online Link: https://www.usbr.gov/research/dwpr/DWPR_Reports.html: 2022.
129. Boards, C. W. Drinking Water Notification Levels. https://www.waterboards.ca.gov/drinking_water/certlic/drinkingwater/NotificationLevels.html (accessed October 1, 2022).
130. Huang, M. E.; Huang, S.; McCurry, D. L., Re-Examining the Role of Dichloramine in High-Yield N-Nitrosodimethylamine Formation from N,N-Dimethyl-α-arylamines. *Environmental Science & Technology Letters* **2018,** *5* (3), 154-159.
131. Plumlee, M. H.; Lopez-Mesas, M.; Heidlberger, A.; Ishida, K. P.; Reinhard, M., N-nitrosodimethylamine (NDMA) removal by reverse osmosis and UV treatment and analysis via LC-MS/MS. *Water Res* **2008,** *42* (1-2), 347-55.
132. Bellona, C.; Drewes, J. E.; Oelker, G.; Luna, J.; Filteau, G.; Amy, G., Comparing nanofiltration and reverse osmosis for drinking water augmentation. *Journal AWWA* **2008,** *100* (9), 102-116.
133. Reny, R.; Plumlee, M. H.; Kodamatani, H.; Suffet, I. H. M.; Roback, S. L., NDMA and NDMA precursor attenuation in environmental buffers prior to groundwater recharge for potable reuse. *Sci Total Environ* **2021,** *762*, 144287.
134. Mitch, W. A.; Sedlak, D. L., Characterization and Fate of N-Nitrosodimethylamine Precursors in Municipal Wastewater Treatment Plants. *Environmental Science & Technology* **2004,** *38* (5), 1445-1454.
135. Gerecke, A. C.; Sedlak, D. L., Precursors of N-Nitrosodimethylamine in Natural Waters. *Environmental Science & Technology* **2003,** *37* (7), 1331-1336.
136. Sedlak, D. L.; Deeb, R. A.; Hawley, E. L.; Mitch, W. A.; Durbin, T. D.; Mowbray, S.; Carr, S., Sources and fate of nitrosodimethylamine and its precursors in municipal wastewater treatment plants. *Water environment research* **2005,** *77* (1), 32-39.
137. Lee, C.; Schmidt, C.; Yoon, J.; von Gunten, U., Oxidation of N-Nitrosodimethylamine (NDMA) Precursors with Ozone and Chlorine Dioxide: Kinetics and Effect on NDMA Formation Potential. *Environmental Science & Technology* **2007,** *41* (6), 2056-2063.
138. Le Roux, J.; Gallard, H.; Croue, J. P., Formation of NDMA and halogenated DBPs by chloramination of tertiary amines: the influence of bromide ion. *Environ Sci Technol* **2012,** *46* (3), 1581-9.

139. Schreiber, I. M.; Mitch, W. A., Influence of the Order of Reagent Addition on NDMA Formation during Chloramination. *Environmental Science & Technology* **2005,** *39* (10), 3811-3818.
140. Fujioka, T.; Ishida, K. P.; Shintani, T.; Kodamatani, H., High rejection reverse osmosis membrane for removal of N-nitrosamines and their precursors. *Water Res* **2018,** *131*, 45-51.
141. Szczuka, A.; Huang, N.; MacDonald, J. A.; Nayak, A.; Zhang, Z.; Mitch, W. A., N-Nitrosodimethylamine Formation during UV/Hydrogen Peroxide and UV/Chlorine Advanced Oxidation Process Treatment Following Reverse Osmosis for Potable Reuse. *Environ Sci Technol* **2020,** *54* (23), 15465-15475.
142. Miyashita, Y.; Park, S.-H.; Hyung, H.; Huang, C.-H.; Kim, J.-H., Removal of N-nitrosamines and their precursors by nanofiltration and reverse osmosis membranes. *Journal of environmental engineering* **2009,** *135* (9), 788-795.
143. Deborde, M.; von Gunten, U., Reactions of chlorine with inorganic and organic compounds during water treatment-Kinetics and mechanisms: a critical review. *Water Res* **2008,** *42* (1-2), 13-51.
144. Lee, C.; Choi, W.; Kim, Y. G.; Yoon, J., UV Photolytic Mechanism of N-Nitrosodimethylamine in Water: Dual Pathways to Methylamine versus Dimethylamine. *Environmental Science & Technology* **2005,** *39* (7), 2101-2106.
145. Mitch, W. A.; Gerecke, A. C.; Sedlak, D. L., A N-Nitrosodimethylamine (NDMA) precursor analysis for chlorination of water and wastewater. *Water Research* **2003,** *37* (15), 3733-3741.
146. Verdu-Andres, J.; Campins-Falco, P.; Herraez-Hernandez, R., Determination of aliphatic amines in water by liquid chromatography using solid-phase extraction cartridges for preconcentration and derivatization. *Analyst* **2001,** *126* (10), 1683-8.
147. Zhang, J.; Hanigan, D.; Westerhoff, P.; Herckes, P., N-Nitrosamine formation kinetics in wastewater effluents and surface waters. *Environmental Science: Water Research & Technology* **2016,** *2* (2), 312-319.
148. Munch, J.; Bassett, M., Method 521 Determination of nitrosamines in drinking water by solid phase extraction and capillary column gas chromatography with large volume injection and chemical ionization tandem mass spectrometry (MS/MS). *National Exposure Research Laboratory Office of Research and Development, US Environmental Protection Agency* **2004**.
149. Goosen, M.; Sablani, S.; Al-Hinai, H.; Al-Obeidani, S.; Al-Belushi, R.; Jackson, a., Fouling of reverse osmosis and ultrafiltration membranes: a critical review. *Separation science and technology* **2005,** *39* (10), 2261-2297.
150. Wang, S.; Patel, M.; Dunivin, B.; Clark, J.; Foellmi, S.; Dipietro, C., Post-treatment Optimization to Enhance Groundwater Recharge Operations. *Journal-American Water Works Association* **2015,** *107* (5), 87-92.
151. Soltermann, F.; Lee, M.; Canonica, S.; von Gunten, U., Enhanced N-nitrosamine formation in pool water by UV irradiation of chlorinated secondary amines in the presence of monochloramine. *Water Res* **2013,** *47* (1), 79-90.
152. Stefan, M. I.; Bolton, J. R., UV direct photolysis of N-nitrosodimethylamine (NDMA): Kinetic and product study. *Helvetica Chimica Acta* **2002,** *85* (5), 1416-1426.

153. Roback, S. L.; Ishida, K. P.; Chuang, Y.-H.; Zhang, Z.; Mitch, W. A.; Plumlee, M. H., Pilot UV-AOP Comparison of UV/Hydrogen Peroxide, UV/Free Chlorine, and UV/Monochloramine for the Removal of N-Nitrosodimethylamine (NDMA) and NDMA Precursors. *ACS ES&T Water* **2020,** *1* (2), 396-406.
154. Chen, Z.; Valentine, R. L., Formation of N-Nitrosodimethylamine (NDMA) from Humic Substances in Natural Water. *Environmental Science & Technology* **2007,** *41* (17), 6059-6065.
155. Bei, E.; Liao, X.; Meng, X.; Li, S.; Wang, J.; Sheng, D.; Chao, M.; Chen, Z.; Zhang, X.; Chen, C., Identification of nitrosamine precursors from urban drainage during storm events: A case study in southern China. *Chemosphere* **2016,** *160*, 323-331.
156. TMWA, Your water: Water resources ⟨http://tmwa.com/water_system/resources/⟩. *Truckee Meadows Water Authority* **2012**.
157. Survey, U. S. G., USGS The National Map: Hydrography Dataset. **2022**.
158. USGS, Water Data for the Nation. *United States Geological Survey* **2020**.
159. USGS, Water Data for the Nation. *United States Geological Survey* **2021**.
160. Bohman, L. R., *Estimation of Traveltime Characteristics for Truckee River Between Truckee, California, and Marble Bluff Dam Near Nixon, Nevada, and for Truckee Canal in Nevada*. US Department of the Interior, US Geological Survey: 2000; Vol. 99.
161. Crompton, E. J.; Bohman, L. R., *Traveltime data for Truckee River between Tahoe City, California, and Marble Bluff Dam near Nixon, Nevada, 1999*. US Department of the Interior, US Geological Survey: 2000.
162. Schreiber, I. M.; Mitch, W. A., Occurrence and Fate of Nitrosamines and Nitrosamine Precursors in Wastewater-Impacted Surface Waters Using Boron As a Conservative Tracer. *Environmental Science & Technology* **2006,** *40* (10), 3203-3210.
163. Pehlivanoglu-Mantas, E.; Sedlak, D. L., The fate of wastewater-derived NDMA precursors in the aquatic environment. *Water Research* **2006,** *40* (6), 1287-1293.
164. Asami, M.; Oya, M.; Kosaka, K., A nationwide survey of NDMA in raw and drinking water in Japan. *Science of The Total Environment* **2009,** *407* (11), 3540-3545.
165. Sanchis, J.; Gernjak, W.; Munne, A.; Catalan, N.; Petrovic, M.; Farre, M. J., Fate of N-nitrosodimethylamine and its precursors during a wastewater reuse trial in the Llobregat River (Spain). *J Hazard Mater* **2020**, 124346.
166. Chen, B.; Nam, S. N.; Westerhoff, P. K.; Krasner, S. W.; Amy, G., Fate of effluent organic matter and DBP precursors in an effluent-dominated river: a case study of wastewater impact on downstream water quality. *Water Res* **2009,** *43* (6), 1755-65.
167. Huy, N. V.; Murakami, M.; Sakai, H.; Oguma, K.; Kosaka, K.; Asami, M.; Takizawa, S., Occurrence and formation potential of N-nitrosodimethylamine in ground water and river water in Tokyo. *Water Res* **2011,** *45* (11), 3369-77.
168. Plumlee, M. H.; Reinhard, M., Photochemical Attenuation of N-Nitrosodimethylamine (NDMA) and other Nitrosamines in Surface Water. *Environmental Science & Technology* **2007,** *41* (17), 6170-6176.
169. Uzun, H.; Kim, D.; Karanfil, T., Seasonal and temporal patterns of NDMA formation potentials in surface waters. *Water Research* **2015,** *69*, 162-172.
170. Koch, B. P.; Dittmar, T., From mass to structure: an aromaticity index for high-resolution mass data of natural organic matter. *Rapid Communications in Mass Spectrometry* **2006,** *20* (5), 926-932.

171. Shannon Roback, M. H. P., Kenneth P. Ishida, Hitoshi Kodamatani, Takahiro Fujioka, Use of Rapid, Novel NDMA Analysis Method to Discern Diurnal and Seasonal Trends in NDMA and NDMA Precursors at an Advanced Water Treatment Facility. In *American Water Works Association International Symposium on Water Reuse*, Austin, TX, 2018.
172. McKenna, E. Disinfection By-Products in Potable Reuse Water and Interpretation of Their Relative Toxicities. University of Nevada, Reno, 2020.

Appendix A – Supplementation information for Chapter 3

Text A-1 Analytical Methods

Sample Extraction with MCX cartridges for NTA samples. MCX cartridges were conditioned with 20 mL of methanol, followed by 30 mL of HPLC-grade water. One liter of acidified sample (pH<3) was loaded onto the MCX cartridges at 5 mL/min. Cartridges were dried for 45 min using ultra high purity nitrogen gas (UHP), then eluted with 10 mL of a 5% ammonium hydroxide solution in methanol. Eluates were evaporated to 1 mL in a TurboVap at 40°C using a gentle stream of UHP nitrogen gas. 2 L of samples were extracted in duplicate on separate cartridges and the isolates combined to expedite the extraction process. The combined 2 mL isolates were transferred to amber vials and stored at -20°C.

LC-qTOF/MS method details

The mobile phase consisted of 0.1% formic acid in water (phase A) and acetonitrile (phase B). The optimized chromatographic method held the initial mobile phase composition (10% B) constant for 5 min, followed by a linear gradient to 100% B after 30 min. The flow-rate used was 0.6 mL/min. A 10-min post-run time was used after each analysis. The LC-qTOF/MS was operated in positive mode using the following parameters: capillary voltage: 3500 V; nebulizer pressure: 45 psi; drying gas: 10 L/min; gas temperature: 250°C; sheath gas flow: 11 L min-1; sheath gas temperature: 350°C; nozzle voltage: 0 V, fragmentor voltage: 190 V; skimmer voltage: 65 V; octopole RF: 750 V. The accurate mass spectra were recorded across the range 50–1000 m/z at 2 GHz. For quality assurance and control, stability of mass accuracy was checked daily and if values were above 2 ppm error, the instrument was re-calibrated. Accurate mass measurements of each peak from the extracted ion chromatograms were obtained by means of a calibrant solution delivered by an external quaternary pump. This solution contained the internal reference masses purine ($C_5H_4N_4$ at m/z 121.0509) and HP-921 [hexakis-(1H, 1H, 3H-tetrafluoro-pentoxy)phosphazene] ($C_{18}H_{18}O_6N_3P_3F_{24}$ at m/z 922.0098). The instrument provided a mass resolving power of 30,000 ± 500 (m/z 1522).

Van Krevelen diagram boundary regions

Each formula that represents the identified chemical composition was further categorized into four groups of compounds (i.e., condensed aromatic compounds, aromatic compounds, olefins, and aliphatic compounds) based on an aromaticity index (AI_{mod}) [170].

$$AI_{mod} = \frac{1+\left(\#\text{of C}\right)-0.5\times\left(\#\text{of O}\right)-\left(\#\text{of S}\right)-0.5\times\left(\#\text{of H}\right)-0.5\times\left(\#\text{of N}\right)}{\left(\#\text{of C}\right)-0.5\times\left(\#\text{of O}\right)-\left(\#\text{of S}\right)-\left(\#\text{of N}\right)}$$

where # of C, # of O, # of S, # of H, and # of N represents the number of carbon atoms, oxygen atoms, sulfur atoms, hydrogen atoms, and nitrogen atoms in each chemical formula determined, respectively. Condensed aromatic compounds were assigned based on $0.67 \leq AI_{mod} \leq 1.5$, aromatic compounds ($0.5 \leq AI_{mod} < 0.67$), olefins ($0 < AI_{mod} < 0.5$), and aliphatic compounds ($AI_{mod} \leq 0$ and $1.5 < AI_{mod}$).

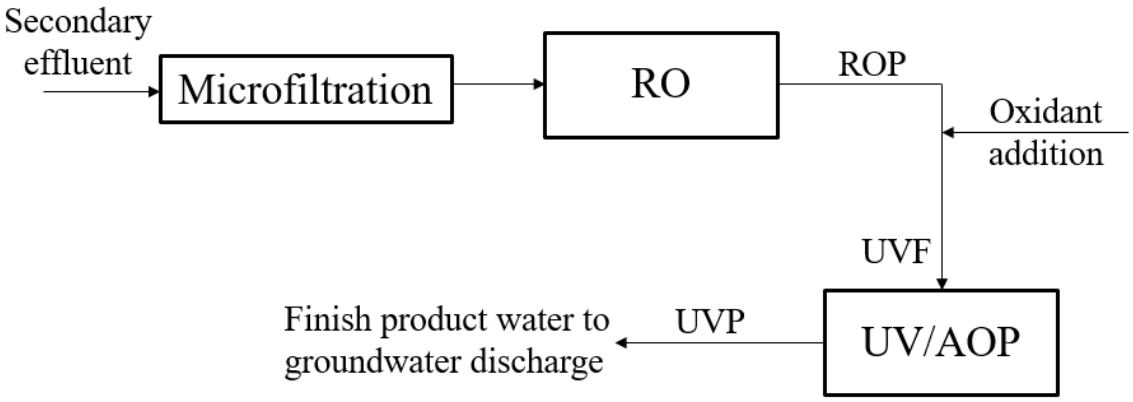

Figure A-1. OCWD AWPF treatment process and sampling locations (ROP = reverse osmosis permeates, UVF = ultraviolet feed, and UVP = ultraviolet product).

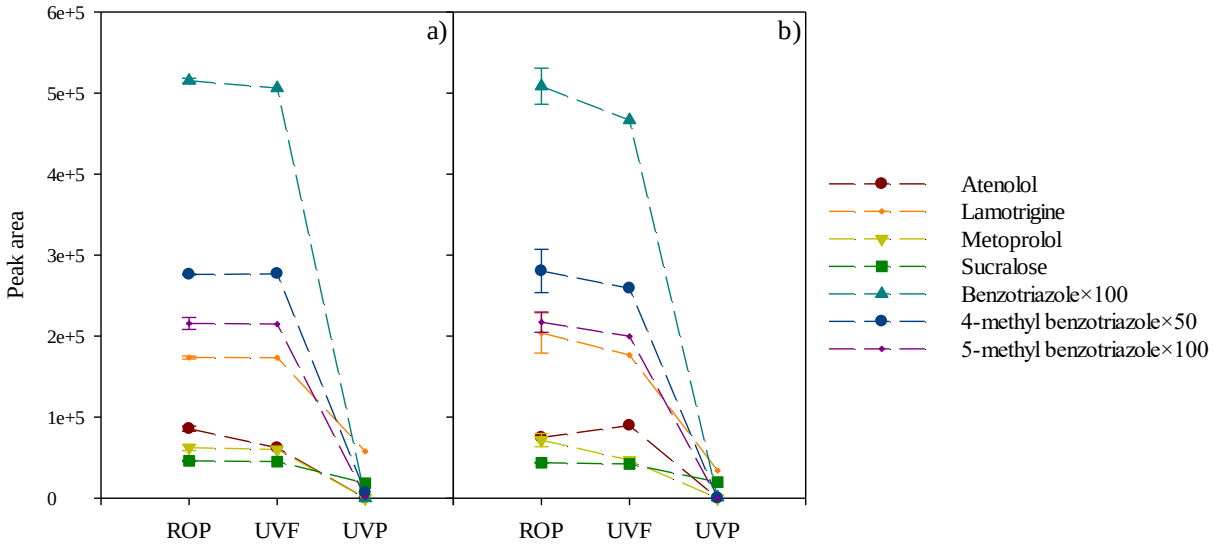

Figure A-2. Peak area of suspect compounds in MCX extracts of samples from 2019 ROP, UVF, and UVP treated by a) UV/HOCl, b) UV/H_2O_2. Compound×factor indicates the offset of the data for clarity.

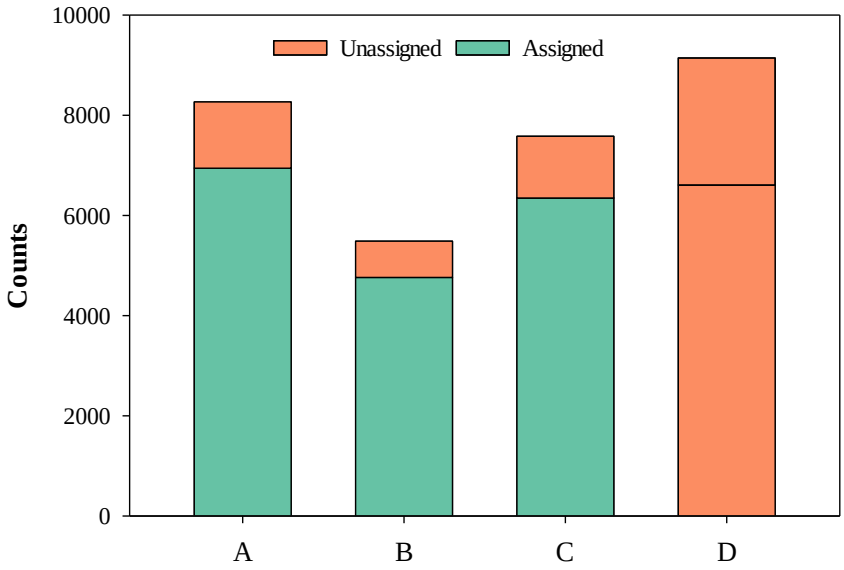

Figure A-3. Number of assigned and unassigned features under different oxidant additions from LC-qTOF/MS data produced from samples taken in 2018 (A: UV/HOCl, B: UV/H_2O_2, C: UV/NH_2Cl, and D: UV/ambient).

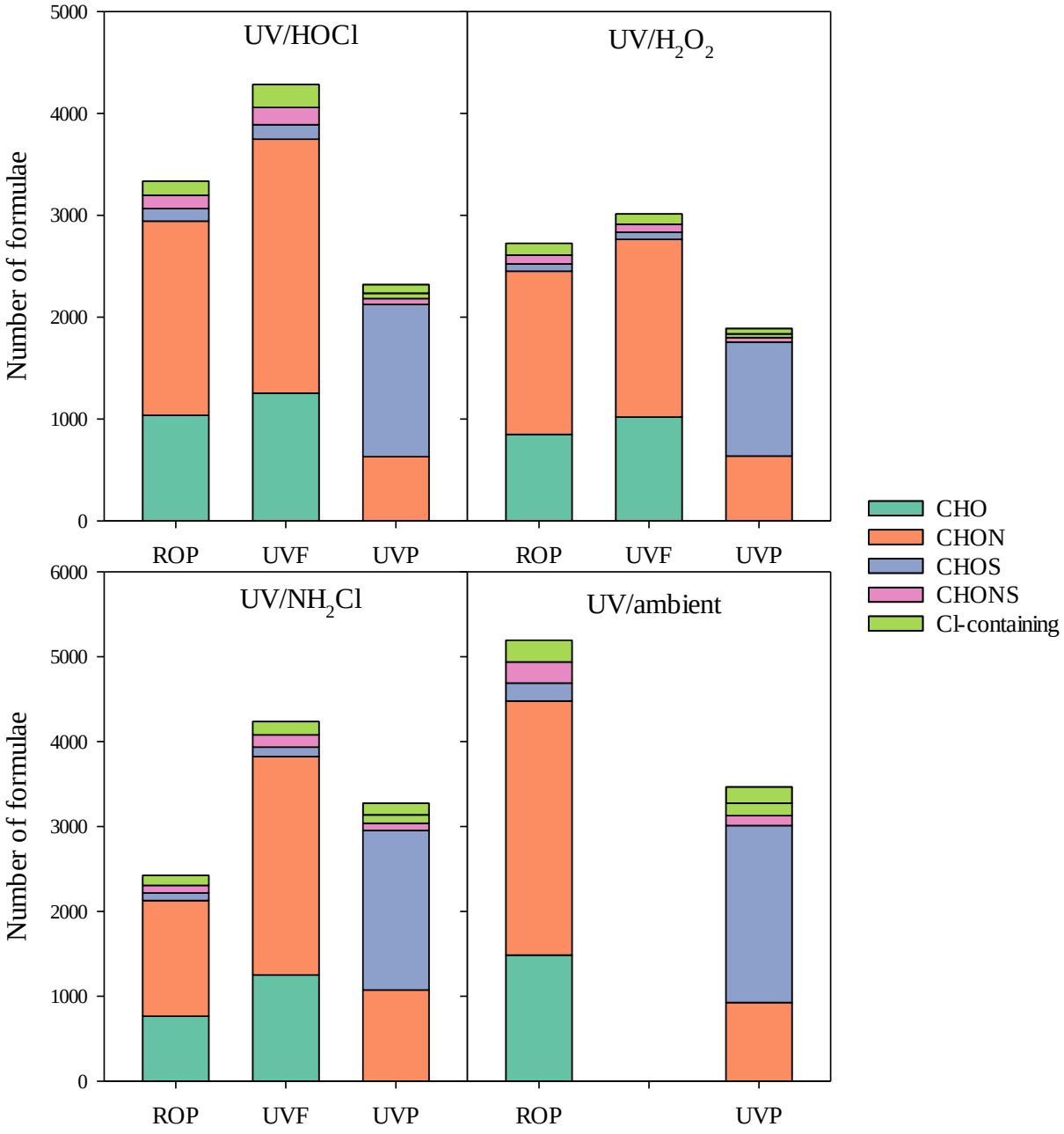

Figure A-4. Elemental composition of the organic compounds sampled in 2018 across the treatment system under varying oxidation conditions of samples extracted with MCX cartridges and analyzed by LC-qTOF/MS. Cl-containing includes all compounds containing any combination of C, H, O, N, or S and at least one Cl.

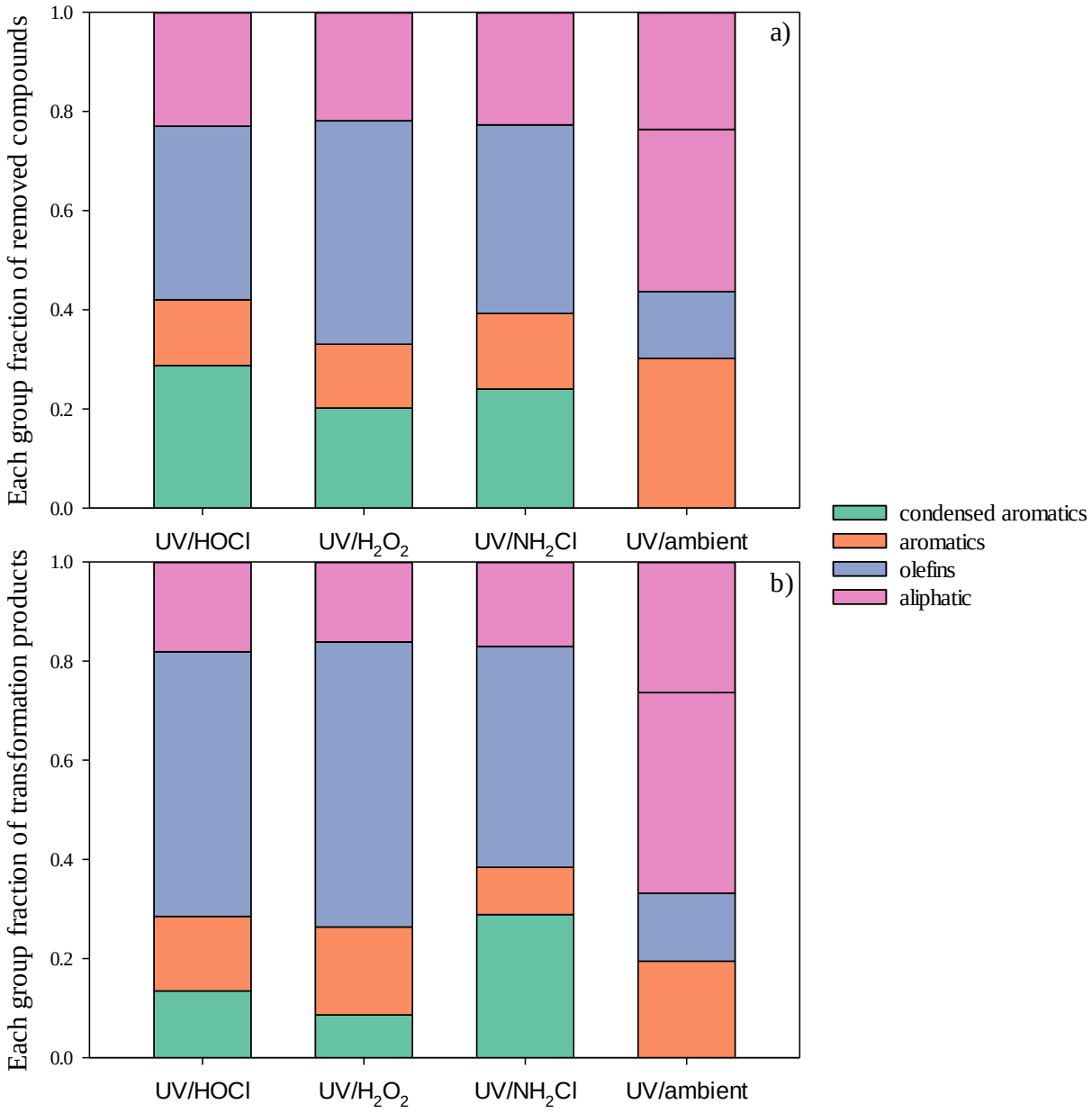

Figure A-5. Fractional representation of a) decomposed compounds and b) transformation products sampled in 2018 across the treatment system under varying oxidation conditions of samples extracted with MCX cartridges and analyzed by LC-qTOF/MS.

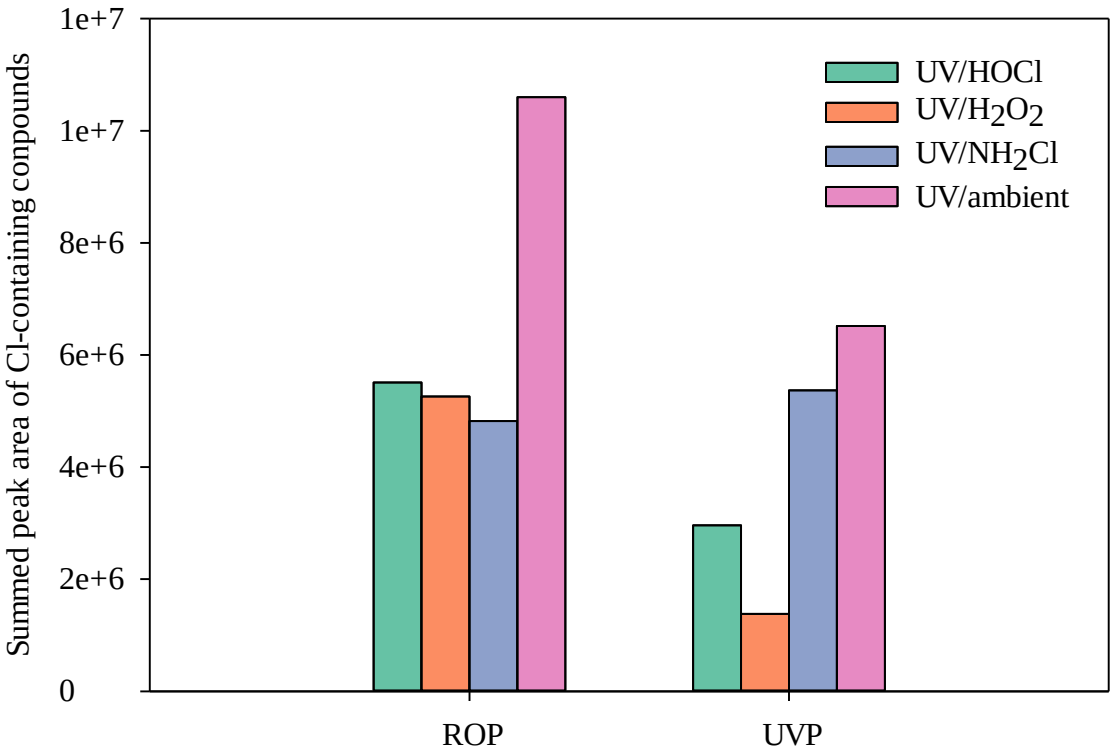

Figure A-6. Summed peak area of Cl-containing compounds across the treatment system under varying oxidation conditions of samples extracted with MCX cartridges and analyzed by LC-qTOF/MS.

Table A-1. Summary of samples and associated water quality.

Sampling events			Sample number	Total Cl_2 (mg-Cl_2/L)	Free Cl_2 (mg-Cl_2/L)	NH_2Cl (mg-Cl_2/L)	NH_3-N (mg-N/L)	H_2O_2 (mg/L)	UVT (%)	pH
2018 Sampling	UV/HOCl	ROP	2	2.3	ND	1.5	ND	/	96.8	/
		UVF	1	4.3	/	/	/	/	70.6	5.90
		UVP	1	1.7	/	/	/	/	76.1	5.78
	UV/H_2O_2	ROP	2	2.3	ND	1.5	0.02	/	98.0	5.90
		UVF	1	3.6	ND	1.6	0.09	2.9	95.9	5.94
		UVP	1	1.7	ND	0.6	0.15	2.4	70.9	5.70
	UV/NH_2Cl	ROP	2	2.1	ND	1.5	0.02	/	80.6	/
		UVF	2	4.3	0.02	3.4	0.13	/	69.0	5.96
		UVP	2	1.8	ND	1.1	0.28	/	98.1	5.68
	UV/ ambient	ROP	1	2.3	0.01	1.5	0.04	/	94.9	5.9
		UVP	1	1.0	ND	0.5	0.14	/	73.5	5.6
2019 Sampling	UV/HOCl	ROP	2	2.0	0.25	0.9	0.06	/	98.8	6.01
		UVF	1	4.3	0.64	1.1	ND	/	98.7	6.06
		UVP	1	2.1	0.39	0.5	ND	/	99.8	6.02
	UV/H_2O_2	ROP	2	3.0	ND	2.2	0.11	/	97.5	5.83
		UVF	1	4.3	ND	2.2	0.08	2.8	97.6	5.89
		UVP	1	2.3	ND	0.9	0.16	2.4	99.5	5.69

ND-Non-detect; /-Not measured.

Table A-2. Preprocessing parameters of peak detection, EIC building and peak picking for all data files.

	Parameters	
Peak detection	Mass Detector	centroid
	Noise level	500
EIC construction	Min group size	7
	Group intensity threshold	1000
	Min highest intensity	2500
	m/z tolerance	0.01
Peak picking	S/N threshold	10
	Min feature height	2500
	Coefficient/area threshold	110
	Peak duration range	0.02-1.00
Alignment	m/z tolerance	0.005 m/z or 5.0 ppm
	Weight for m/z	20
	Retention time tolerance	3%
	Weight for retention time	10
	Require same charge state	Yes

Table A-3. Broad-spectrum bioassays used to assess water quality.

Bioassay	Test Species (strain/cell line)	Endpoint	Detected Signal
p53 assay	Luciferase reporter gene under the control of the p53 response element in Hela stable cell line	Monitor activation of p53 by treatment; responsive to DNA damage and cellular stress.	Luciferase RLU of treated cells compared to negative control
SOS-Chromotest™	B-galactosidase reporter gene under the control of SOS response element and alkaline phosphatase reporter gene for general metabolism in *E.coli* PQ17 bacterial strain	Activation of the DNA repair pathway to direct (mutagenic) and indirect (oxidative) in response to DNA damage	Ratio of blue (OD at 605nm) to green fluorescence emission (OD at 420 nm) excitation of reporter enzyme substrates
ARE-Nrf2	Luciferase reporter under the control of the NRf2 anti-oxidant response element in human breast cancer cell line MCF7	Activation of the oxidative stress response pathway NRf2-ARE	Luciferase RLU of treated cells compared to negative control
MTT cell viability	MTT dye added to exposed human breast cancer cell line MCF7	Indicates metabolic activity and cell viability	OD at 540 nm as marker for MTT cell viability

Table A-4. Suspect compounds in all water samples. Matches with a score of <80 were disregarded. In prior experiments with this instrument, molecular features with high scores (> 80, full score 100) were nearly always a correct hit.

Name	Formula	Retention time (min)	Calculated m/z	Compound group
Atenolol	$C_{14}H_{22}N_2O_3$	4.4	267.1703	blood pressure medication
Carbendazim	$C_9H_9N_3O_2$	7.6	192.0768	fungicide
Thiabendazole	$C_{10}H_7N_3S$	9.3	202.0433	fungicide
Trimethoprim	$C_{14}H_{18}N_4O_3$	10.6	291.1452	antibiotic
Phthalic acid	$C_8H_6O_4$	11.3	167.0339	plasticizer
Sucralose	$C_{12}H_{19}Cl_3O_8$	11.5	419.0038	artificial sweetener
Benzotriazole	$C_6H_5N_3$	12.0	120.0556	anti-corrosion agent
Lamotrigine	$C_9H_7Cl_2N_5$	12.3	256.0151	anti-seizure medication
Metoprolol	$C_{15}H_{25}NO_3$	12.3	268.1907	blood pressure medication
4-methyl benzotriazole	$C_7H_7N_3$	14.0	134.0713	anti-corrosion agent
5-methyl benzotriazole	$C_7H_7N_3$	14.2	134.0713	anti-corrosion agent

Table A-5. Summed peak area of all suspect compounds in MCX extracts of samples from 2018 and 2019 sampling.

		ROP	**UVF**	**UVP**
2018	UV/HOCl	1.39×10^{8}	1.43×10^{8}	7.78×10^{5}
	UV/H_2O_2	1.33×10^{8}	1.05×10^{8}	2.64×10^{6}
	UV/NH_2Cl	1.38×10^{8}	1.43×10^{8}	5.37×10^{7}
	UV/ambient	1.28×10^{8}	/	4.42×10^{7}
2019	UV/HOCl	8.73×10^{7}	8.63×10^{7}	9.43×10^{5}
	UV/H_2O_2	8.70×10^{7}	8.00×10^{7}	1.51×10^{5}

Appendix B – Supplementary information for Chapter 4

Text B-1: Chemicals and Materials

HPLC-grade methanol, acetone, methylene chloride, and sodium hypochlorite (5.65%-6%) were purchased from Fisher Scientific (Pittsburgh, PA). Reagent water was either ≥ 18.2 MΩ-cm (Milli-Q) or HPLC-grade from Fisher Scientific. Sodium carbonate, sodium bicarbonate, and sodium sulfite were purchased from Fisher Scientific. Sodium hydroxide (NaOH, 5M) and acetic acid (CH_3COOH, 0.1M) were used to adjust pH when needed. Acros Organics 4-methoxybenzenesulfonyl chloride (99%, Geel, Belgium) in acetone was used without further purification. Dimethylamine hydrochloride, dimethyl-d6-amine hydrochloride (DMA-d6) and hydrogen peroxide (30% w/w) were purchased from Sigma-Aldrich (St. Louis, MO). Chlorinated dimethylamine (CDMA) stock solutions were prepared by mixing DMA and hypochlorite at equimolar concentrations. An EPA 521 Nitrosamine Mix (Sigma-Aldrich) was used for the NDMA standard. The isotopically labeled NDMA-d6 standard was from Cambridge Isotopes (Tewksbury, MA, USA). EPA 521 activated carbon (2 g) SPE cartridges from Restek (Bellefonte, PA, USA) were used for NDMA analysis, and Sep-Pak C_{18} (1 g) SPE cartridges from Waters (Milford, MA, USA) were utilized for DMA analysis. Sodium sulfate drying cartridges were purchased from Agilent Technologies (Santa Clara, CA, USA). Total chlorine was measured by Hach DPD colorimetric assay (Method 10070; Loveland, CO), and monochloramine was measured by indophenol colorimetric Monochlor F reagent (Hach Co., Method 10171).

Text B-2: Sample Collection

Sample collection at full-scale water reclamation facilities. Samples were collected on three occasions over an approximately one-year period (January 2020, September 2020, and February 2021) at OCWD AWPF. While the exact units that were operational during each event cannot be confirmed, certain membranes were cleaned during this period. Between January 2020 and February 2021, each unit (containing three stages of membranes) was cleaned 1-3 times, with the average being twice. The cleanings consisted of either an entire unit clean or just a single stage and three of the 19 units had the membranes replaced in either September or October 2020. Prior work by co-authors indicated that seasonal and diurnal trends in NDMA occurrence were observed at this facility[171] and that membrane age and cleaning can also impact rejection of trace organics including NDMA precursors.[20] Thus, three sampling events allowed the team to capture variation associated with water quality (warmest in September and coldest in January of the region) and membrane age/cleaning.

Pilot UV-AOP Reactor. A flow through single-lamp reactor equipped with a low-pressure mercury amalgam lamp (Trojan Technologies, London, Ontario, CA) was fed RO permeate from the AWPF. The flow rate was set at 22.7 L/min (6 gpm) with a contact time of approximately 25 s with UV light at an estimated 900–1000 mJ/cm^2 dose. Hydrogen peroxide was delivered to an inline static mixer (Koflo Corporation, Cary, IL) upstream of the UV reactor with a peristaltic pump at targeted dose of 3 mg/L.

Control experiments were conducted with deionized (DI) water free of NDMA (<0.5 ng/L). HDPE totes (275 gal) were filled with DI water from the OCWD Philip Anthony

Water Quality Laboratory then moved to the location of the pilot UV reactor. NDMA or DMA was spiked into the DI water and manually mixed with a PVC “plunger” device.

Text B-3: DMA Method Development and Optimization

Optimization of derivatization reaction and extraction conditions. Since DMA is semi-volatile a study of the derivatization reaction and extraction procedure was conducted to improve the recovery process. The peak area of DMA and DMA-d6 at static concentrations and varying operational conditions is presented in Figure B-4. Peak area of DMA and DMA-d6 with shaking during derivatization was greater. Similarly, more derivatization DMA and DMA-d6 was extracted with longer extraction time. Therefore, in order to achieve greater DMA and DMA-d6 peak area and thus lower method detection limit (MDL), shaking during derivatization reaction and 2 min extraction were used going forward.

Optimization of derivatization reagent dose. Along with the optimizing derivatization reaction and extraction conditions, the derivatization reagent dose was evaluated. We assessed the effect of various derivatization reagent (4-methoxybenzensulfonyl chloride) doses and the results are summarized in Table B-2. The slope of calibration curves increased by decreasing the derivatization reagent dose, meaning the method is more sensitive at higher dose. Above 1 mg or derivitization reagent dose derivatized DMA was detected even when none was spiked, indicating some contamination of the reagent with DMA. Because of this, 1 mg of reagent was selected.

Procedures of optimized method. The optimized method used Sep-Pak C_{18} cartridges conditioned with 0.1 M acetic acid, methanol, and HPLC grade water. Samples (1 L, pH >12) were spiked with 0.4 μg/L dimethyl-d6-amine hydrochloride (DMA-d6), and loaded onto cartridges. Cartridges were eluted with 20 mL of 0.1 M acetic acid. Extracts

were titrated with sodium hydroxide to circumneutral pH, followed by buffering at pH 10 with 0.5 g of an equimolar mixture of sodium carbonate and sodium bicarbonate. DMA was derivatized with 4-methoxybenzensulfonyl chloride (20 μL of 50 g/L solution in acetone) in 35-mL borosilicate vials on a rotary shaker at room temperature for 3 h. Derivatized DMA was transferred into separatory funnels, 5 mL dichloromethane (DCM) was added, and the funnels were agitated to partition derivatized DMA to the DCM. The DCM was removed via the stopcock, evaporated at 40°C to 0.5 mL under a gentle stream of ultra-high purity nitrogen gas, transferred to 2-mL amber vials, and stored at -20 °C. Calibration curves were made by spiking DMA (1 to 100 μg/L) into 20 mL Milli-Q water containing 20 μg/L DMA-d6. The calibration standards were derivatized following the same procedure described above.

Text B-4: Method validation, Calibration, and MDL. The calibration linearity for a wide range of DMA concentrations from 1 to 100 μg/L was tested and the results are presented in Figure B-5. The results displayed good calibration linearity with correlation coefficient (R^2) > 0.999. Relative standard deviations (RSDs) were 10%-4% as DMA concentration was lower than 10 μg/L, whereas RSDs were decreased to 2% as DMA concentration increased to 20 μg/L. The MDL of this method was determined as 0.15 μg/L by measuring 11 fully processed blanks (SPE, derivatization, and extraction processes) according to the U.S. EPA method (i.e., calculated by the standard deviation of replicate blanks and a statistic coefficient).

Method recoveries and RSDs in tap water and Milli-Q water were checked with spiked DMA at 0.6 to 2.0 μg/L. As shown in Table B-3, 92%-113% recoveries were obtained with higher recovery in tap water. In addition, the RSDs of all tested samples were less than 15%, indicating good precision was received by the modified DMA method. Lower RSD was obtained at higher spiked concentrations in Milli-Q water, and the highest RSD was obtained with spiked DMA in tap water.

Text B-5: NDMA analysis. NDMA was extracted from samples with an automated Dionex AutoTrace 280. Cartridges were first conditioned with methylene chloride, methanol, and HPLC grade water. Then 500m mL samples with NDMA-d6 were loaded at a rate of 5 mL/min. After loading, cartridges were dried for 30 min using ultra high purity (UHP) nitrogen gas, then eluted using 5 mL of methylene chloride. The extracted samples were then passed through sodium sulfate drying cartridges to remove any residual water and into glass conical centrifuge vials. Samples were evaporated to 1 mL in a TurboVap at 40°C using a gentle stream of UHP nitrogen gas. Using a 1 mL syringe, samples were transferred to 2 mL amber vials and placed in the freezer.

The extracted samples were analyzed using Shimadzu GC-MS/MS TQ8040 with a capillary column (Stabilwax-MS, 30 m × 0.25 mm × 0.25 μm) operated in electron impact ionization mode. 2 μL splitless injections were injected into a 200°C injection port with helium as the carrier gas. The inlet pressure was pulsed at 300 kPa for 1 minute, followed by 1.22 mL/min column flow. The initial oven temperature was held at 50°C for 2 min, ramped to 130°C at 15°C/min (no hold), ramped to 220°C at 20°C/min and held for 4 min. The MS acquisition mode was set to MRM using argon as the collision gas. The interface temperature was 220°C and the ion source temperature was set to 200°C. NDMA and NDMA-d6 were quantified using the 80 *m/z* parent ion and 50.1 daughter ions for NDMA and the 74 *m/z* parent ion and 44.1 daughter ion. The method detection limits were 1 ng/L based on a S:N ratio of 5.

Text B-6. Batch-scale UV experiment. The experimental methods are provided in previously published work.[172] Briefly, a UV lamp emitting 254 nm light (Phillips TUV 8W, G8T5) was allowed to warm up for 20 min before samples were exposed. The lamp was placed as close as possible to quartz cuvettes (<1 cm). A common UV dose at water reuse facilities was achieved (1000 mJ/cm^2) by irradiating 5 mg/L CDMA samples for 20 min. 5 mL of irradiated solution was pipetted into 495 mL DI water to achieve 50 µg/L CDMA. 72-hour NDMA FP tests of the UV-exposed 50 µg/L CDMA solutions were then conducted.

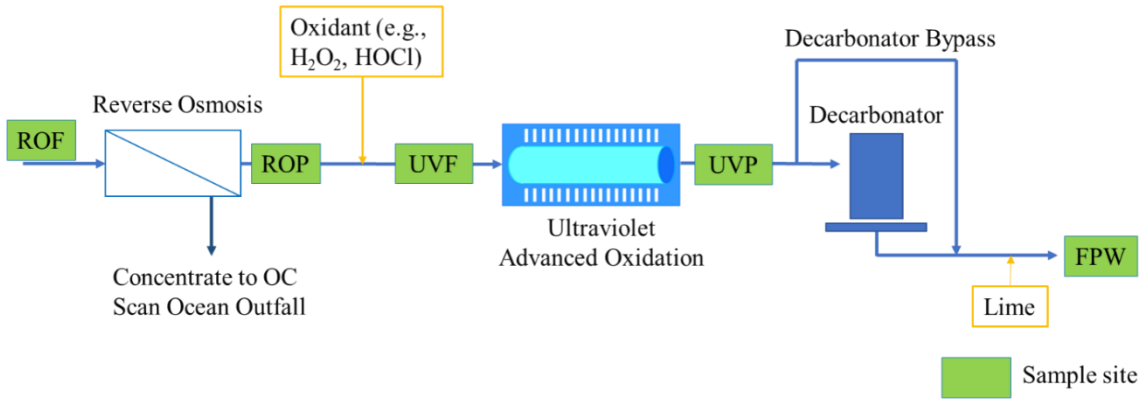

Figure B-1. Orange County Water District (OCWD) Advanced Water Purification Facility (AWPF) sampling sites. The OCWD Groundwater Replenishment System (GWRS) AWPF treats a blend of activated sludge effluent (80%) and trickling filter effluent (20%) by MF or UF, RO, and UV/H_2O_2.

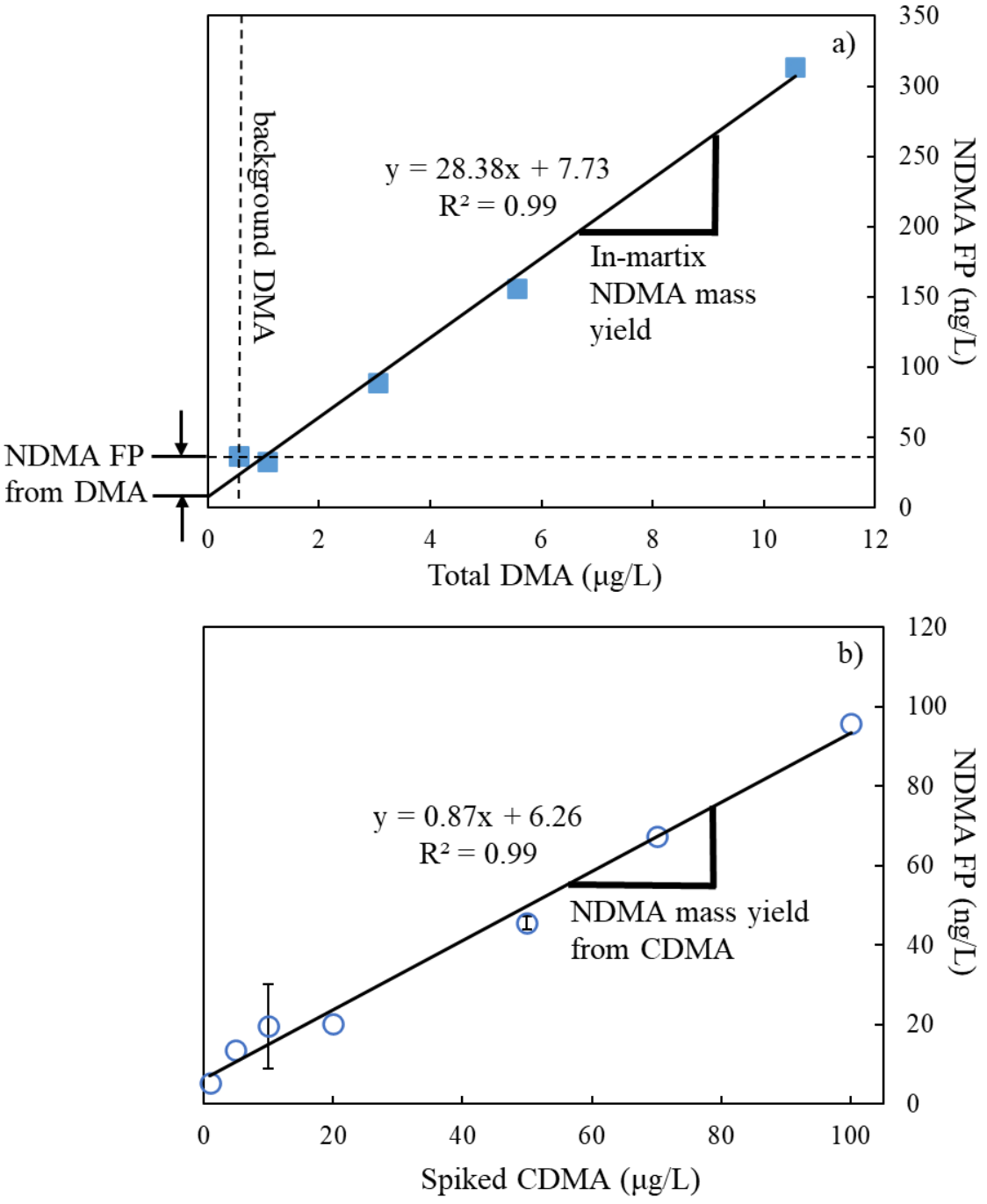

Figure B-2. NDMA FP of a) spiked DMA in AWPF UVP water and b) spiked CDMA in DI water. the y-intercept represents the NDMA that would have formed had no DMA/CDMA been present (non-DMA precursor loading). No replicates were conducted for the DMA addition experiments due to the limited volume of UVP samples shipped. The p-value of the linear regressions were 2.09×10^{-4} and 3.75×10^{-6} for spiked DMA and CDMA, respectively.

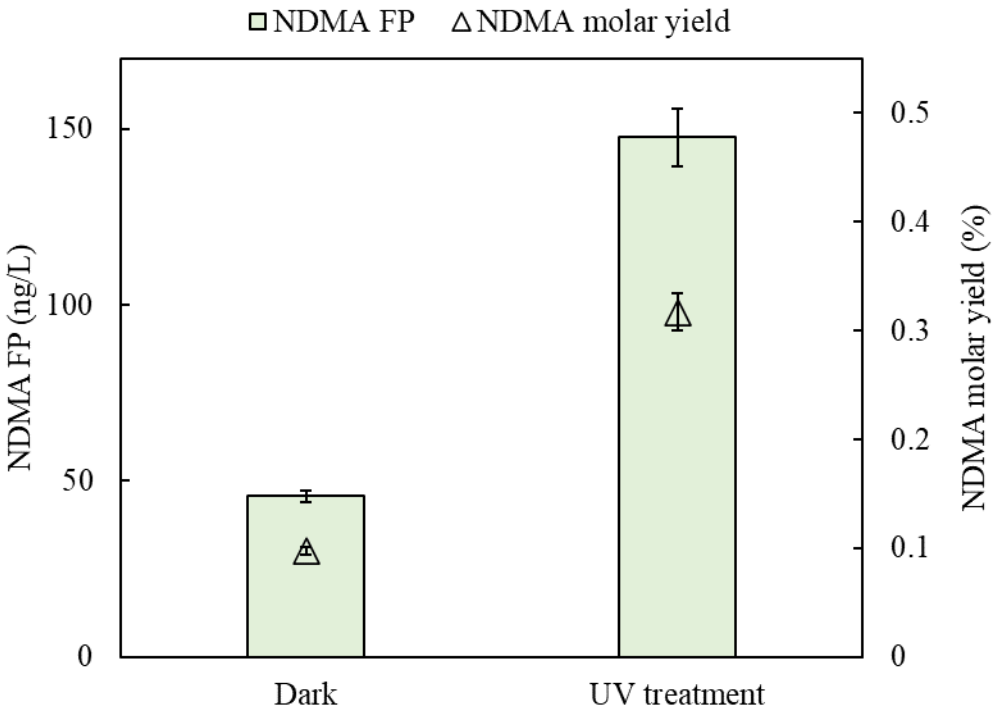

Figure B-3. NDMA FP and NDMA molar yield from CDMA with and without 1000 mJ/cm^2 UV treatment.

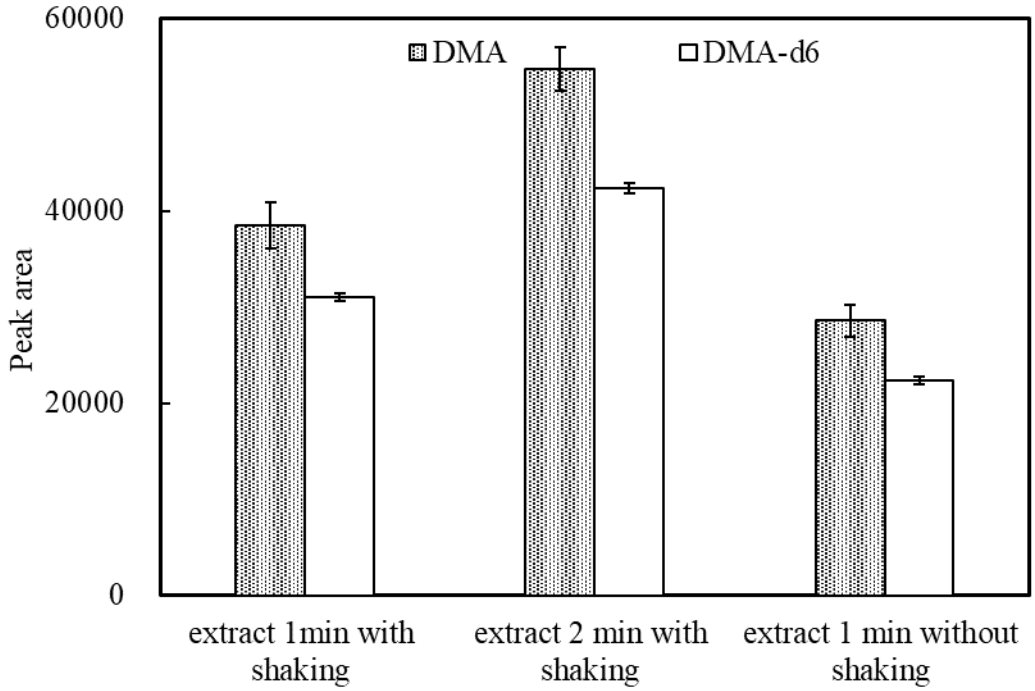

Figure B-4. Comparison of derivatization reaction and extraction conditions on the peak area of DMA and DMA-d6 ([DMA] = 30 μg/L, [DMA-d6] = 20 μg/L).

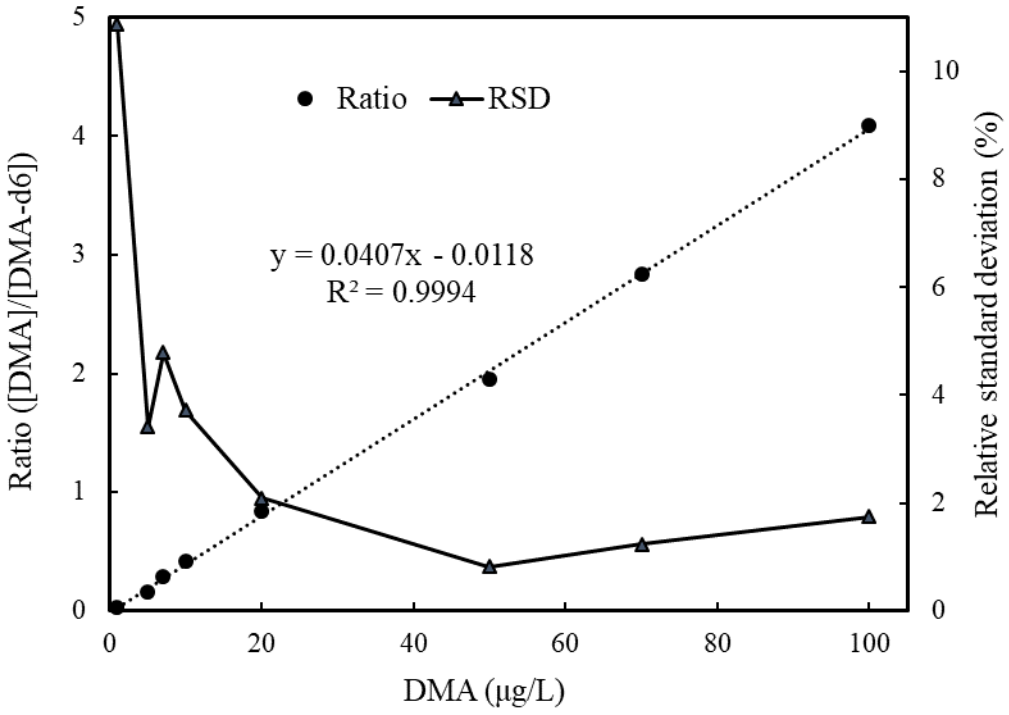

Figure B-5. Calibration curve and relative standard deviations (RSDs, n=3).

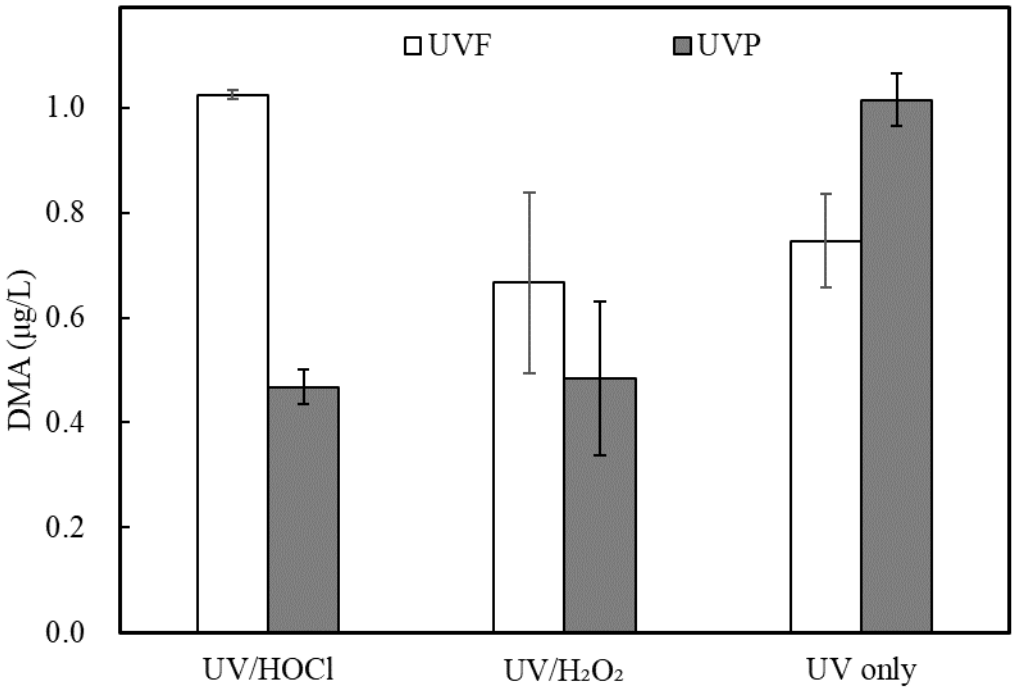

Figure B-6. The effect of different type of UV/AOPs on DMA concentration with ROP water from OCWD advanced water purification facility. Error bars indicate the range of triplicates and the bar is the average.

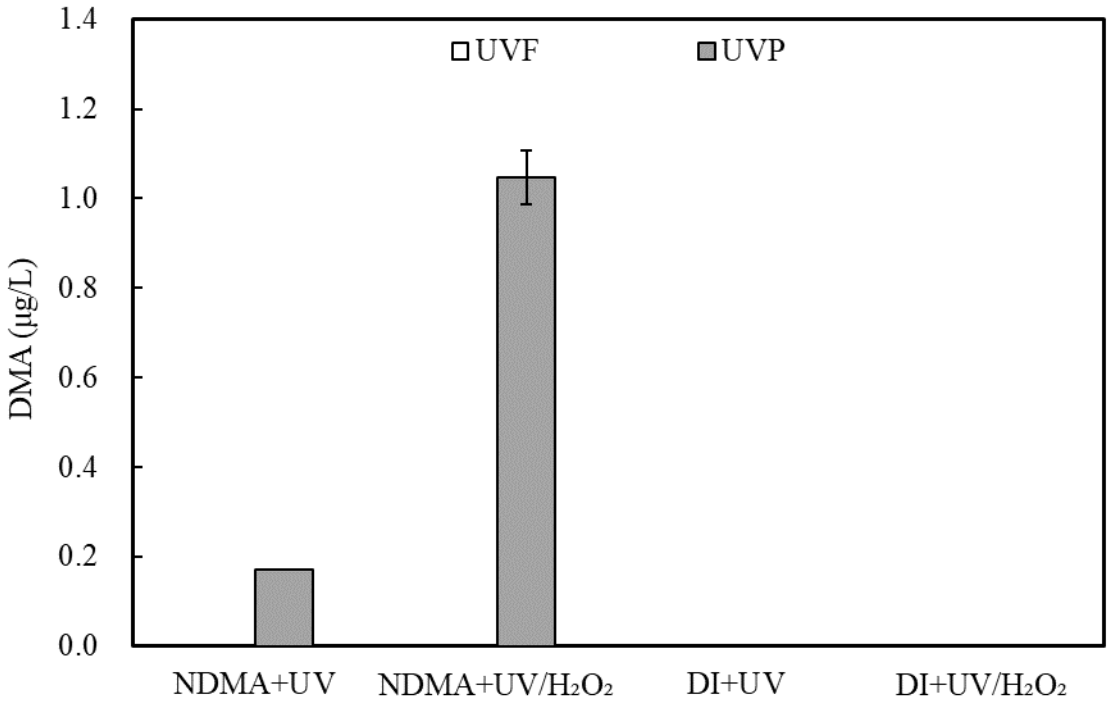

Figure B-7. The effect of NDMA photolysis on DMA formation. DMA concentrations in deionized water (DI) only were below MDL (0.15 µg/L).

Table B-1. GC-MS/MS instrument conditions for DMA analysis.

GC-MS/MS Parameters	
Injection port temperature	250 °C
Injection mode	Splitless
Column flow	1.16 mL/min (Linear Velocity)
Oven Program	Initial Temp at 100 °C (1 min hold), 100 °C to 250 °C at 8 °C/min (4 min hold)
MS acquisition mode	MRM
Interface temperature	260 °C
Ion Source Temperature	150 °C
Total Run Time	22.75 min

Table B-2. Calibration curves and peak area at varying reagent dose.

Derivatization reagent dose (mg)	Calibration curve	DMA peak area of a sample that was not spiked with DMA	DMA to DMA-d6 ratio of a sample which was not spiked with DMA
10	[DMA]=21.128×Ratio-0.4463	6276	0.05
5	[DMA]=25.071×Ratio+1.8916	221	0.02
2.5	[DMA]=24.997×Ratio-0.2732	120	0.01
1	[DMA]=24.601×Ratio+0.1027	0	-
0.4	[DMA]=30.37×Ratio-0.754	0	-

Table B-3. Method recoveries of DMA in different water matrices ($n \geq 3$).

Water matrix	Spiked DMA (μg/L)	Detected DMA (μg/L)	Recovery (%)	RSD (%)
Milli-Q water	0.6	0.62	104	7.53
Milli-Q water	1.5	1.47	98	4.65
Milli-Q water	2.0	1.84	92	3.63
Tap water	1.0	1.13	113	15.07

Table B-4. Water quality parameters for full-scale water reclamation facilities.

			pH	Total Cl_2 (mg Cl_2/L)	H_2O_2[a] (mg/L)	TOC (mg/L)[c]
OCWD AWPF	January 2020	ROP	5.42	2.9	3.0	0.056
		UVP	5.34	1.1	3.0	-
	September 2020	ROP	5.54	2.1	3.0	0.060
		UVP	5.04	1.0	3.0	-
	February 2021	ROP	5.44	2.8	3.0	0.046
		UVP	4.80	1.4	3.0	-
Plant 1		ROP	5.8	0.8	0	0.027
		UVF	-	1.8	0	<0.3
		UVP	-	0.7	0	<0.3
Plant 2		ROP	-	-	3.0	14
		UVF	-	-	3.0	0.16
		UVP	7.8	-	3.0	0.18

- not measured;

Water quality data from Plant 3 was lost and is no longer available;

a target concentration;

c TOC data provided by the participating utilities using varying standards methods and instrumentation.

Table B-5. Water quality parameters for the pilot-scale UV-AOP reactor.

		pH	Temperature (°C)	Total Cl_2 (mg/L)	Free Cl_2 (mg/L)	Monochloramine (mg/L)	H_2O_2 (mg/L)
UV/HOCl	ROP	5.40	25.1	1.8	-	-	-
	UVF	5.67	25.4	2.9	0.9	0.3	-
	UVP	5.40	25.6	1.9	1.1	0.2	-
UV/H_2O_2	ROP	-	-	-	-	-	-
	UVF	5.47	25.5	3.2	0.0	1.4	3.2
	UVP	5.30	25.7	1.9	0.0	0.6	2.9
UV/Ambient	ROP	5.30	25.6	2.3	-	-	-

	UVF	-	-	2.2	0.0	1.4	-
	UVP	5.17	25.8	1.0	0.1	0.6	-

-: not measured.

Appendix C – Supplementary information for Chapter 5

Text C-1: GC-MS/MS condition for NDMA analysis.

The extracted samples were analyzed using Shimadzu GC-MS/MS TQ8040 with a capillary column (Stabilwax-MS, 30 m × 0.25 mm × 0.25 μm) operated in electron impact ionization mode. 2 μL splitless injections were injected into a 200°C injection port and used helium as the carrier gas. The inlet pressure was pulsed at 300 kPa for 1 minute, followed by 1.22 mL/min column flow. The initial oven temperature was held at 50°C for 2 min, ramped to 130°C at 15°C/min (no hold), ramped to 220°C at 20°C/min and held for 4 min. The MS acquisition mode was set to MRM using argon as the collision gas. The interface temperature was 220°C and the ion source temperature was set to 200°C. NDMA and NDMA-d6 were quantified using the 80 parent ion and 50.1 daughter ions for NDMA and the 74 parent ion and 44.1 daughter ion. The method detection limits were 1 ng/L based on a S:N ratio of 5.

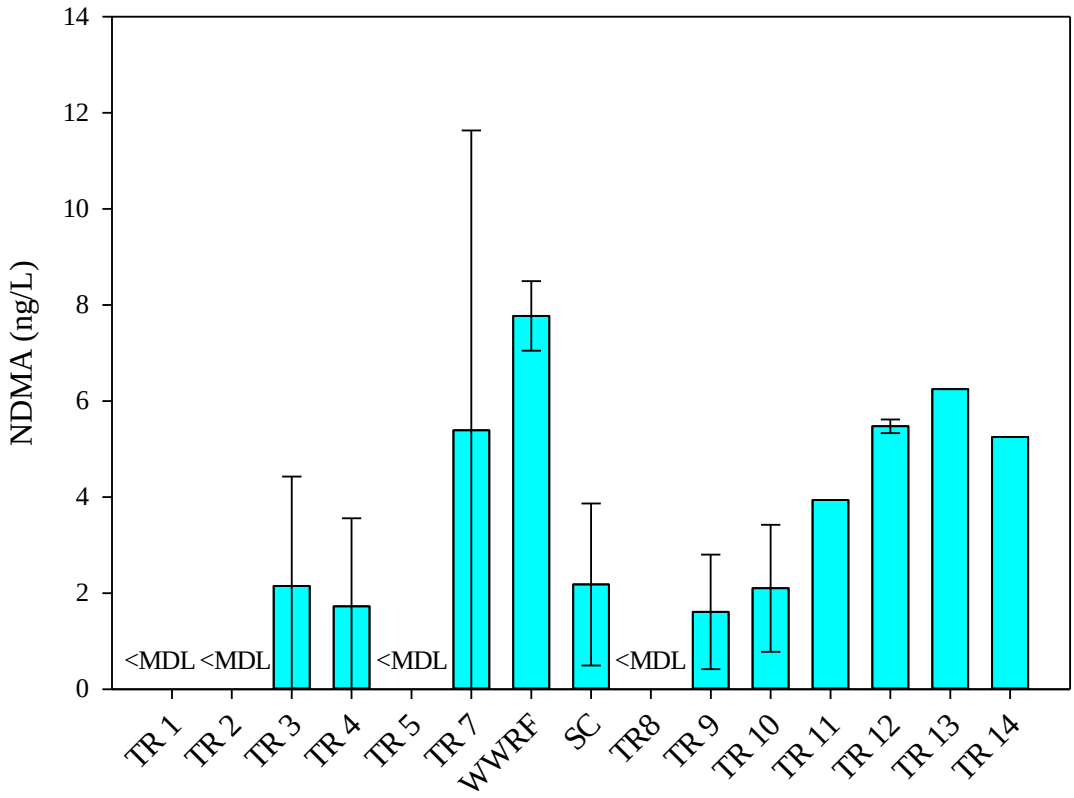

Figure C-1. NDMA concentrations in Truckee River. The error bars indicate the one standard deviation of triplicates. SC indicates Steamboat Creek.

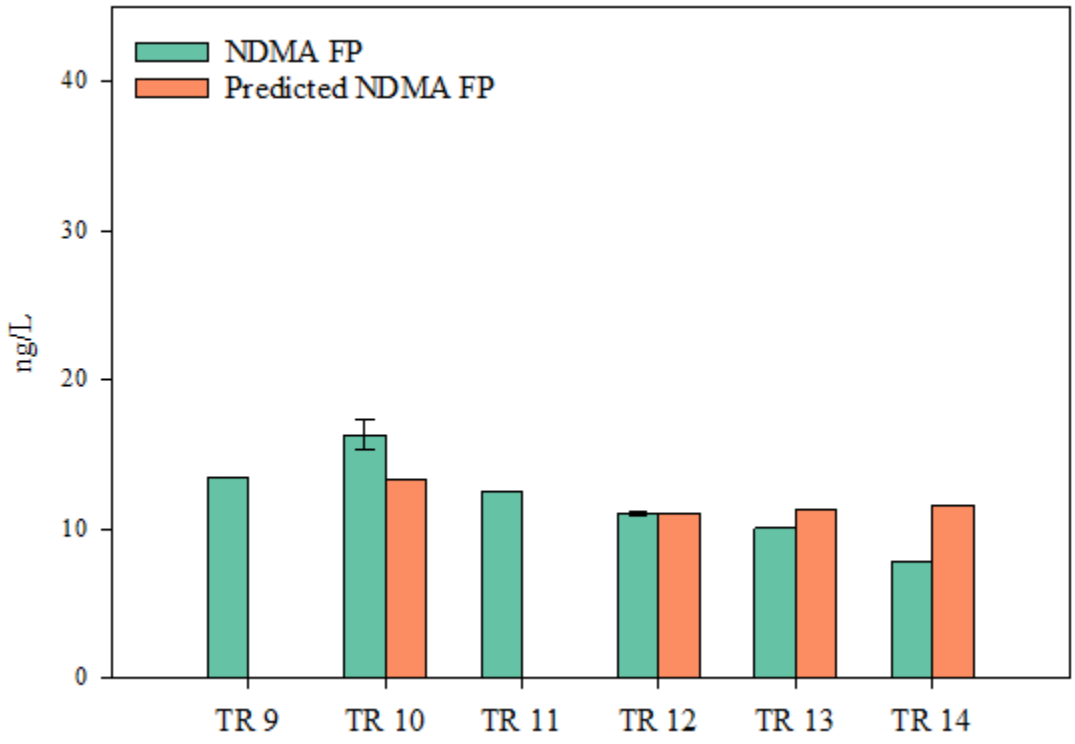

Figure C-2. NDMA FP and predicted NDMA FP based on conservation of precursors and change in flow from the prior site to the current site from TR 9 to TR 14 along Truckee River in June 2022.

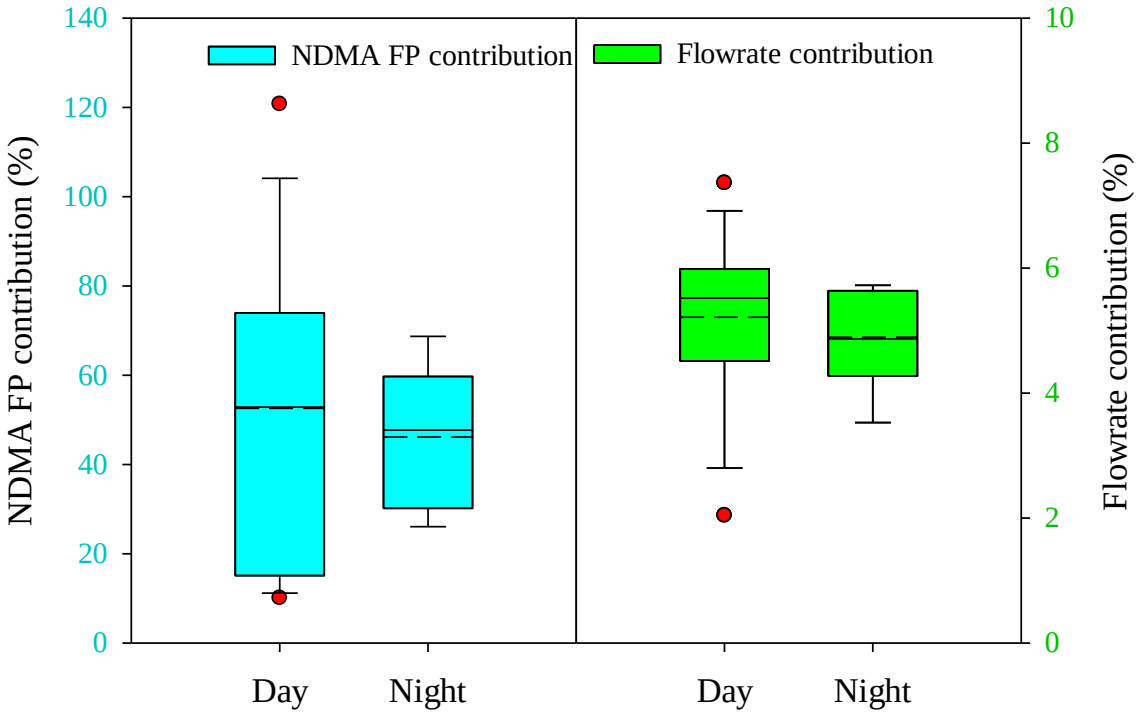

Figure C-3. Boxplot of NDMA FP contribution from reclaimed wastewater (the ratio of NDMA FP at WWRF final effluent flowrate (WWRF) to NDMA FP at Truckee River [TR 8]) and flowrate contribution from reclaimed wastewater (the ratio of TMWRF 1 flowrate to TR 8 flowrate) during continuous 24-hr sampling in June 2022. Day time is from 5:31 to 20:25 based on the sunrise and sunset time at Reno. For the boxplots, the ends of the boxes define the 25th and 75th percentiles, with a solid line at the median and a dash line indicating mean value.

Table C-1. Location description, latitude, and longitude of each sampling site.

Location	Description	Latitude	Longitude
TR 1	Truckee River at State Highway 267	39˚19′57.7″ N	120˚9′46.7″ W
TR 2	Truckee River at Glenshire Road bridge	39˚21′11.8″ N	120˚7′21.9″ W
TR 3	Truckee River at Boca Bridge	39˚23′7″ N	120˚5′12″ W
TR 4	Truckee River at Farad, Calif.	39˚25′41″ N	120˚1′59″ W
TR 5	Truckee River at Mayberry Drive	39˚30′24″ N	119˚42′13.2″ W
TR 6	Truckee River at West McCarran	39˚30′41.2″ N	119˚51′38.7″ W
TR 7	Truckee River before WWRF	39˚31′15.7″ N	119˚42′13.2″ W
WWRF	WWRF final effluent from the WWRF outfall	39˚31′8.2″ N	119˚42′15.2″ W
SC	Steamboat Creek after receiving WWRF discharge	39˚31′11.8″ N	119˚42′13.4″ W
TR 8	Truckee River at Vista	39˚31′20.4″ N	119˚41′35.9″ W
TR 9	Truckee River at Lockwood	39˚30′34.4″ N	119˚38′55.9″ W
TR 10	Truckee River at Patrick	39˚32′50.2″ N	119˚34′59″ W
TR 11	Truckee River at Derby Dam	39˚35′21.9″ N	119˚27′14.3″ W
TR 12	Truckee River at US 40 Bridge, near Wadsworth	39˚37′56.5″ N	119˚16′59.4″ W
TR 13	Truckee River at Dead Ox Wash	39˚44′17.8″ N	119˚19′20.7″ W
TR 14	Truckee River below Marble Bluff Dam	39˚51′11.1″ N	119˚23′41.5″ W

Table C-2. Sampling time and flowrates of each sampling site.

Location	2020 Sampling		2021 Sampling		2022 Sampling	
	Sampling time	Flowrates (cfs)	Sampling time	Flowrates (cfs)	Sampling time	Flowrates (cfs)
TR1	Day 1, 7:05 am	195.2	Day 1, 6:40 am	18.3	/	/
TR 2	Day 1, 10:05 am	206.0	Day 1, 11:35 am	30.4	/	/
TR 3	/		Day 1, 4:00 pm	84.4	/	/
TR 4	/		Day 2, 10:00 am	102.0	/	/
TR 5	/		Day 3, 8:00 am	25.02	/	/
TR 6	Day 2, 6:00 am	334.0	/		/	/
TR 7	Day 2, 2:00 pm	261.6	Day 4, 3:15 pm	41.1	/	/
WWRF	Day 2, 2:15 pm	3 8.4	Day 4, 4:00 pm	40.2	/	/
SC	Day 2, 2:30 pm	65.6*	Day 4, 4:10 pm	56.8*	/	/
TR 8	Day 2, 3:00 pm	333.0	Day 4, 5:00 pm	105.0	/	/
TR 9	Day 2, 4:45 pm	336.0	Day 4, 10:00 pm	107.2	Day 1, 12:45 pm	476.5
TR 10	/	/	/	/	Day 1, 3:45 pm	479.0
TR 11	/	/	/	/	Day 1, 11:42 pm	198.0
TR 12	/	/	/	/	Day 2, 7:58 am	223.0
TR 13	/	/	/	/	Day 2, 4:19 pm	217.5
TR 14	/	/	/	/	Day 3, 1:06 pm	213.0

* Summed Flowrates of TMWRF effluent (WWRF) and Steamboat Creek before WWRF.

Table C-3. Sampling time and flowrates at WWRF effluent (WWRF) and SC during continuous 24-hr sampling in May 2022.

Sampling time	WWRF (cfs)	SC* (cfs)
May 11st 11:05 am	44.2	96.4
May 11st 12:05 pm	46.2	99.0
May 11st 1:05 pm	45.1	98.5
May 11st 2:05 pm	39.7	92.5
May 11st 3:05 pm	35.8	89.2
May 11st 4:05 pm	35.4	88.8
May 11st 5:05 pm	21.0	73.8
May 11st 6:05 pm	32.3	85.1
May 11st 7:05 pm	34.6	88.0
May 11st 8:05 pm	21.9	75.3
May 11st 9:05 pm	30.0	82.7
May 11st 10:05 pm	32.6	85.3
May 11st 11:05 pm	32.4	85.1
May 12nd 12:05 am	27.6	80.3
May 12nd 1:05 am	32.8	84.9
May 12nd 2:05 am	21.4	73.5
May 12nd 3:05 am	37.2	88.7
May 12nd 4:05 am	31.9	83.4
May 12nd 5:05 am	32.6	83.4
May 12nd 6:05 am	26.8	77.6
May 12nd 7:05 am	44.1	94.9
May 12nd 8:05 am	15.1	66.5
May 12nd 9:05 am	47.0	98.4
May 12nd 10:05 am	53.1	105.2

* Summed Flowrates of TMWRF effluent (WWRF) and Steamboat Creek before WWRF.

Table C-4. Sampling time and flowrates at WWRF effluent (WWRF) and TR 8 during continuous 24-hr sampling in June 2022.

Sampling time at TMWRF effluent	TMWRF effluent (cfs)	Sampling time at TR 8	TR 8 (cfs)
June 8th 11:20 am	34.3	June 8th 12:50 am	675
June 8th 12:20 pm	49.0	June 8th 1:50 pm	666
June 8th 1:20 pm	43.5	June 8th 2:50 pm	657
June 8th 2:20 pm	38.3	June 8th 3:50 pm	657
June 8th 3:20 pm	36.3	June 8th 4:50 pm	657
June 8th 4:20 pm	39.5	June 8th 5:50 pm	660
June 8th 5:20 pm	29.8	June 8th 6:50 pm	660
June 8th 6:20 pm	33.7	June 8th 7:50 pm	666
June 8th 7:20 pm	39.1	June 8th 8:50 pm	669
June 8th 8:20 pm	43.5	June 8th 9:50 pm	666
June 8th 9:20 pm	27.5	June 8th 10:50 pm	660
June 8th 10:20 pm	36.9	June 8th 11:50 pm	660
June 8th 11:20 pm	37.5	June 8th 12:50 am	660
June 8th 12:20 am	37.6	June 8th 1:50 am	657
June 8th 1:20 am	23.2	June 8th 2:50 am	657
June 8th 2:20 am	35.5	June 8th 3:50 am	654
June 8th 3:20 am	31.6	June 8th 4:50 am	648
June 8th 4:20 am	28.7	June 8th 5:50 am	654
June 8th 5:20 am	31.0	June 8th 6:50 am	660
June 8th 6:20 am	25.8	June 8th 7:50 am	663
June 8th 7:20 am	13.7	June 8th 8:50 am	669
June 8th 8:20 am	22.5	June 8th 9:50 am	681
June 8th 9:20 am	34.6	June 8th 10:50 am	693
June 8th 10:20 am	39.5	June 8th 11:50 am	699

Appendix D - Standard Operation Procedures of GC-MS/MS

D.1. Realtime Analysis

All the following operations in Section 1 needs to be completed by “GCMS Real Time Analysis”. When you open the program, it will ask for a password with the “admin” user, but none is set. Click “OK”. If you get the error 1317, “The hardware configuration for this method…”, just click “OK”. More details about the error will be discussed at Section 3.

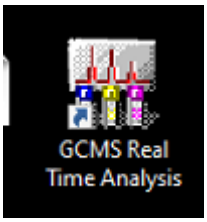

D.1.1. Turn ON/OFF

1. Two daily checks first. If everything goes well, follow step 2 to turn on the machine.
    - Check gas levels of helium and argon tanks. Around 500 psi, keep a close eye on the tanks and order a backup tank. There are currently two oxygen traps and one scrubber in series between the helium and the GC. While oxygen is well removed, it is important to check these occasionally to see if they have expired.
    - Check pump oil levels and color. If oil level is low, add oil. If it looks brown or yellow, change the pump oil. Make sure you turn off the vacuum pump using the software BEFORE servicing the pump.

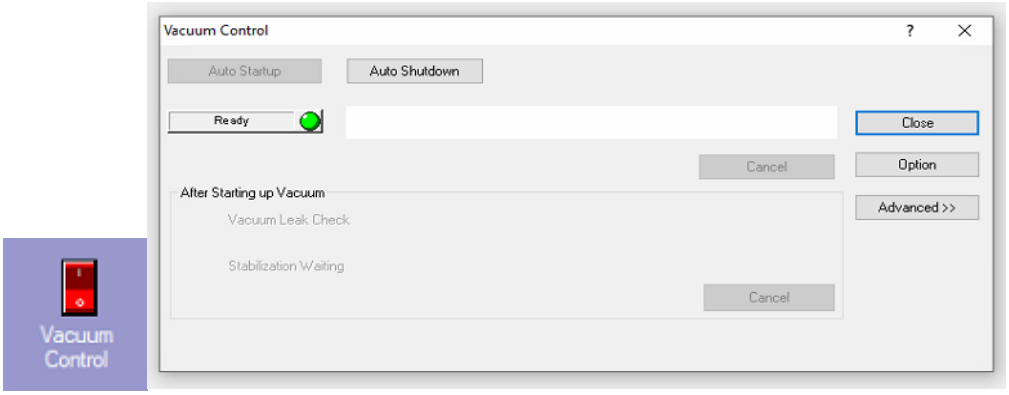

2. Turn on: click the “Vacuum Control” button in the left purple column. Then click “Auto Startup” in the pop-up window.
    - It will take around 15 min for pump startup. Click “Advanced” to check “Lower Vacuum”. If the “Lower Vacuum” keeps higher than 9.0e+000 Pa, there must be some leaks.
        i. Leaks from MS part: tighten the knob of the MS front door.
        ii. Leaks from GC part: tighten the MS side column nut with the wrench ¼ inch.

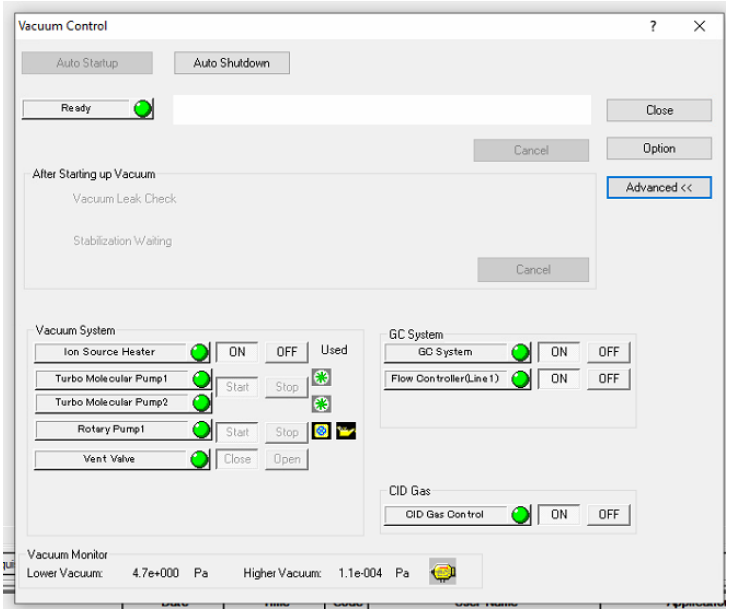

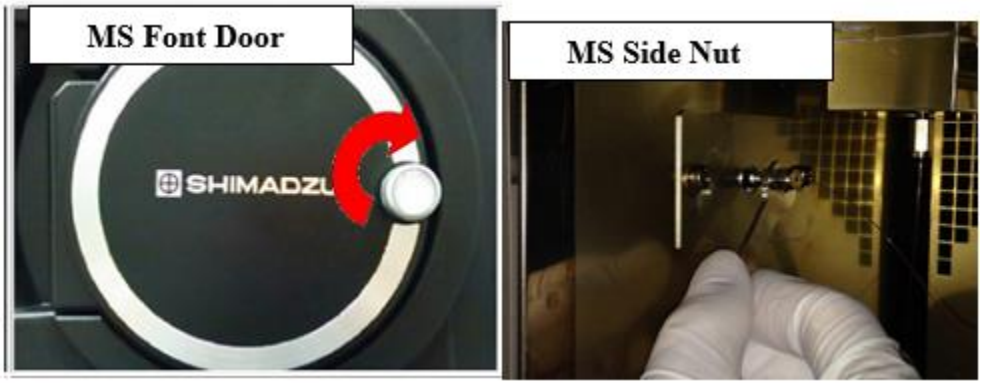

- After starting up Vacuum, “Vacuum Leak Check” will start automatically.

i. It will take ~10 min waiting for ion source temperature stabilizing at 200 °C.

ii. PASS will show up with a green " √ " at most time. If it doesn't show up, please check the leaks or the errors displayed.

- Stabilization will start automatically after "Vacuum Leak Check". It will take 2 hours, but I usually wait for 8 hours. Don't close the Vacuum Control window until the Stabilization completed.

3. Turn off: go to "Vacuum Control", then click "Auto shutdown", and wait until "system shutdown" appears. This will take at least 20 minutes to properly shut down the pump. This function also reduces source and inlet heat, so it is a good opportunity to clean the source, change the inlet liner, change the septa, and change the column if necessary.

C.1.2. Auto-tuning

1. Make sure that the loaded method is an MRM method. If not, the machine will only do a scan tuning.
    - For loading an MRM method (e.g. NDMA method), go to "Data Acquisition" (1) → open file (2) →open your own fie (3) → choose "Method" (4) →double click the method file "ndma mrm 0911" (5) → Acquisition →Download Initial parameters.

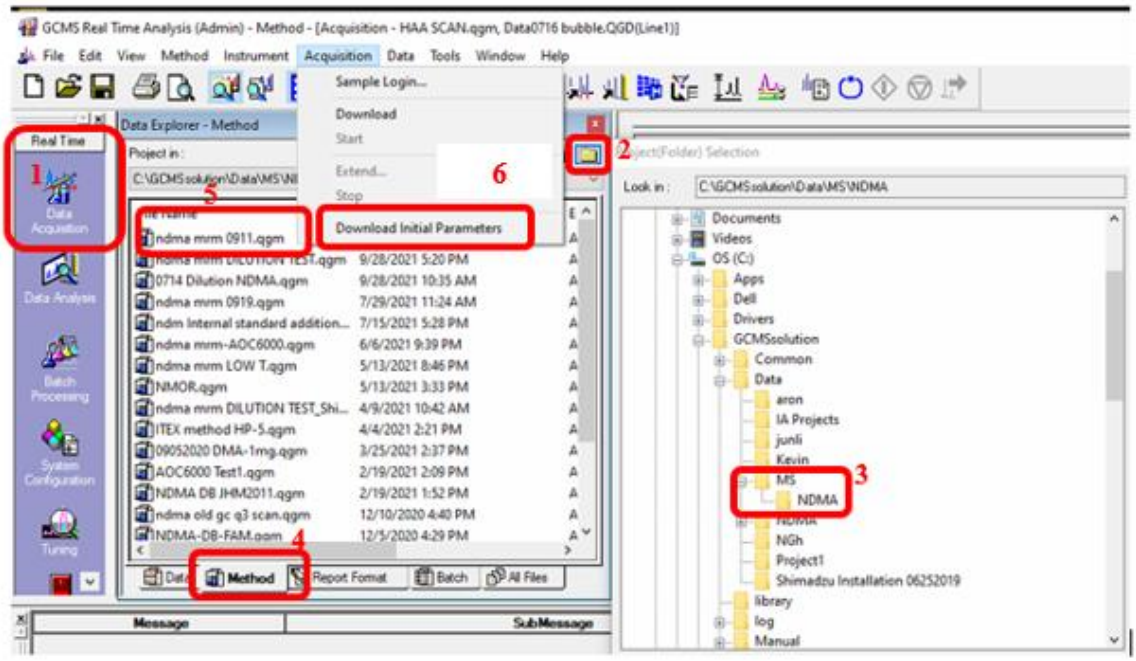

2. Click the “Tuning” button in the left-hand panel. If you cannot see the button, click “Top” button to go back the main panel.

Click “New” blank page icon in the top left corner (1). In the pop-up box, select “High Sensitivity”. Finally, click “Start Auto Tuning” button (2).

3. 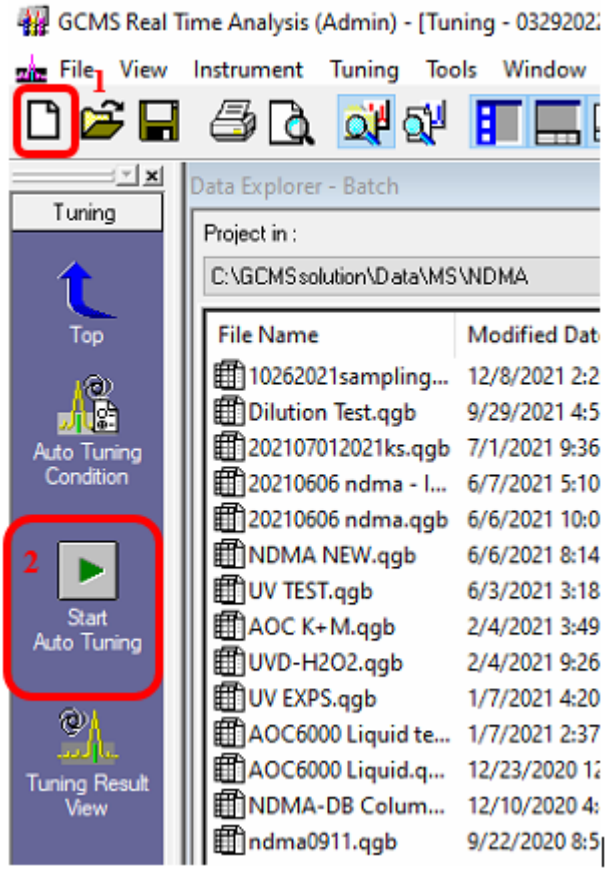

After ~30 min, you will be prompted to save THREE times: 1) first pdf page of the tuning report, 2) second page of tuning report with collision gas on, and 3) the tuning file (.qgt) to be used during liquid injection. The tuning reports are saved to the desktop in the folder, "TUNING FILES". The tuning files are saved in the folder (C) → GCMS Solution → System → Tune1.

Note:

- Log some tuning data to quickly determine if the source needs to be cleaned. On the desktop, open the Excel file, "TUNE DATA." Open the two pdf tuning files you just saved. In the Excel file, enter the following data from your pdf files: Tuning date, Lens 1-4, CC Lens 1-4, Detector, Low Vacuum, High Vacuum. Source generally needs to be cleaned when you notice an increase in detector voltage. After cleaning the source, indicate this in the logbook as done previously.

- For the Detector, please make sure the Voltage is <2.5 V in the tuning report. If it becomes greater than 2.5, the detector needs to be replaced.
- If you met an error and the auto tuning stopped, there should be two reasons:
  - The ion source is dirty (See section 3).
  - The standard needs to be refilled (See section 3).

D.1.3. Liquid Injection

D.1.3.1. Create “MRM” or “Scan” method

I recommended to create a new method by modifying a current method.

1. Create a folder that house all your data files, method files, and the batch file. If you already have your own folder, please skip this step and go to next.
   - Click “File” icon (1) →Select “C:\GCMS Solution\Data” location in the pop-up box (2) → Click “New Folder” (3) → Name the new folder and click OK (4).

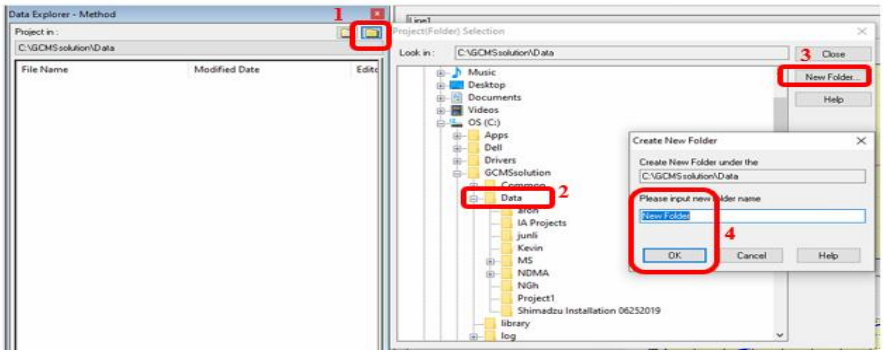

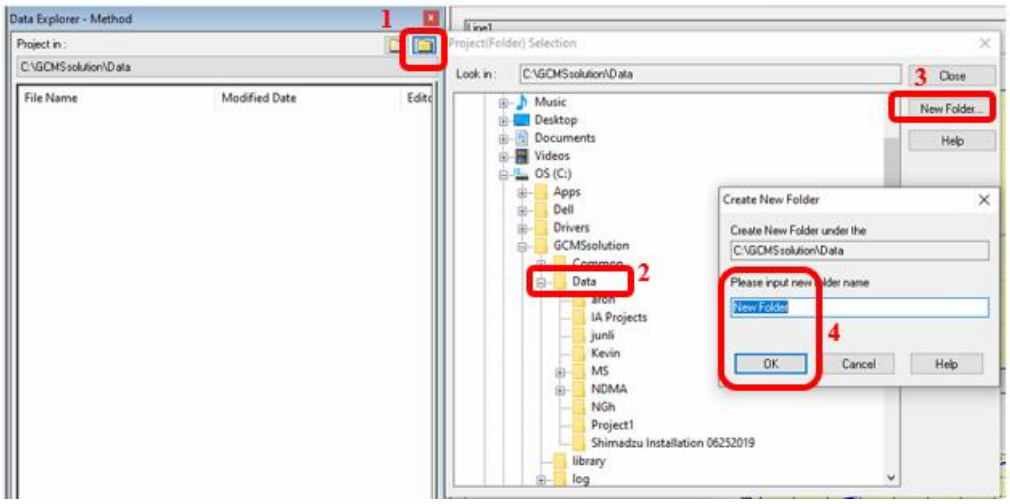

2. Copy the current method (e.g., NDMA method) and paste it into your own folder and change the name to avoid confusion.
    - The current NDMA method is located in C:\GCMS solution\Data\MS\NDMA\ndma mrm 0911.qgm
    - Double click on the displayed method file to open it. You can toggle between the Sampler, GC, and MS setting (1). Injection method is same as the method described in Section 1.3.2.

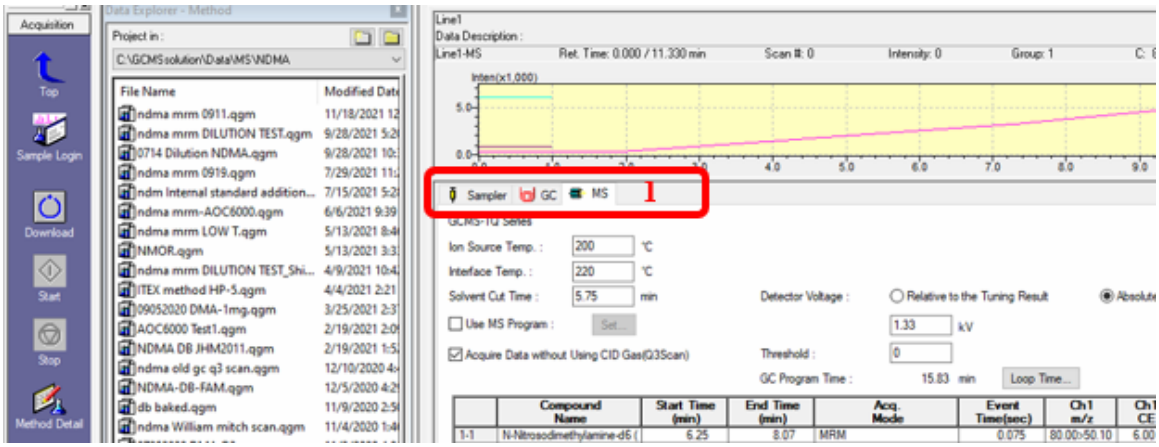

C.1.3.2. Create Injection Method

1. Click “Edit” on “Sampler” tab page (1) → choose Method and then click “Liquid Injection”.

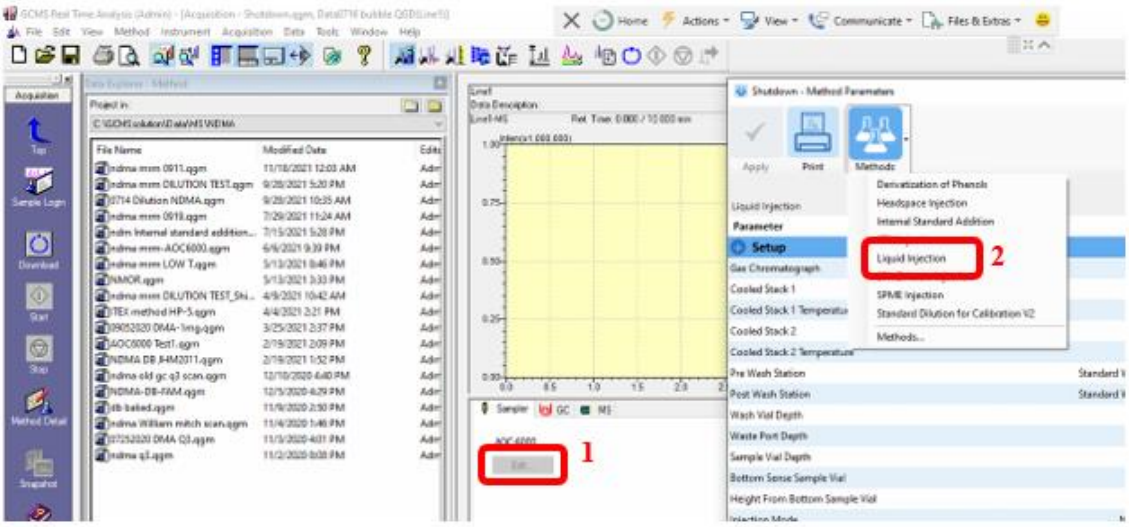

2. Choose/fill the exact same parameter values in the following pictures.

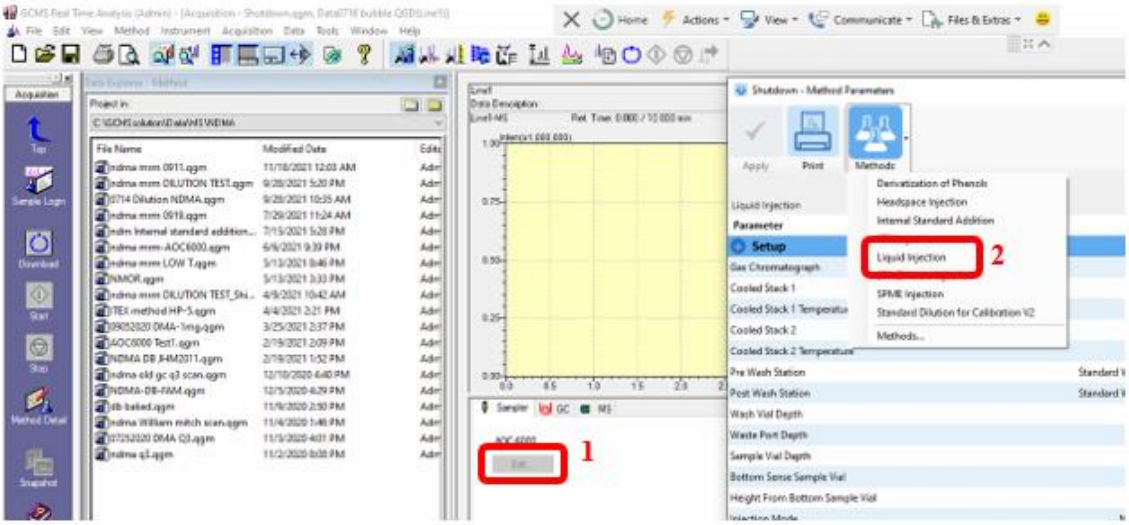

3. Choose/fill the exact same parameter values in the following pictures.

Shutdown - Method Parameters

Apply Print Methods

Liquid Injection

Parameter	Value	Unit
Setup		
Gas Chromatograph	GC1	
Cooled Stack 1		
Cooled Stack 1 Temperature	20	°C
Cooled Stack 2		
Cooled Stack 2 Temperature	20	°C
Pre Wash Station	Standard Wash 1	
Post Wash Station	Standard Wash 1	
Wash Vial Depth	40	mm
Waste Port Depth	10	mm
Sample Vial Depth	30	mm
Bottom Sense Sample Vial	Off	
Height From Bottom Sample Vial	3	mm
Injection Mode	Normal	
Injection Signal Mode	PlungerDown	
Injector Penetration Depth	40	mm
Prep Ahead Option	Disabled	
Analysis		

Analysis		
Syringe Tool	LS 1	
Pre Wash Cycles	3	
Sample Rinse Cycles	0	
Sample Aspirate Flow Rate	1	µL/s
Sample Post Aspirate Delay	2	s
Injector	Injector 1	
Injection Flow Rate	50	µL/s
Post Wash Cycles	3	

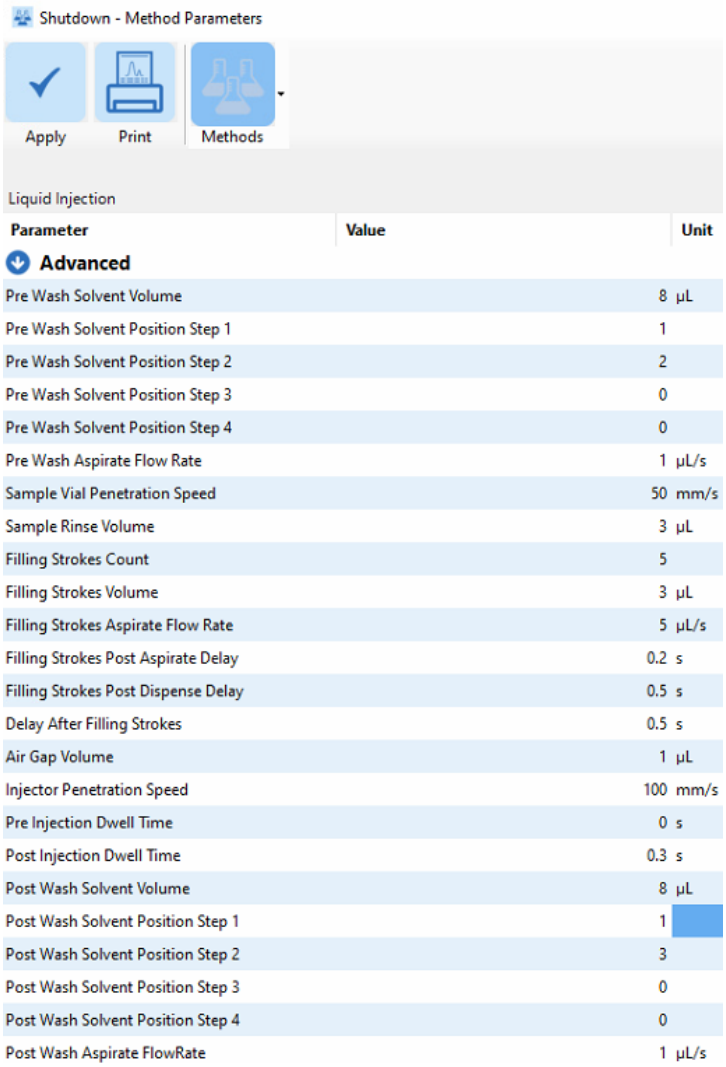

Parameter	Value	Unit
Advanced		
Pre Wash Solvent Volume	8	µL
Pre Wash Solvent Position Step 1	1	
Pre Wash Solvent Position Step 2	2	
Pre Wash Solvent Position Step 3	0	
Pre Wash Solvent Position Step 4	0	
Pre Wash Aspirate Flow Rate	1	µL/s
Sample Vial Penetration Speed	50	mm/s
Sample Rinse Volume	3	µL
Filling Strokes Count	5	
Filling Strokes Volume	3	µL
Filling Strokes Aspirate Flow Rate	5	µL/s
Filling Strokes Post Aspirate Delay	0.2	s
Filling Strokes Post Dispense Delay	0.5	s
Delay After Filling Strokes	0.5	s
Air Gap Volume	1	µL
Injector Penetration Speed	100	mm/s
Pre Injection Dwell Time	0	s
Post Injection Dwell Time	0.3	s
Post Wash Solvent Volume	8	µL
Post Wash Solvent Position Step 1	1	
Post Wash Solvent Position Step 2	3	
Post Wash Solvent Position Step 3	0	
Post Wash Solvent Position Step 4	0	
Post Wash Aspirate FlowRate	1	µL/s

4. Click “Apply” to save injection method.

D.1.3.3. Run Liquid Injection

1. Ensure solvents are filled in the AutoSampler and that correct solvents are in the correct location vial. Vials 1, 2, 3, and 5 correspond to methanol, DCM, DCM, and Waste. The number is showing on the cap of the “standard wash”, showing as following.

2. Check smart syringe: LS1 is 10 µL syringe, usually needed for liquid rejection.
    - Park the syringe first: Click the main button on the remote robot to select “LS1 10 uL; NL: 57 mm” (1) → rotate to select “Park Tool” (2) →click the first button on the left panel (3).
    - Check if LS1 was stuck. If so, use acetic acid to wash the syringe.
    - Select the syringe: Click the main button on the remote robot to select “LS1 10 uL; NL: 57 mm” (1) → rotate to select “Select Tool” (2) →click the first button on the left panel (3).

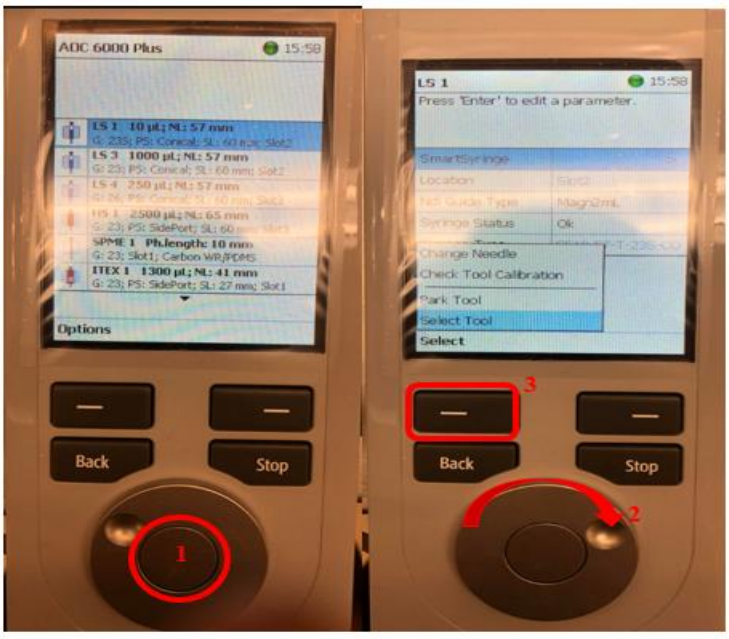

3. Open your own folder and open your “bath file”.
    - The simple way is copy old batch file (e.g., C:\GCMS solution\Data\MS\NDMA\20210606 ndma.qgb), paste it into your batch folder, change the name, and delete all lines.

Folder: C:\GCMSsolution\Data\MS\NDMA

	Rack #	Vial#	Sample Name	Sample ID	Sample Type	Analysis Type	Method File	Data File	Level#	Inj. Volume	ISTD Amt.	Tuning File
1	1	1			0:Unknown	IT QT	00 Test1.qgm	d test1.qgd	1	2	(Level1 Con	
2	1	1		001	0:Unknown	IT QT	rm 0911.qgm	cm001.qgd	1	2	(Level1 Con	06042021.qgt
3	1	2		002	1:Standard:(I)	IT QT	rm 0911.qgm	h-001.qgd	1	2	(Level1 Con	06042021.qgt
4	1	3		003	1:Standard	IT QT	rm 0911.qgm	h-002.qgd	2	2	(Level1 Con	06042021.qgt
5	1	4		004	1:Standard	IT QT	rm 0911.qgm	h-003.qgd	3	2	(Level1 Con	06042021.qgt
6	1	5		005	1:Standard	IT QT	rm 0911.qgm	h-004.qgd	4	2	(Level1 Con	06042021.qgt
7	1	6		006	1:Standard	IT QT	rm 0911.qgm	h-005.qgd	5	2	(Level1 Con	06042021.qgt
8	1	7		007	1:Standard	IT QT	rm 0911.qgm	h-006.qgd	6	2	(Level1 Con	06042021.qgt
9	1	8		008	1:Standard	IT QT	rm 0911.qgm	h-007.qgd	7	2	(Level1 Con	06042021.qgt
10	1	9		009	1:Standard	IT QT	rm 0911.qgm	h-008.qgd	8	2	(Level1 Con	06042021.qgt
11	1	10		010	1:Standard	IT QT	rm 0911.qgm	h-009.qgd	9	2	(Level1 Con	06042021.qgt

- Another way is to create a new one. All steps are listed below to avoid forgetting. Click “New” blank page icon in the top left corner to create a new one (1) → right click the blank area of the new batch file (2) → choose “Table Style…) in the pop-up box (3) → add “Option 1” (4) to Display Items (5) → make “Option 1” the top item of the Display Items by clicking “Up” and Click “OK” (6) → right click the blank area of the new batch file and choose “Settings”(7) → change the name of “Option 1” to “Rack #” (8).

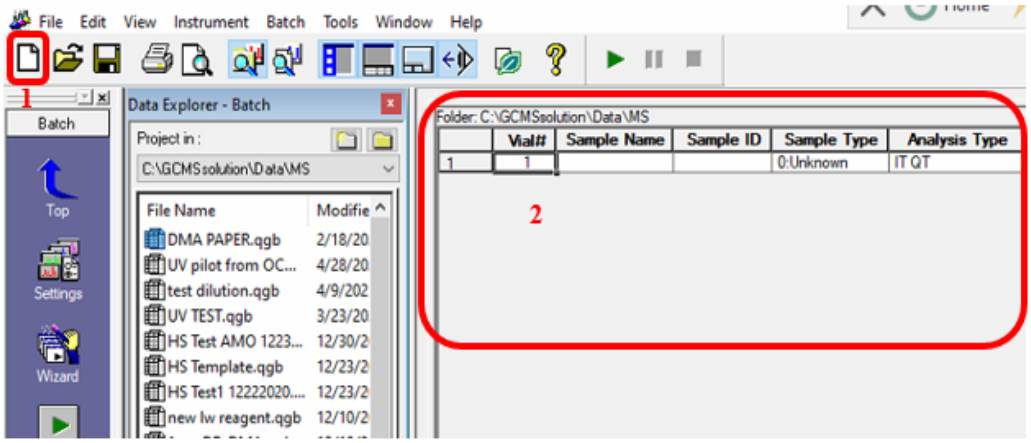

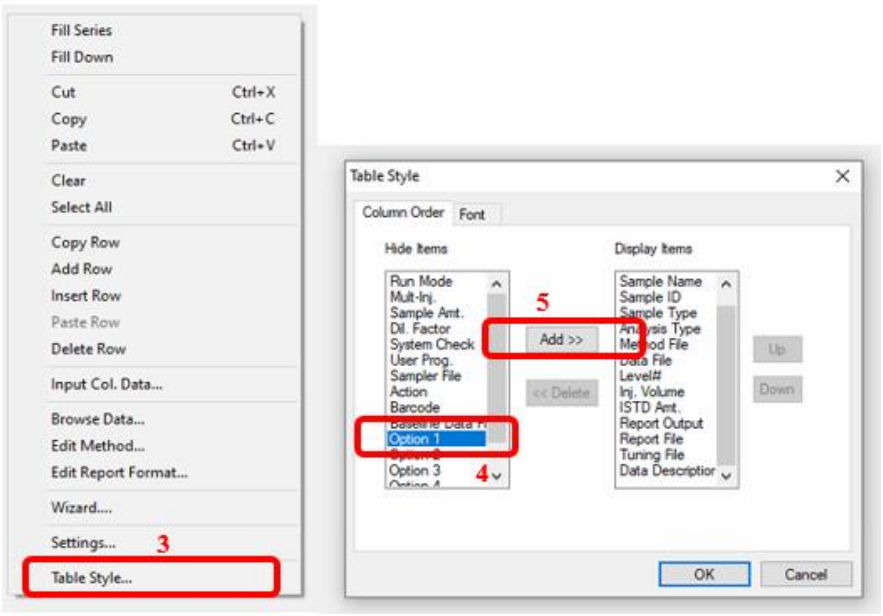
Fill Series
Fill Down
Cut Ctrl+X
Copy Ctrl+C
Paste Ctrl+V
Clear
Select All
Copy Row
Add Row
Insert Row
Paste Row
Delete Row
Input Col. Data...
Browse Data...
Edit Method...
Edit Report Format...
Wizard....
Settings...
Table Style...
3
Table Style
Column Order
Font
Hide Items
Display Items
Run Mode
Mult-Inj.
Sample Amt.
Dil. Factor
System Check
User Prog.
Sampler File
Action
Barcode
Option 1
Option 3
4
5
Add >>
<< Delete
Sample Name
Sample ID
Sample Type
Level#
Inj. Volume
ISTD Amt.
Report Output
Report File
Tuning File
Data Description
Up
Down
OK
Cancel

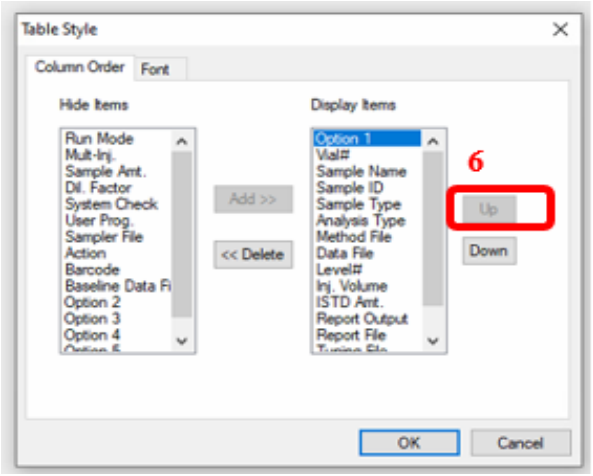
Table Style
Column Order
Font
Hide Items
Display Items
Run Mode
Mult-Inj.
Sample Amt.
Dil. Factor
System Check
User Prog.
Sampler File
Action
Barcode
Option 2
Option 3
Option 4
Add >>
<< Delete
Option 1
Vial#
Sample Name
Sample ID
Sample Type
Analysis Type
Method File
Data File
Level#
Inj. Volume
ISTD Amt.
Report Output
Report File
6
Up
Down
OK
Cancel

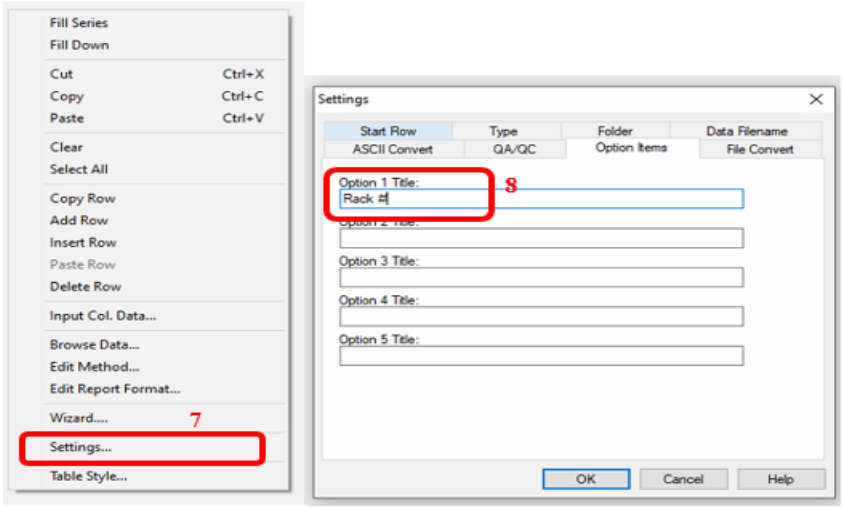

4. After opening your own batch file, use “Wizard” to fill in the batch table FIRST, and fill in the Rack # and Tuning file at last.
    - “Wizard” steps: “Wizard” → “Append” → “Line 1” → “Unknown/Standard” → Choose method file by click the green folder → Type the first Vial#, “Sample Count”, and “Injection Volume” (for NDMA, it is usually 2 uL) → name the data files and click Finish.

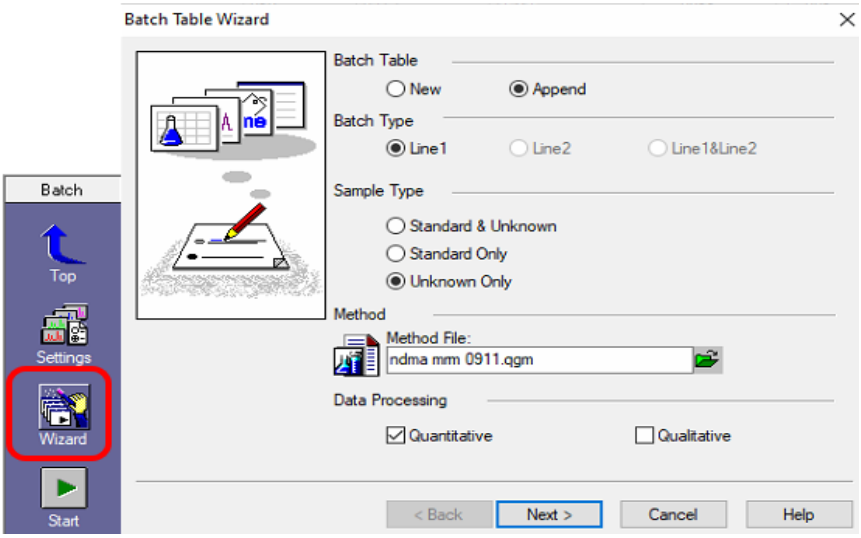
Batch Table Wizard
Batch
Top
Settings
Wizard
Start
Batch Table
New
Append
Batch Type
Line1
Line2
Line1&Line2
Sample Type
Standard & Unknown
Standard Only
Unknown Only
Method
Method File:
ndma mm 0911.qgm
Data Processing
Quantitative
Qualitative
< Back
Next >
Cancel
Help

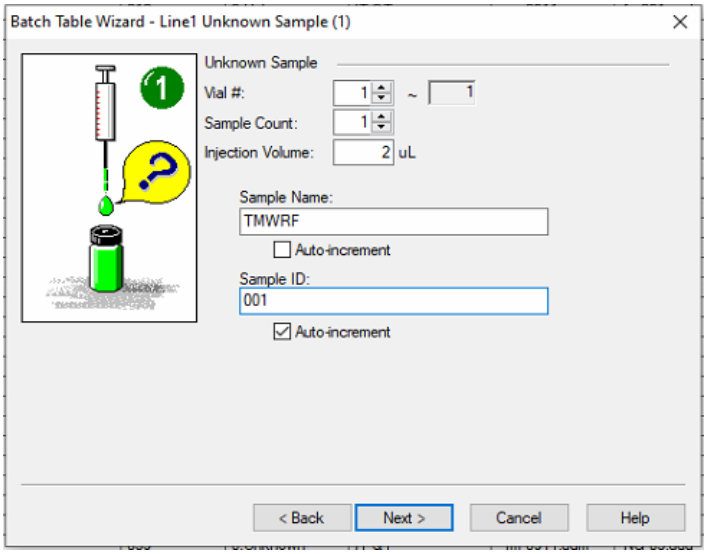
Batch Table Wizard - Line1 Unknown Sample (1)
Unknown Sample
Vial #:
1
~
1
Sample Count:
1
Injection Volume:
2
uL
Sample Name:
TMWRF
Auto-increment
Sample ID:
001
Auto-increment
< Back
Next >
Cancel
Help

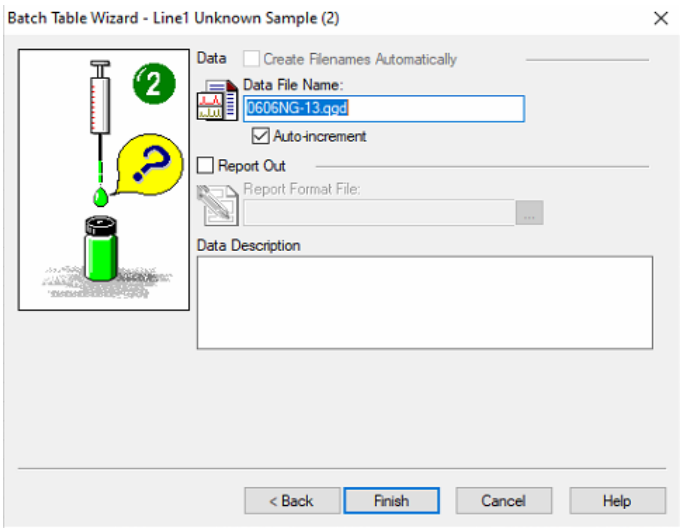

Folder: C:\GCMSsolution\Data\MS\NDMA

	Rack #	Vial#	Sample Name	Sample ID	Sample Type	Analysis Type	Method File	Data File	Level#	Inj. Volume	ISTD Amt.	Tuning File
3		2		002	1:Standard:(I)	IT QT	rm 0911.qgm	h-001.qgd	1	2	(Level1 Con	
4		3		003	1:Standard	IT QT	rm 0911.qgm	h-002.qgd	2	2	(Level1 Con	
5		4		004	1:Standard	IT QT	rm 0911.qgm	h-003.qgd	3	2	(Level1 Con	
6		5		005	1:Standard	IT QT	rm 0911.qgm	h-004.qgd	4	2	(Level1 Con	
7		6		006	1:Standard	IT QT	rm 0911.qgm	h-005.qgd	5	2	(Level1 Con	
8		7		007	1:Standard	IT QT	rm 0911.qgm	h-006.qgd	6	2	(Level1 Con	
9		8		008	1:Standard	IT QT	rm 0911.qgm	h-007.qgd	7	2	(Level1 Con	

NOTE:

- For every batch run, I suggested run blank first. If your sample solvent is Methanol, your first sample should be Methanol.
- Rack # is 1,2, and 3, indicating the location of your vials.

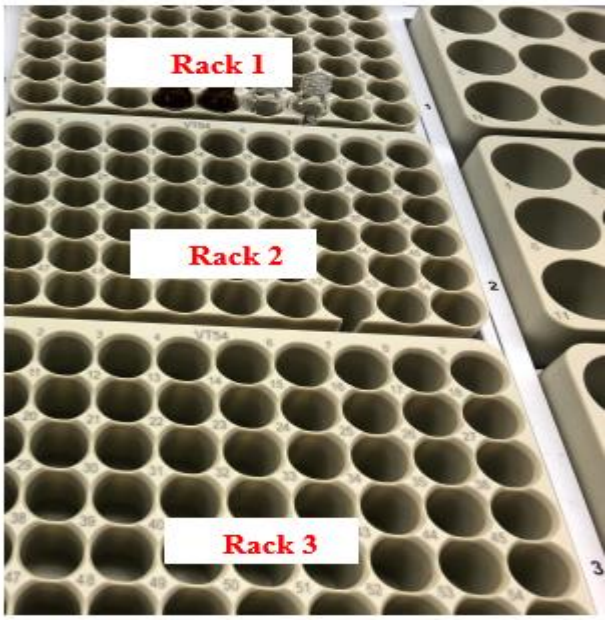

- Sample Type: Standard and Unknown. If you want to change the sample type after doing “Wizard”. Click the inside the box, then click the small arrow that appears on the right side. If the sample is a calibration standard, select “Standard”. If it is your first point of your calibration curve, click “Initialize Calibration Curve”. The rest of your standards should automatically have “Add Calibration Level” selected. If you are entering an unknown (e.g., a sample), select “Unknown”.
- Level #: Indicate what point in your calibration curve each standard corresponds to. For example, if 0.5 ppb NDMA is your fist point of your calibration curve, the Level # should be Level 1. For Unknowns (Not standards), it should be Level 1 by default.
- Tuning file: Choose most recent one (should do auto-tuning every month). If there isn’t a tuning file created within one month, do auto-tuning following Section 1.2.

5. Highlight all samples, then click the green triangle to start your batch of samples. MAKE SURE all rows you want processed are listed in “Selected Rows”. Then click “Start”.

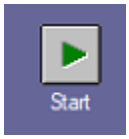

6. Waiting in front of the GC/MS until the first samples injected. Sometimes it may stop during wash syringe or sample wash. If it happens, please check the needle length setting in your injection method (See parameters in Section 1.3.2).

Note:

- There is a BUUBBLE issue when sucking liquid samples, please make sure your sample volume is greater than 0.4 mL.
- Don’t run GC/MS for continuously 24 hrs. It might cause AOC error.
- Turn off the AOC 6000+ and turn it on from time to time to avoid AOC error. For example, once a week.

D.1.4. Dilution Calibration Curve

D.1.4.1. Create Dilution method

1. Copy your analysis method and paste it into your own folder. If you don't have your own folder, see Section 1.3.1 to create your own folder.
2. Double click the pasted method to open your method.
3. Click "Edit" on the Sampler tab page (1) → Click the "Methods" icon (2) and select "Standard Dilution for Calibration V2" (3) to open the "Method Parameters" sub-window.

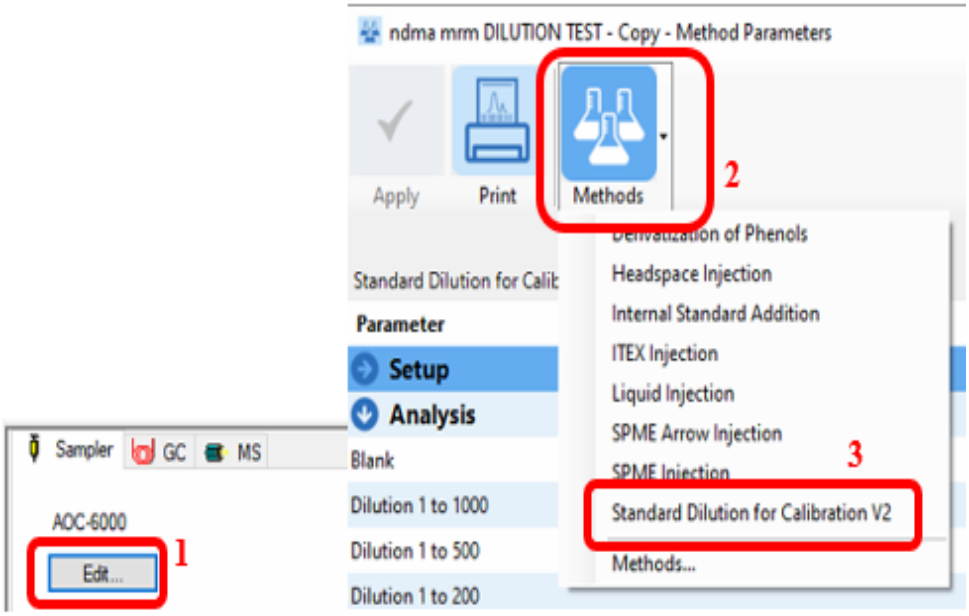

4. Fill in the parameters exactly same as the following the picture.

ndma mrm DILUTION TEST - Copy - Method Parameters

Apply | Print | Methods

Standard Dilution for Calibration V2

Parameter	Value	Unit
Setup		
Gas Chromatograph	GC1	
Syringe Tool 10µL	LS 1	
Syringe Tool 250µL	LS 4	
Syringe Tool 1000µL	LS 3	
Dilution Rack	Rack 1	
Vial Dispense Depth	10	mm
Standard Rack	Rack 2	
Standard Index	1	
Bottom Sence Standard	Off	
Heigth From Bottom Standard	2	mm
Standard Penetration Depth	30	mm
Large Volume Wash Station	Large Wash 1	
Solvent Penetration Depth	45	mm
Wash Vial Depth	45	mm
Waste Port Depth	12	mm
Vortex Mixer	Vortex Mixer 1	
Analysis		

Dilution Rack: Empty vials with magnetic caps.

Standard Rack: In order from the left, the standard sample, internal standard sample, and analyte protectant (usually not included by NDMA analysis) vials.

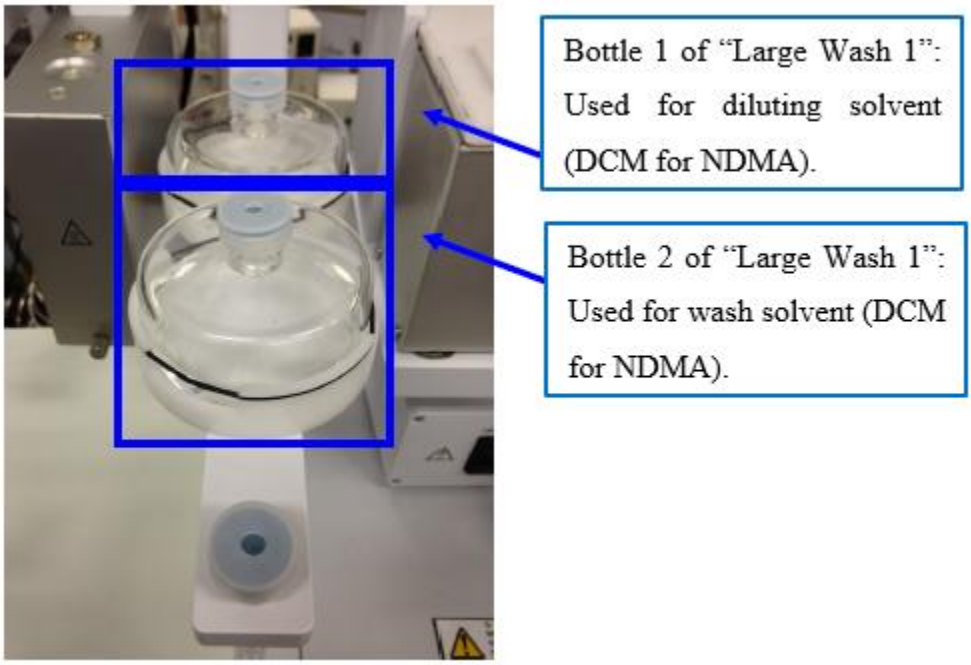

5. Choose the dilution factor under "Analysis" tab. Because there are some bubbles in the syringe, I recommend use small dilution factors less than 500 times.

    - Use "Dilution 1 to 200", "Dilution 1 to 100", "Dilution 1 to 50", "Dilution 1 to 20", "Dilution 1 to 10", "Dilution 1 to 5", "Dilution 1 to 2".

Analysis	
Blank	Skip
Dilution 1 to 1000	Skip
Dilution 1 to 500	Skip
Dilution 1 to 200	Skip
Dilution 1 to 100	Skip
Dilution 1 to 50	Skip
Dilution 1 to 20	Prepare
Dilution 1 to 10	Prepare
Dilution 1 to 5	Prepare
Dilution 1 to 2	Skip
Rinse Cycles	2
Wash Cycles	3

6. Select Internal standard parameters under "Internal Standard" tab.

- Internal Standard Index: Vial# of the internal standard you prepared for dilution.
- For the internal standard volume, need to calculate based on the equation $V_{add} = \frac{C_{final} \times V_{Total}}{C_{IS}}$
  - V_{add} is the value (volume) you need to typed in, ranged from 0-1000 uL.
  - C_{final} is the internal standard concentration of calibration point samples. For NDMA, 100 ug/L.
  - V_{total} is the total volume of calibration point samples. For one-time dilution, the total volume is 0.5 mL. But I recommend use two-time dilution for total 1 mL of calibration point sample to decrease the effects of bubble issue during liquid injection.
  - C_{IS} is the concentration of the internal standard you prepared for dilution.

Internal Standard		
Internal Standard	Include	
Internal Standard Rack	Rack 2	
Internal Standard Index	2	
Internal Standard Volume	10	µL
Bottom Sence Internal Standard	Off	
Heigth From Bottom Internal Standard	3	mm
Intarnal Standard Penetration Depth	30	mm

7. Set “Omit” for Analyte Protectant Agent.

Analyte Protectant Agent		
Analyte Protectant Agent	Omit	
Analyte Protectant Agent Rack		
Analyte Protectant Agent Index	3	
Analyte Protectant Agent Volume	1	µL
Bottom Sence Analyte Protectant Agent	Off	
Heigth From Bottom Analyte Protectant Agent	3	mm
Analyte Protectant Agent Penetration Depth	30	mm

8. Set other parameters.

Advanced	
Repetitions	1
Rinse Volume 10µL Syringe	2 µL
Rinse Volume 250µL Syringe	10 µL
Rinse Volume 1000µL Syringe	50 µL
Aspirate Flow Rate 10µL Syringe	2 µL/s
Aspirate Flow Rate 250µL Syringe	20 µL/s
Aspirate Flow Rate 1000µL Syringe	100 µL/s
Post Asprate Delay	3 s
Penetration Speed	50 mm/s
Filling Strokes Counts	5
Filling Strokes Post Aspirate Delay	1 s
Filling Strokes Post Dispense Deley	2 s
Delay After Filling Strokes	0.5 s
Vortex Frequency	1200 rpm
Vortex Time	10 s

9. Click “Apply” to save the method parameters and close the “Method Parameters” sub-window.

10. Save the whole method by clicking  or use “Same as” to give it a new name.

Note: If the internal standard was not added into the vials because AOC 6000+ stopped in the middle of the run, please uncheck the “High Pressure Injection” under “Injection Unit Advanced”.

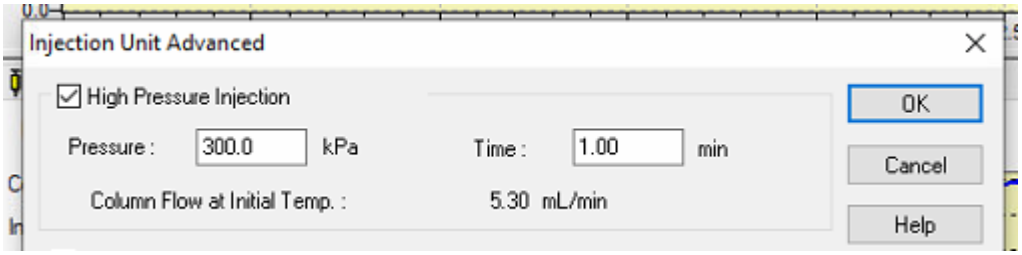

D.1.4.2. Prepare the calibration point samples (run the method)

1. Ensure solvents are filled in the Large Wash Station. For NDMA, both use DCM.

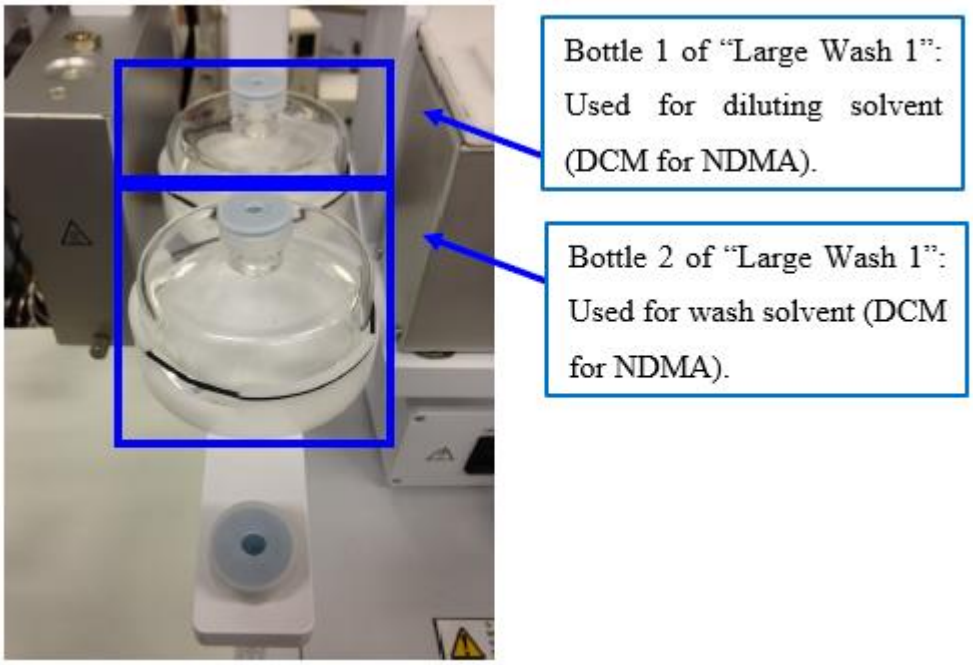

2. Check your Smart Syringe (LS1, LS3, LS4) and open your own batch file (See Section 1.3.3 for details).
3. Type in the exact same parameters in the following picture to prepare the calibration curve point samples. These parameters have no effect on the action of preparing calibration point samples, but tell machine to do Auto dilution.
    - Rack #: **Rack 2**; Vial#: **1**; Sample Type: **0: Unknown**; Analysis Type: **IT QT**; Method File: **The one you just created or "ndma mrm Dilution TEST.qgm" for NDMA calibration curve**; Level #: **1**; Inj. Volume: **1**.

	Rack #	Vial#	Sampl	Sam	Sample Type	Analys	Method File	Data File	Level#	Inj. Volum	ISTD Amt.
1	Rack 2	1	NDMA		0:Unknown	IT Q	ndma mrm DILUTION TEST.qgm	0714 2nd _7142021_1.qgd	1	1	(Level1 Con

4. Highlight the Line and click 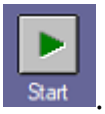

.
5. If you have time, please wait until the first solvent was added to make sure the machine works well.

Note:

- For single dilution, the total volume of the calibration point samples (V_{total}) is 0.5 mL. In order to decrease the effects of bubble issue, I recommend to do two-time dilution (First time without internal standard addition, and second with internal standard addition) to get total of 1 mL sample.
- If the dilution method doesn't work (e.g., AOC 6000+ doesn't move), please create a new method. If you only modify the method, the machine won't recognize.

D.2. Postrun Analysis

All the following operations in Section 2 needs to be completed by "GCMS Postrun Analysis". This software is design for processing your data to obtain the final results. If the following instructions are slightly different from the manual provided by the GCMS software, please follow this SOP.

D.2.1. Calibration Curve

1. Open your own folder and click "Quantitative".
    - If you cannot see the list of files, click the "Toggle Data Explorer" button.

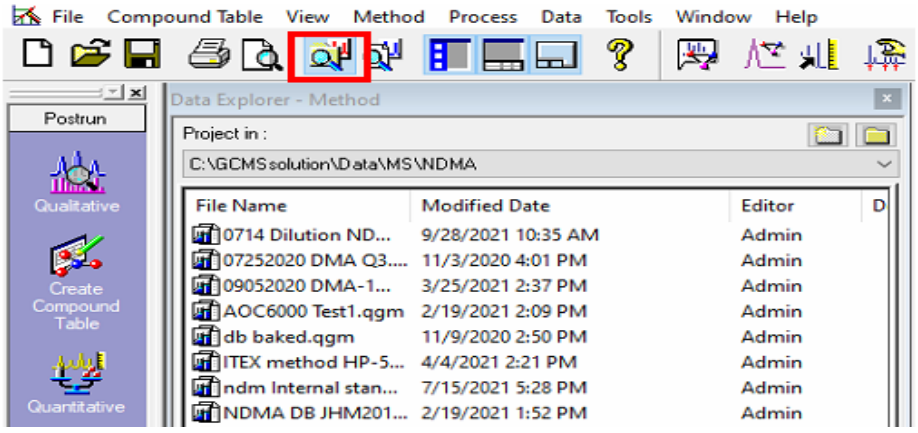

- If you cannot see your data file, check if you select “Data” tab in the data Explorer first. If you have already selected the right tab, reopen/refresh your folder.

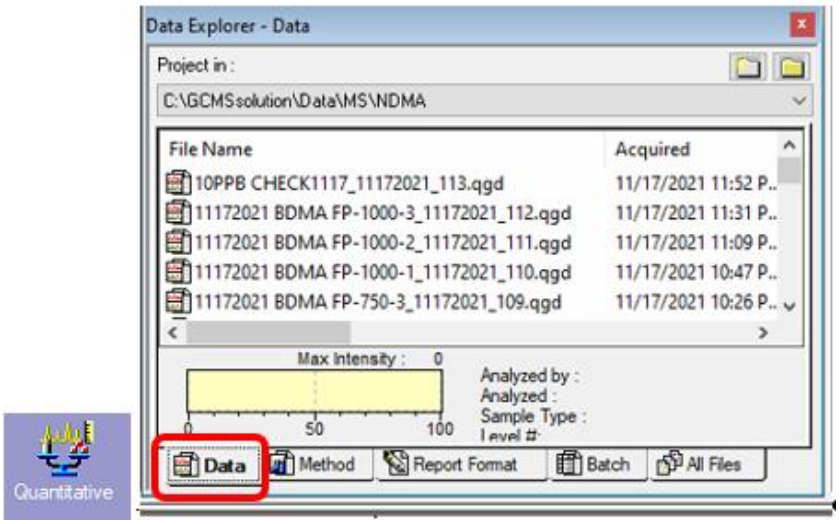

2. Go through all your calibration point samples, and make sure the software recognized the right peaks for every compound. You can click the ID#/Name in the right-most window to see the peak of each compound.
    - If the wrong peak was selected with the right Ret. Time, right click the blank area of the chromatography (1) → select “Manual Identification” (2) → click the right peak (3) → save the data file by clicking  .

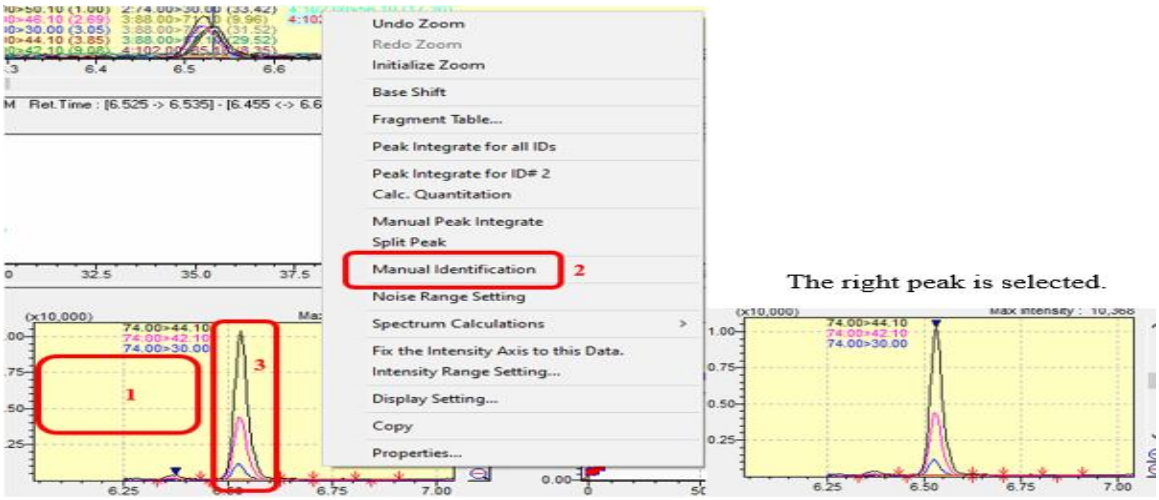

- If the wrong peak was selected because the wrong Ret. Time was wrong, the Ret. Time needs to be changed first and save it as a new method.
    - Choose “Param’s” (1), click “Edit” (2), type in the right Ret. Time (3), and click “View” to save.

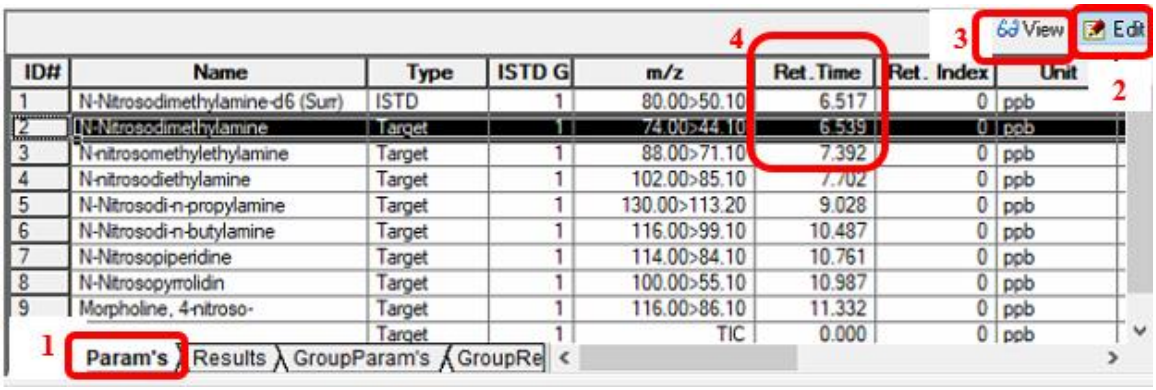

ID#	Name	Type	ISTD G	m/z	Ret. Time	Ret. Index	Unit
1	N-Nitrosodimethylamine-d6 (Surr)	ISTD	1	80.00>50.10	6.517	0	ppb
2	N-Nitrosodimethylamine	Target	1	74.00>44.10	6.539	0	ppb
3	N-nitrosomethylethylamine	Target	1	88.00>71.10	7.392	0	ppb
4	N-nitrosodiethylamine	Target	1	102.00>85.10	7.702	0	ppb
5	N-Nitrosodi-n-propylamine	Target	1	130.00>113.20	9.028	0	ppb
6	N-Nitrosodi-n-butylamine	Target	1	116.00>99.10	10.487	0	ppb
7	N-Nitrosopiperidine	Target	1	114.00>84.10	10.761	0	ppb
8	N-Nitrosopyrrolidin	Target	1	100.00>55.10	10.987	0	ppb
9	Morpholine, 4-nitroso-	Target	1	116.00>86.10	11.332	0	ppb
		Target	1	TIC	0.000	0	ppb

    - If the Ret. Time was changed, please save the method as a new one with a different name (go to File → Save Method As…) and load the new method first (go to File → Load Method → check all parameters in the pop-up window and click OK → click  “Peak Integrate for All IDs”) when going through other data files.

3. Go to Calibration Curve, and make sure the right method is open. If you cannot see the button, click the blue arrow “TOP” first in the left panel.

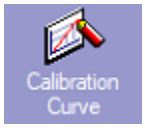

4. Click the compounds name to check the calibration curve of each compound.

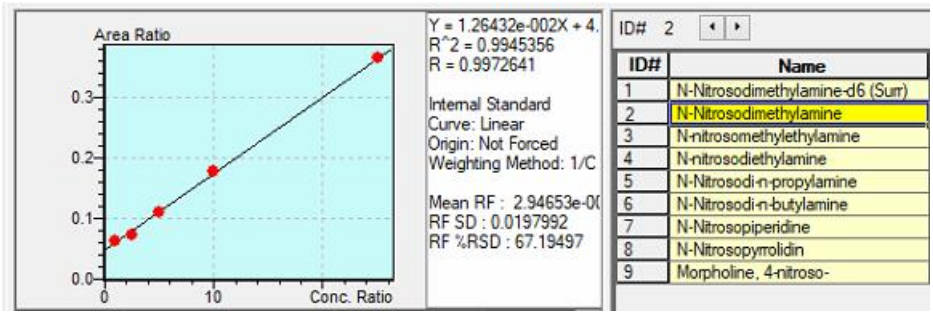

ID#	Name
1	N-Nitrosodimethylamine-d6 (Surr)
2	N-Nitrosodimethylamine
3	N-nitrosomethylethylamine
4	N-nitrosodiethylamine
5	N-Nitrosodi-n-propylamine
6	N-Nitrosodi-n-butylamine
7	N-Nitrosopiperidine
8	N-Nitrosopyrrolidin
9	Morpholine, 4-nitroso-

- If the calibration curve is not great,
    - Check if the data files are in right order. If not, deleted the wrong data files and drag the right ones from your folder.

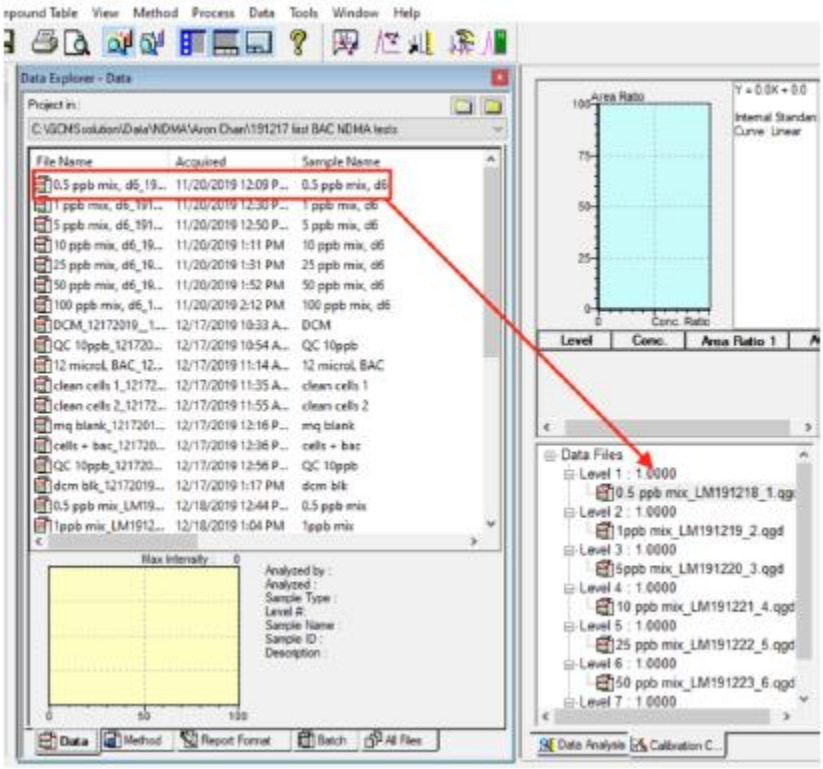

    - If the order is right, clicking the boxes could remove the calibration points which might not fit with the calibration curve.

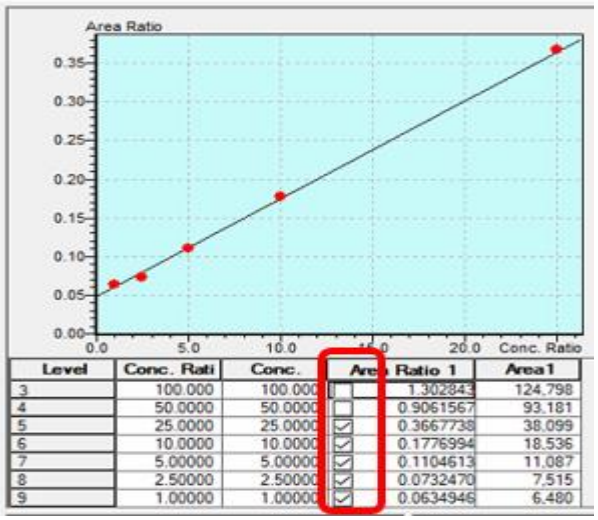

Level	Conc. Rati	Conc.	Area Ratio 1	Area1
3	100.000	100.000	1.302843	124.798
4	50.0000	50.0000	0.9061567	93.181
5	25.0000	25.0000	0.3667738	38.099
6	10.0000	10.0000	0.1776994	18.536
7	5.00000	5.00000	0.1104613	11.087
8	2.50000	2.50000	0.0732470	7.515
9	1.00000	1.00000	0.0634946	6.480

- If you want to change the level number of your calibration curve (point number of your calibration curve), go to "Method" (1) → click "Quantitative Parameters…" (2) → choose "Quantitative" in the pop-up window (3) → change the "# of Calib. Levels" (4).

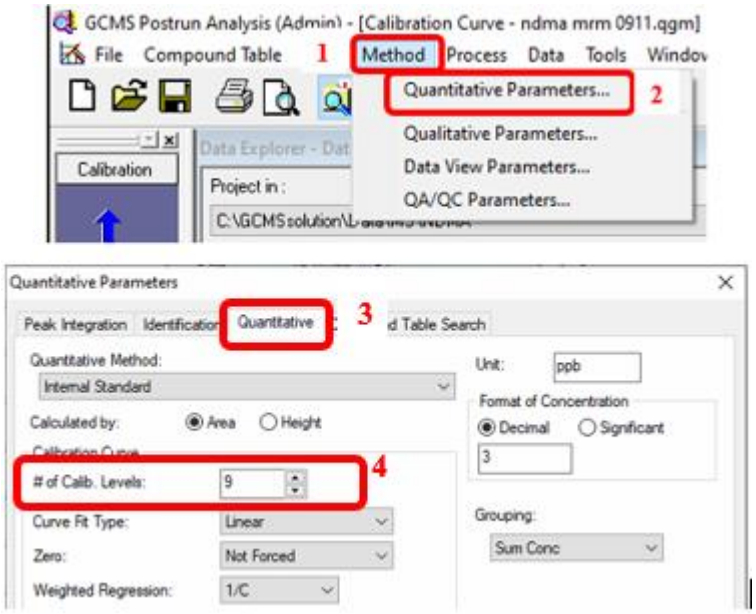

- If you want to change the concentration of each level in the calibration curve, go to the right most window and click "Param's" tab (1) → click "Edit" → change the concentration values (3) → click "View" to save it (2). Remember, the concentration of internal standard (ISTD) should be 1 all the time.

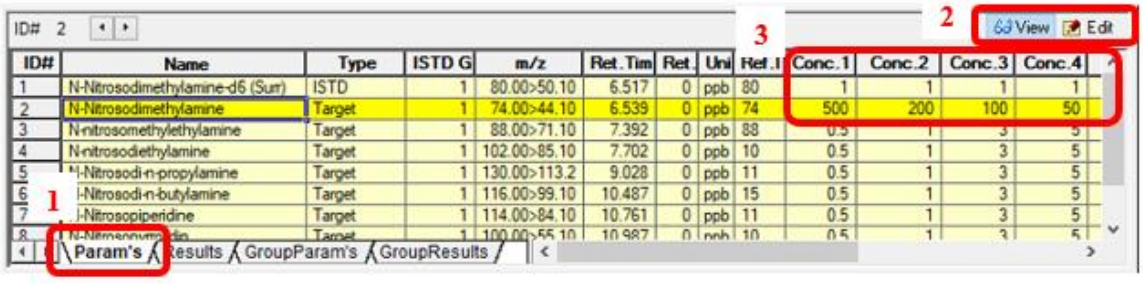

5. Save the method by clicking  .

D.2.2. Concentration of Unknown samples

1. Open your folder and click "Quantitative".

2. Double click on a data file from the “File Explorer - Data”.
3. Similar to Step 2 of Section 2.1, make sure the software recognized the right peak for every compound you are measuring first (1) → check the calibration curve (2) → the right concentration for each compound is displayed in the second column (Conc.) of the most-right window.

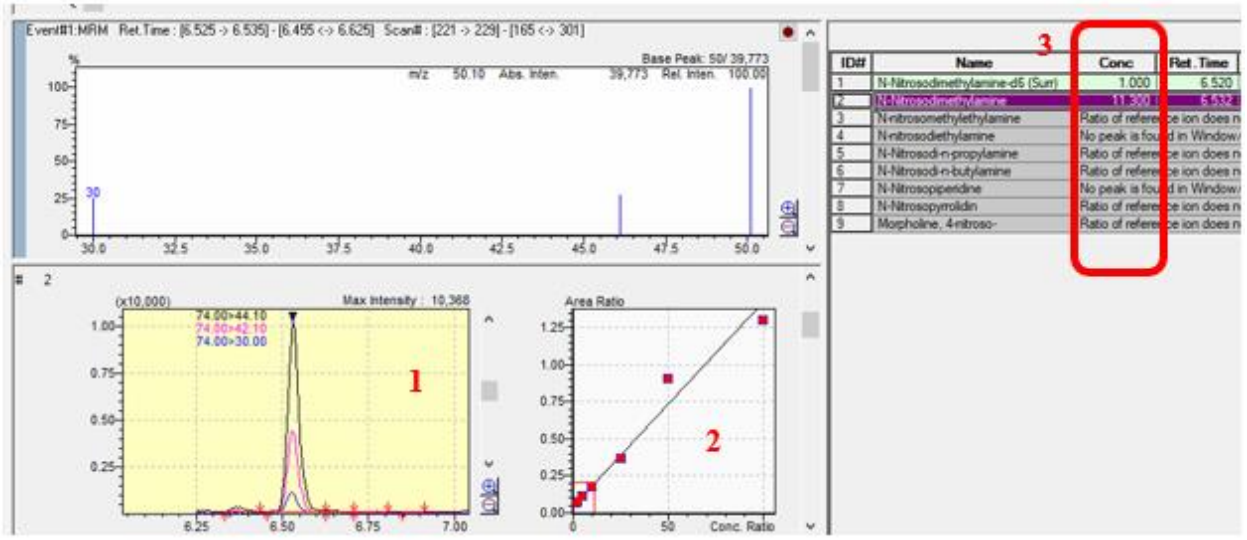

- If the peak is not right, select the right one following Step 2 of Section 2.1.
- If you cannot see the “Conc.” column, please click “Result” tab in the most-right window.

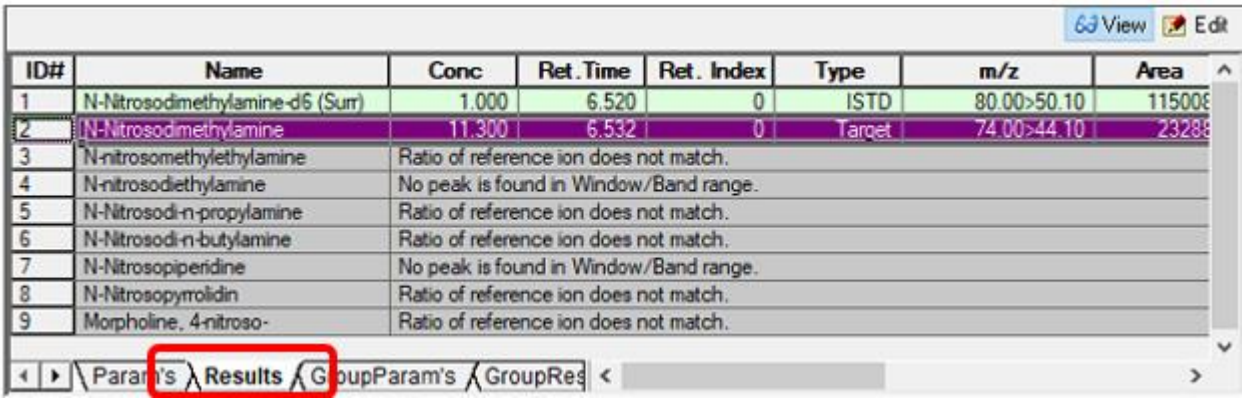

- If the calibration curve is not great, modify the calibration curve following Section 2.1. After that, load the new calibration curve by loading method (go to

File → Load Method → check all parameters in the pop-up window and click OK → click  "Peak Integrate for All IDs"). Then, make sure the software recognized the right peak for every compound again, and then the right concentrations should be displayed.

D.2.3. Similarity Search (Library)

Similarity Search is usually used for identifying unknown peaks of the chromatography from "SCAN" method.

1. Open your folder and click "Qualitative".
2. Double click on a data file from the "File Explorer - Data".
3. The full chromatography is shown in the top figure (A); draw a rectangle to select the unknown peaks (1), and the selected peaks would be enlarged and shown in the middle figure (B); double click the peak (a) you want to identify, and the *m/z* would be displayed in the bottom figure (C).

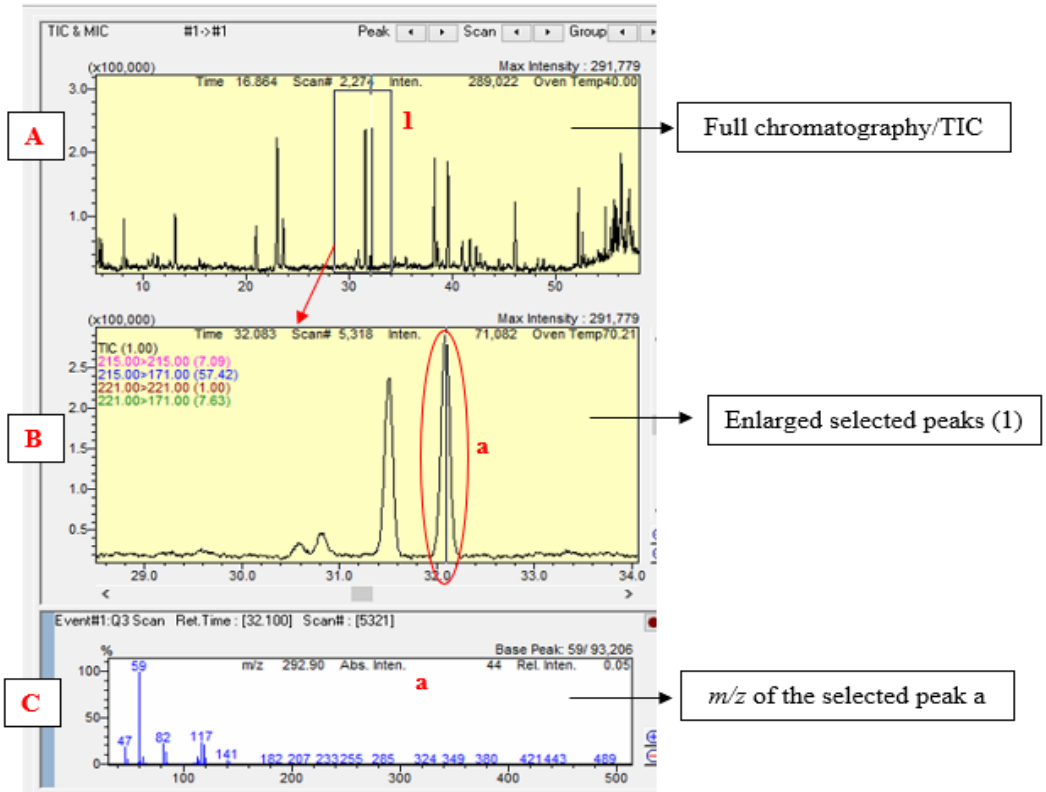

4. Right click the blank area of the bottom figure (C) and click “Similarity Search…” in the pop-up window.

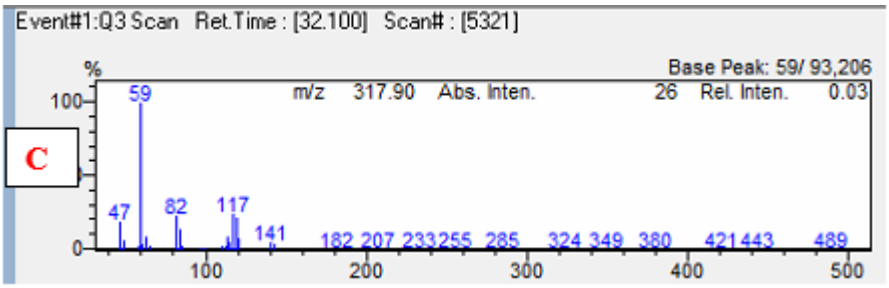

5. The result will be showed up automatically.

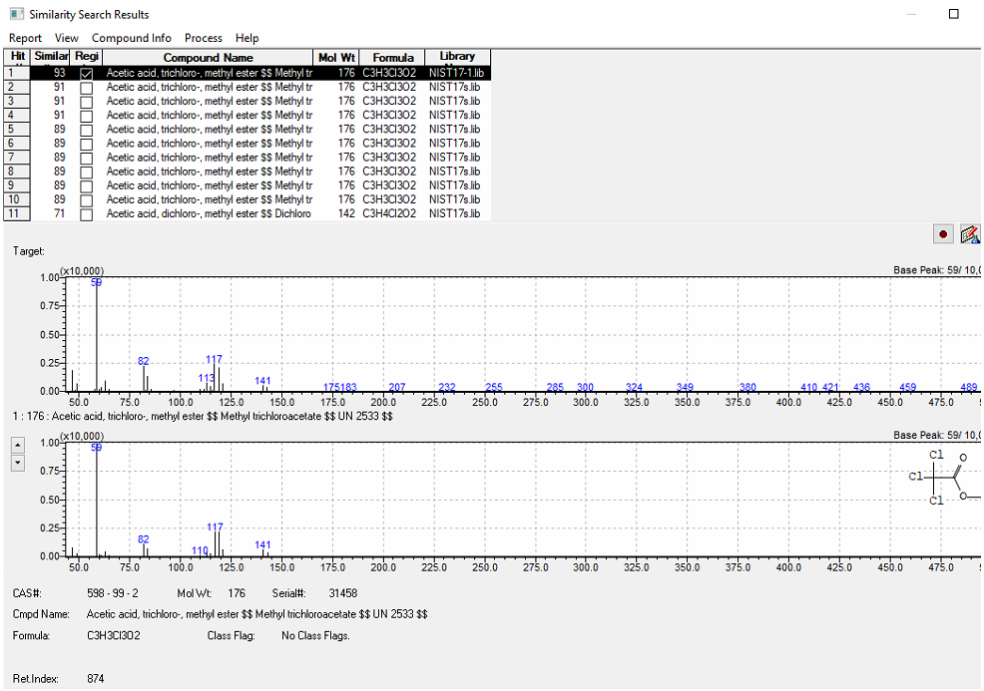

Note: If the following error occurs (1), click OK first, and do Step 4 again → Figure 2 will show up → click first "…" (a) and the Library will show up (3) → double click to select one (b) → click second "…" (a) and select another library (b) → … →click the last "…" and choose another library. Make sure every library to be selected at least once.

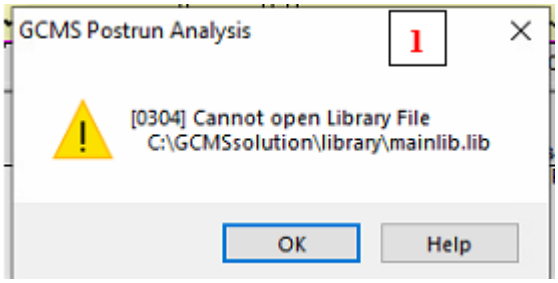

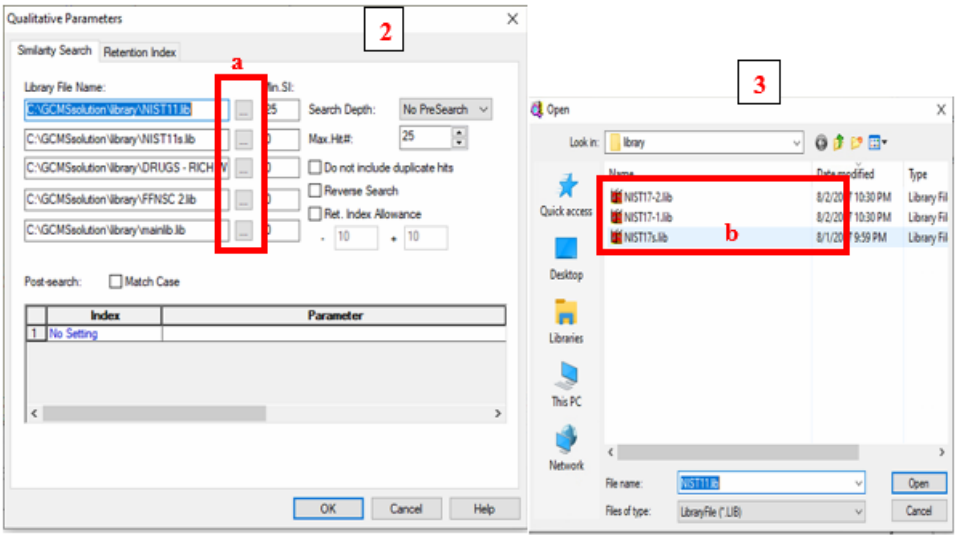

D.3. Maintenance

All maintenance instructions including column change, septum and insert replacement, ion source cleaning, filament replacement, and standard reagent for tuning (PFTBA) addition are provide by all GC/MS software. The following figures will tell you how to find them and some notes.

1. Click “Guide”, which are always on the left purple panel. 

2. In the sub-window, click “Maintenance” and choose “GC/MS TQ8040”.

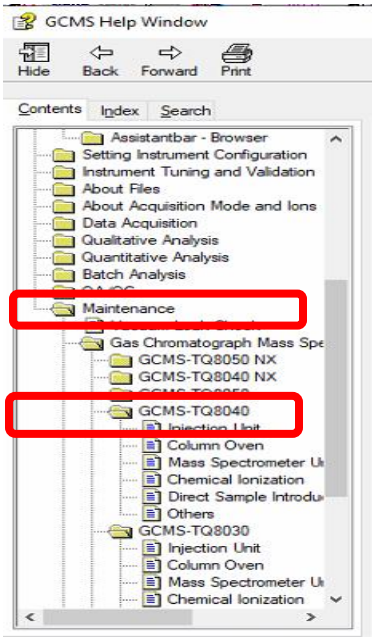

3. The GC/MS picture will show up.

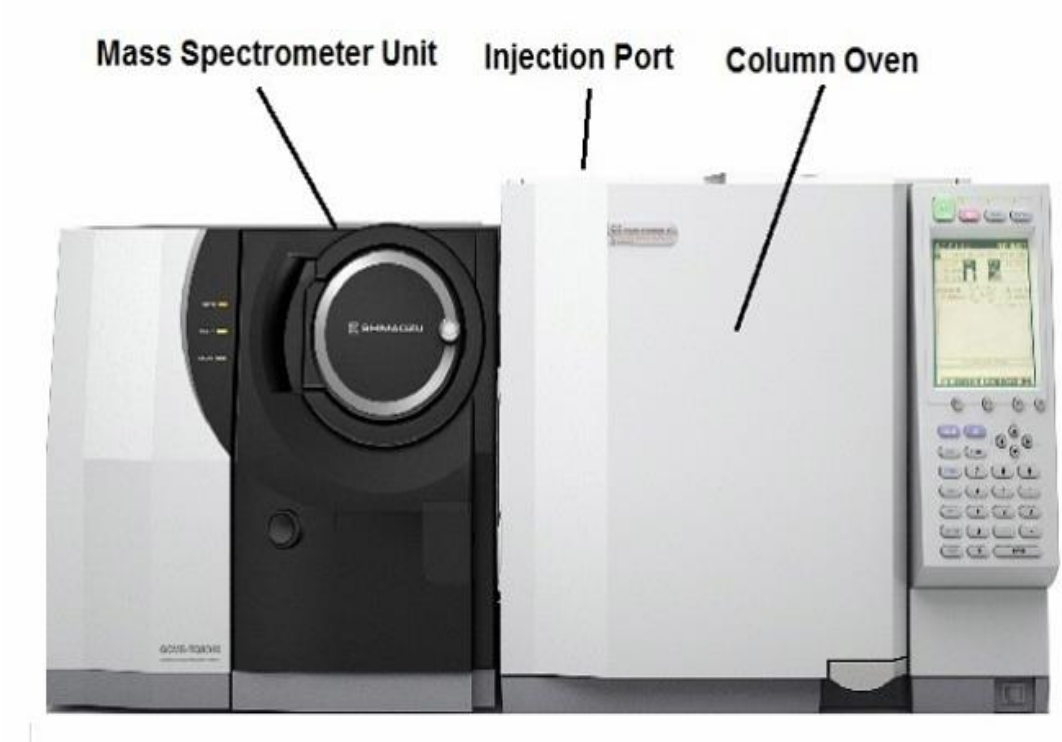

- If you click “Column Oven”, the procedure of column change will show up.

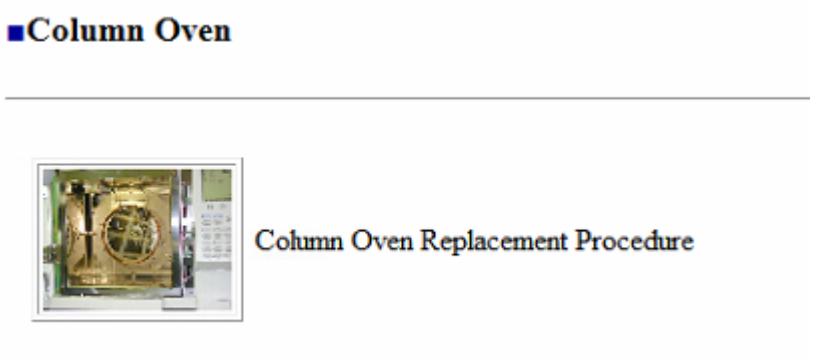

Note: Don't forget to do Step 17-18, after the machine stabilization completes. Otherwise, it will cause the error 1317, "The hardware configuration for this method…", which I mentioned in Section 1.

- If you click "Injection Port", four procedures including syringe rinsing, septum replacement, insert replacement, and filter trap replacement will show up.

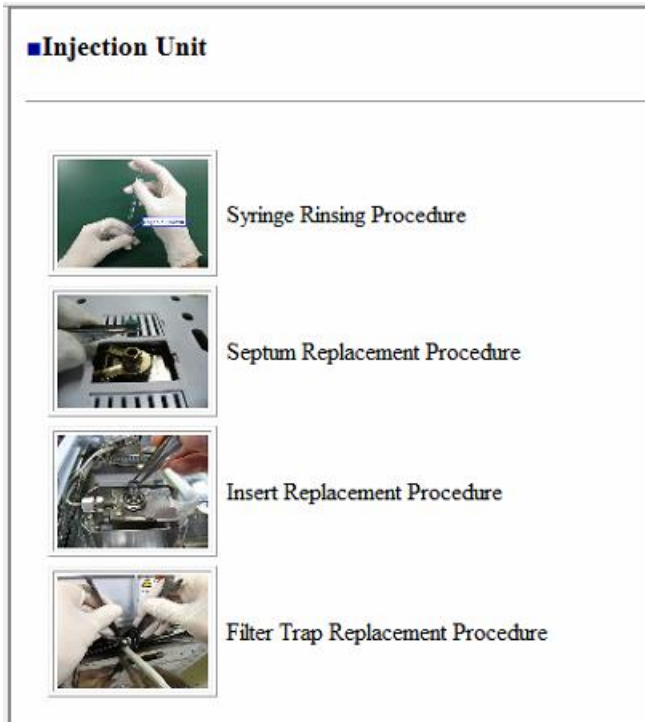

Note: For the insert replacement, please double check which types of glass inert you are using. We usually use SPLITLESS. If you'd like to use a different type, don't forget to modify your method.

- If you click "Mass Spectrometer Unit", three procedures including ion source cleaning, filament replacement, and tuning standard (PFTBA) addition procedure will show up.

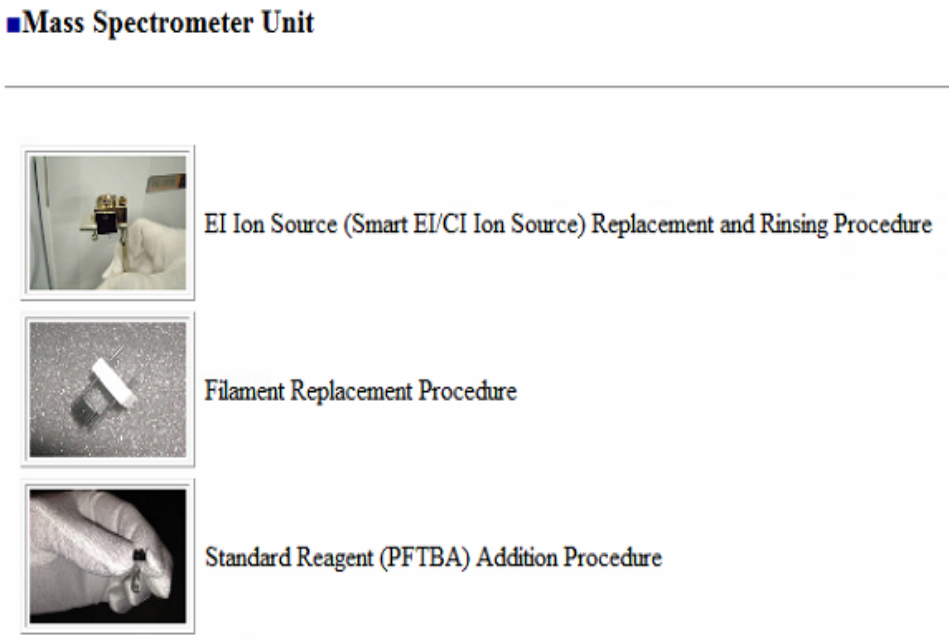

Note: For ion source cleaning,

  - During Step 19-21, in addition to ion source box and repeller, shield also needs to be cleaned.
  - In Step 24, no need to bake cleaning parts at 400 ℃, which might oxidize them. Drying them at 105 ℃ is enough.